Ispitivanje potencijala ubrzane karbonatizacije recikliranog betonskog agregata

Mikulić, Zdravka

Master's thesis / Diplomski rad

2023

Degree Grantor / Ustanova koja je dodijelila akademski / stručni stupanj:
University of Split, Faculty of Civil Engineering, Architecture and Geodesy / Sveučilište u Splitu, Fakultet građevinarstva, arhitekture i geodezije

Permanent link / Trajna poveznica: https://urn.nsk.hr/urn:nbn:hr:123:402517

SVEUČILIŠTE U SPLITU
FAKULTET GRAĐEVINARSTVA, ARHITEKTURE I GEODEZIJE

DIPLOMSKI RAD

Zdravka Mikulić

Split, 2023.

SVEUČILIŠTE U SPLITU
FAKULTET GRAĐEVINARSTVA, ARHITEKTURE I GEODEZIJE

Zdravka Mikulić

Ispitivanje potencijala ubrzane karbonatizacije recikliranog betonskog agregata

Diplomski rad

Split, 2023.

Ispitivanje potencijala ubrzane karbonatizacije recikliranog betonskog agregata

Sažetak:

Proizvodnja cementa čini približno 5 % globalne emisije CO_2 tako što se u cementnoj peći CO_2 oslobađa kalcinacijom vapnenca (2/3) i izgaranjem goriva (1/3). Nakon izlaganja zraku beton s vremenom ponovo apsorbira atmosferski CO_2 koji se trajno ugrađuje. Taj proces se naziva karbonatizacija. Javlja se tijekom vremena trajanja betonske konstrukcije, ali i nakon rušenja. Beton nastao rušenjem betonskih konstrukcija odlaže se kao otpad. Njegovom ponovnom upotrebom, recikliranjem, bi se reducirao nastali otpad kao i korištenje prirodnog agregata za proizvodnju betona čije rudarenje iziskuje veliku potrošnju energije. To bi također imalo veliki utjecaj na prirodu, krajolik i čovjekov okoliš. Dobivanje novog betona od recikliranog betonskog agregata, koji bi zadovoljio propisane standard za konstrukcijski beton, zahtjeva primjenu tehnologije ubrzane karbonatizacije. Međutim, primjena ove tehnologije je još uvijek novost i nije do kraja razvijena.

U ovom diplomskom radu je ispitan potencijal ubrzane karbonatizacije recikliranog betonskog agregata na različitim frakcijama agregata. Korištena je standardna tehnologija ubrzane karbonatizacije ugljikovim dioksidom. Na temelju mjerenja protoka plina, koncentracije CO_2, relativne vlažnosti, temperature i mase napravljena je analiza podataka. Dobivena je krivulja za procjenu apsorpcije CO_2 u reciklirani betonski agregat tijekom vremena za različite frakcije.

Ključne riječi: Reciklirani betonski agregat; ubrzana karbonatizacija; dubina karbonatizacije; apsorpcija CO_2.

Investigation on the forced carbonation potential of recycled concrete aggregate

Abstract:

Cement production accounts for approximately 5 % of global CO_2 emissions, by releasing CO_2 in a cement kiln by calcination of limestone (2/3) and fuel combustion (1/3). After exposure to air, concrete eventually reabsorbs atmospheric CO_2. This process is called carbonation. It occurs during the duration of the concrete structure, and after demolition. Concrete formed by the demolition of concrete structures is disposed of as waste. Its reuse, recycling, would reduce the resulting waste and the use of natural aggregate to produce concrete whose mining requires high energy consumption. This would have a great impact on nature, landscape and human environment as well. One of the possibilities for obtaining concrete from recycled concrete aggregate is the application of forced carbonation technology. However, the application of this technology is still a novelty and has not been fully developed.

In this graduate thesis, the potential of accelerated carbonation of recycled concrete aggregate on different fractions of aggregates was examined. The standard technology of accelerated carbonation by carbon dioxide was used. Based on the measurement of gas flow, CO_2 concentration, relative humidity, temperature and mass, data analysis was made. A curve was obtained to assess the absorption of CO_2 into a recycled concrete aggregate over time for different fractions.

Key words: Recycled concrete aggregate; forced carbonation; carbonation depth; CO_2 uptake.

SVEUČILIŠTE U SPLITU
FAKULTET GRAĐEVINARSTVA, ARHITEKTURE I GEODEZIJE

UNIVERSITY OF SPLIT
FACULTY OF CIVIL ENGINEERING, ARCHITECTURE AND GEODESY

STUDIJ: **DIPLOMSKI SVEUČILIŠNI STUDIIJ GRAĐEVINARSTVA**

SMJER: **KONSTRUKCIJE**

KANDIDAT: **Zdravka Mikulić**

JMBAG: **0083223158**

KATEDRA: **Katedra za Betonske konstrukcije i mostove**

PREDMET: **Betonske konstrukcije**

ZADATAK ZA DIPLOMSKI RAD

Tema: **Ispitivanje potencijala ubrzane karbonatizacije recikliranog betonskog agregata**

Opis zadatka: Zadatak diplomskog rada je ispitivanje potencijala ubrzane karbonatizacije recikliranog betonskog agregata kombinacijom standardne metode karbonatizacije i metode karbonatizacije pod tlakom. Analizom mjerenja tijekom procesa (protok plina, CO_2 koncentracija i kontinuirano mjerenje promjena težine) potrebno je odrediti ukupnu količine pohranjenog CO_2.

U Splitu, ožujak, 2023.

Voditelji diplomskog rada:

O.Univ.Prof.dr.sc. Alen Harapin

O.Univ.Prof. Dipl.-Ing. Dr.phil. Dr.techn. Konrad Bergmeister

Komentori diplomskog rada:

Dipl.-Ing. Johannes Hron

Dipl.-Ing. Dr. Oliver Zeman

Predsjednik Povjerenstva
za završne i diplomske ispite:

Doc. dr. sc. Ivan Balić

Ovaj diplomski rad je izrađen na Institutu za konstrukcijsko inženjerstvo, Sveučilišta prirodnih resursa i životnih znanosti u Beču, Austrija.

Erasmus+

University of Split
International Relations Office
Erasmus coordinator
Ruđera Boškovića 31
21000 Split

Letter of Confirmation

This is to confirm that student Zdravka MIKULIĆ from the **University of Split** spent 6 months at the Institute for Structural Engineering, Department of Civil Engineering and Natural Hazards at the University of Natural Ressources and Life Sciences, within the framework of the Erasmus + Programme and for the purpose of research for her Master thesis entitled:

Ispitivanje potencijala ubrzane karbonatizacije recikliranog betonskog agregata

Investigation on the forced carbonation potential of recycled concrete aggregate

Additional comments: Mrs. Zdravka MIKULIĆ worked very professional and demonstrated great interest and engagement in the field of resource-efficient Structural Engineering with passion for sustainability, novel technologies, and resource-efficient material combinations.

Name and surname: Konrad Bergmeister
Title: o.Univ.-Prof. Dipl.-Ing. Dr.phil. Dr.techn. DDr.-Ing. E.h. MSc. Ph.D.
Function: Chair of the Institute for Structural Engineering

Signature:

Date: Vienna, 28.08.2023

Stamp of the Institution: University of Natural Resources and Life Sciences, Vienna

BOKU | IKI

INSTITUT FÜR KONSTRUKTIVEN INGENIEURBAU
Universität für Bodenkultur
Peter Jordan Str. 82. 1190 Wien

Affidavit

I hereby declare that I have authored this master thesis independently, and that I have not used any assistance other than that which is permitted. The work contained herein is my own except where explicitly stated otherwise. All ideas taken in wording or in basic content from unpublished sources or from published literature are duly identified and cited, and the precise references included.

Vienna, 8/29/2023 Zdravka MIKULIĆ *(manu propria)*

Acknowledgments

I would like to express my gratitude to O. Univ. Prof. Dipl. Ing. Dr. Alen Harapin for supporting me in the decision to do this master thesis through the Erasmus + student exchange program at the University of Natural Resources and Life Sciences in Vienna. I thank him for his patience, understanding and guidance during the creation of this work.

Furthermore, I would like to express my gratitude to O.Univ.Prof. Dipl.-Ing. Dr.phil. Dr.techn. Konrad Bergmeister for accepting to be my supervisor, recognizing my efforts and giving me the opportunity to develop at the Institute of Structural Engineering through this master thesis.

I also want to express my sincere gratitude to Dipl.-Ing. Johannes Hron for advising in every part of the work. I really appreciate that I was able to learn from him and I am extremely grateful to him for his patience and selfless sharing of knowledge with me. His help was of huge importance to me during the entire creation of this work.

I also thank Dipl.-Ing. Dr. Oliver Zeman for all the help in the laboratory and the trust he showed me by enabling me to do everything I needed to create the laboratory part of the work.

Thanks to colleagues from the Institute of Structural Engineering BOKU for cheering me up and making the time spent at the institute more comfortable.

Also, I thank to all my friends who accompanied me on this journey. Without them, this period of my life would not be the same.

Finally, I am grateful to my parents Dijana and Mario and brother Blago for supporting me in all my decisions throughout my life. I thank them for every sacrifice they made for me and their efforts to make my life more beautiful. Special thanks to my boyfriend Kajo, who brightened my student days and supported me through all the obstacles I encountered on this way.

This thesis is dedicated to my family and boyfriend.

Content

1. Introduction

Due to its durability and easy application, concrete is the most used material in the construction industry. When concrete structures are no longer usable or are repurposed, that concrete is demolished and disposed of as demolition waste. About 70 to 80 % of the total volume of concrete is aggregate. Natural aggregate (NA) is a limited resource. It is obtained by mining. Mining requires heavy equipment and energy consumption, which incurs high costs. Also, if the nearby source of natural aggregate is insufficient or dried up, it is necessary to open a new source, which represents an additional cost. These problems can be solved at least partially with recycled concrete aggregate (RCA) [1] .

Replacing the natural aggregate with recycled aggregates in the production of new concrete would significantly affect these problems. Using recycled aggregates to replace natural aggregate has some negative effect on the performance of the new concrete, especially mechanical properties [2]. It is shown that one of the ways to achieve better mechanical properties is the application of forced carbonation technology of recycled concrete material [3; 4]. This technology rests on the fact that the carbonation that takes place naturally in concrete has a positive effect on the mechanical properties of concrete [5]. By filling the cavities with limestone, a higher strength of hardened concrete is obtained. Therefore, it was determined that the mechanical properties of the newly formed concrete would be improved if the recycled concrete aggregate was treated in such a way that the carbonation takes place rapidly [6].

Considering what the stated, the aim of this thesis is to investigate the potential of forced carbonation of recycled concrete material to further use the same material to produce new concrete. In addition, the thesis paper will examine equipment designed for accelerated carbonation and the possibility of its application for further testing.

The following 3 research questions are addressed in this thesis:

- What is the potential for recycled aggregate treated with accelerated carbonation?
- Which equipment exists to accelerate carbonation?
- Which amount of CO2 can be stored within various grain fractions of recycled aggregate?

Accordingly, this master thesis is divided into two parts: theoretical background and experimental part including results with discussion.

In the theoretical part firstly is described recycled concrete, its production, properties and mechanical properties of concrete with different proportions of RCA. Secondly, the carbonation of concrete, its positive and negative impact on the properties of hardened concrete and the factors that affect it are described. The third part of the theoretical background describes the technology of accelerated carbonation and the possibilities of its application.

In the experimental part, there is a characterization of the basic raw material as well as description of used methods and equipment. Furthermore, a determination of the forced carbonation potential is carried out.

1. Research on different grain fractions:

   0-0,25 mm; 0,25-0,5 mm; 0,5-1 mm; 1-2mm; 2-4mm; 4-8mm; 8-16mm; 16-22mm

2. Determination of the total amount of stored CO_2 by analyzing the measurements taken during the process (gas flow, concentration and continuous measurement of the weight changes)

The aim of this work is to obtain curves according to which carbon dioxide uptake could be predicted for different fractions of recycled concrete aggregate and examine the possibility of applying this technology for further tests.

2. Theoretical background

2.1. Recycled concrete aggregate

Use of recycled concrete began at the end of World War II [1]. It was necessary to rebuild Europe, and at the same time to get rid of waste material. Then the use of RCA decreased. Reuse began in the 1970s in the United States, but for non-structural purposes like fill material, foundations and base course [7]. Since then, research into RCA, properties and application possibilities has begun. Although there has been a decrease in the use of recycled concrete in construction since then, this does not mean that the amount of decomposed concrete waste is decreasing. Indeed, today there are many sources of concrete waste. The main reasons for the increase of this volume of demolition concrete waste are: “many old buildings and other structures have overcome their limit of use and need to be demolished; structures, even adequate to use, are under demolition because there are new requirements and necessities and creation of building wastes which result from natural destructive phenomena (earthquakes, storms...)” [8]. Therefore, the demolition rate is high, but unfortunately the storage space is small and the costs of storing such materials are increasing. If we turn around the problem of harmful use of natural aggregate to produce new concrete, then recycling of concrete offers a unique solution to this spectrum of problems.

Natural aggregate	Recycled concrete aggregate 1	Recycled concrete aggregate 2

Fig. 1. Natural aggregate and different RC aggregates [9]

Recycling involves proper collection and grinding of demolished concrete. As a product, RCA is obtained. **Fig. 1** shows natural aggregate and two different recycled concrete aggregates. Opposed to NA, RCA consists of two different materials: natural aggregate and adhered mortar (see **Fig. 2**). Adhered mortar makes RCA heterogeneous compared to NA and limits its application in concrete due to its inability to predict its behavior. This property of RCA creates an obstacle to achieve the required quality of RCA concrete and requires research technologies to improve the properties of RCA and to enable mass production of RCA concrete. Even though recycled concrete has already been applied in the past, its use in new construction applications in many countries is still a new technique.

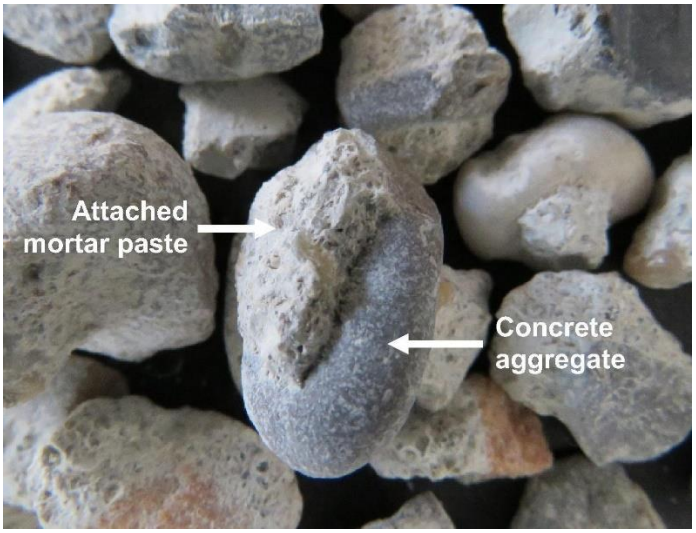

Fig. 2. Residual mortar paste attached to RCA [10]

2.1.1. RCA properties

In this theoretical part, the properties of RCA are discussed compared to the properties of NA. The purpose of this description is to understand the behavior of RCA in concrete mixtures. RCA is different in composition from NA, so it is not surprising that it shows differences in some basic properties such as density, porosity and shape of aggregates. These properties further influence the remaining and dictate the behavior of RCA in the concrete mixtures.

2.1.1.1. Density, porosity and water absorption

The main factor affecting the density of RCA is the residual of the adhesion mortar on the aggregate. Due to the lower density of mortar enveloping the natural aggregate in RCA, the density of RCA is lower than the density of NA [7]. The relative density of RCA (in the saturated surface dry state) is approximately 7–9 % lower than that of NA [11]. Density values also vary depending on which aggregate recycled concrete is made of. When it comes to bulk density, RCA also showed lower values. The value of bulk density RCA and NA was 2,394 and 2,890 kg/m^3, 17% respectively [12]. This means that adhesion mortar can be less weight compared to an aggregate of the same volume and causes a decrease in RCA density.

Porosity and water absorption are also associated with the residual mortar on the aggregate. RCA adhered mortar has a higher porosity and allows the aggregate to retain more water in its pores than NA which has low water absorption due to low porosity [7]. The water absorption value for NA it was from 0,5-1,0 %, and for RCA it was 4-4,7 % in saturated surface dry conditions reported from Shayan and Xu [13]. Other studies [11; 12], showed values for porosity and permeability of 5,6 % and 4,9-5,2% for

RCA and 1,0 and 2,5% for NA. These characteristics are of great importance when it is necessary to determine the appropriate concrete mixtures. McNeil et al. [7] limited the ability of absorbing aggregates to a maximum of 5 % for structural concrete.

2.1.1.2. Shape and gradation

The shape of the aggregate pieces is a property that affects the workability of concrete. The shape of the aggregate pieces is greatly influenced by the method of production, i.e. type of used crusher [14]. When it comes to RCA, the mortar that envelops the aggregate can smooth the hard edges of the original aggregate. Angular aggregates have a larger contact surface than rounded aggregates, so they can absorb more water. In order to achieve the same workability as with NA concrete, it is necessary to increase the w/c ratio. Matias, Brito et a.[15] confirmed this by increasing the proportion of RCA, resulting in a decrease in the workability of concrete. Which means that in order to successfully replace NA with RCA, RCA must have similar geometrical characteristics.

Gradation of concrete aggregate is prescribed according to the standards for concrete aggregates. Concrete aggregate must be within prescribed range to be acceptable as an aggregate for structural concrete. RCA falls into that range [12; 13].

2.1.1.3. Crushing and L.A. abrasion

The crushing test and L.A. abrasion are measures in order to verify the hardness and therefore the durability of the aggregate [7]. Aggregate crushing value test on coarse aggregates gives a relative measure of the resistance of an aggregate crushing under gradually applied compressive load. Coarse aggregate crushing value is the percentage by weight of the crushed material obtained when test aggregates are subjected to a specified load under standardized conditions [16]. The LA abrasion test is widely used as an indicator of the relative quality of aggregates. It measures the degradation of standard gradings of aggregates when subjected to abrasion and impact in a rotating steel drum with an abrasive charge of steel balls [5]. Predictions are that the RCA shows higher values in both crushing tests and L.A. abrasion tests. Therefore, crushing tests showed values for crushing resistance of 23,1% for RCA and 15,7% for NA [12; 13]. This means that by crushing coarse RCA, a higher measure of crushing resistance is given by RCA than NA. L.A. abrasion tests showed values of 32% and 26,4–42,7% for RCA versus 11 % and 22,9 % for NA [13; 17]. Which means when crushed or hit with steel balls in

L.A. test, RCA have more fine particles. The answer for such a result is given by residual plaster that can be easily broken in the intermediate transition zone[1].

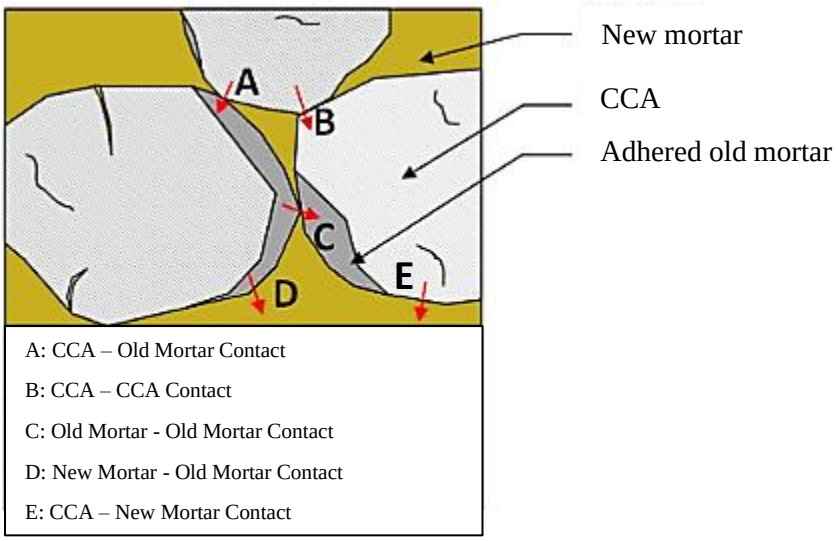

Fig. 3. Load transfer mechanism in RCA concrete [14]

In RCA there are five types of interphase transition zones: between aggregates and old cement mortar between aggregates and new cement mortar, between old cement mortar and new cement mortar, between aggregate and old adhered mortar, between aggregate and aggregate, between old mortar and old mortar (see **Fig. 3**). The transition zone between the aggregate and the old adhered mortar is generally the weakest amongst the various interfaces [18]. It confirms the predictions and indicates the weakness of the adhered mortar. There is a high probability that the mortar will break off the aggregate itself. However, there are also assumptions that a layer of adhered mortar creates a weak connection inside the concrete [7].

[1] Intermediate transition zone (ITZ) - region of the cement paste around the aggregate particles, which is perturbed by the presence of the aggregate. Typically, weak area of concrete through which the load transfer is most often carried out.

2.1.2. RCA concrete material properties

As already described in the previous chapter, RCA has different properties than NA. Therefore, RCA also behaves differently in a concrete mixture. In this section, material properties of RCA concretes are discussed and compared to conventional NA concretes for the purpose of reviewing the application possibilities of RCA concrete mixtures.

2.1.2.1. Compressive strength of RCA concrete

The compressive strength of RCA concrete may depend on the properties and quantity of recycled concrete aggregate. The factors that affect the compressive strength are the water cement ratio (w/c), the amount of RCA adhesion mortar and the percentage of replaced RCA. It is recommended that 25 to 30% of NA can be replaced with RCA without changing the w/c ratio and without compromising compressive strength [7]. This is confirmed by Thomas et al. [19] who tested concrete mixtures with different w/c ratios of 0.40, 0.45 and 0.50 and different proportions of replaced RCA were tested.

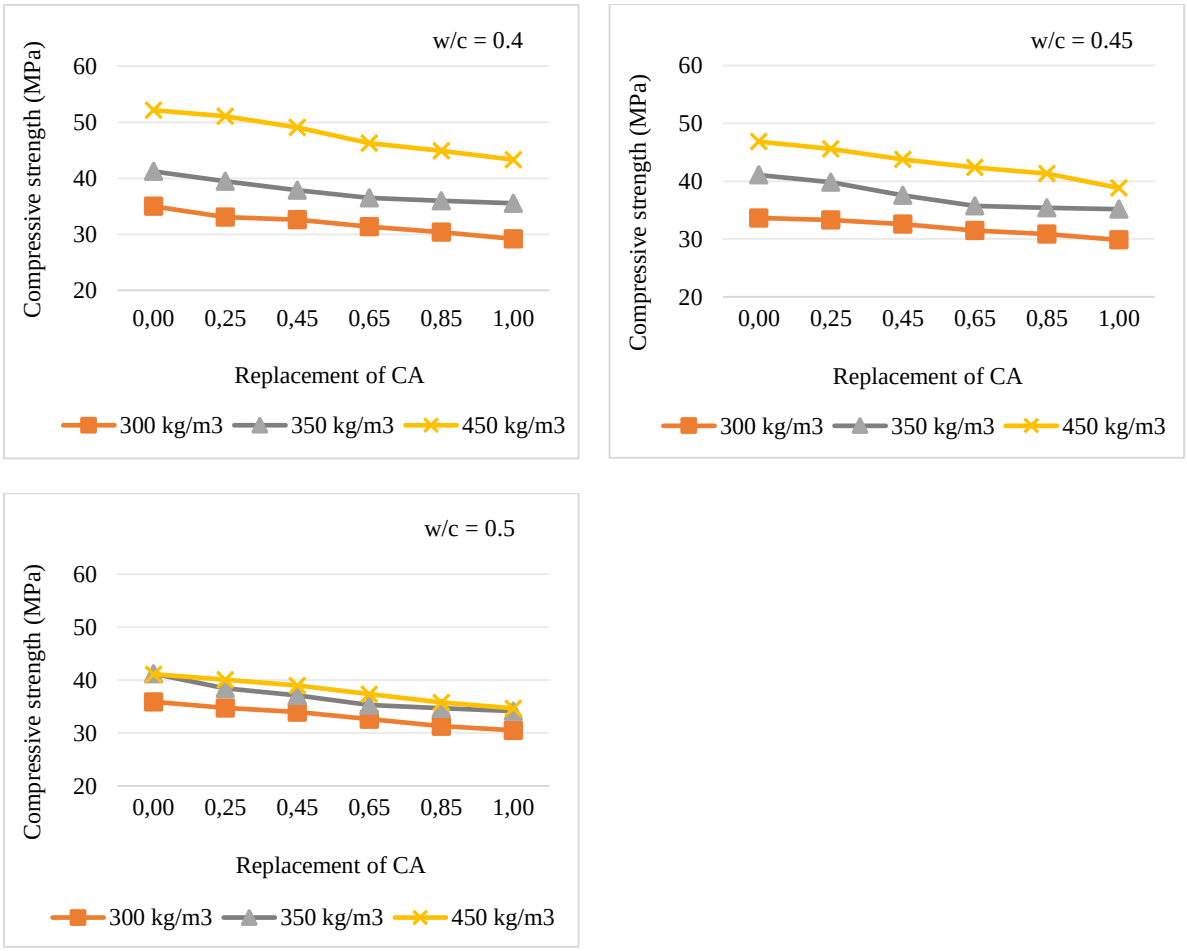

Fig. 4. Effect of aggregate replacement on compressive strength of concrete. Data from [19].

As shown on **Fig. 4**, when only 25 % of natural aggregate is replaced with RCA, the reduction in compressive strength is minimal (1.5-5%). With a further increase in the ratio of aggregate replacement, there can be a significant decrease in compressive strength. When 100% of aggregates have been replaced with RCA, the strength reduction was around 11-19%. In addition, Limbachiya et al. [11] also obtained similar results. Reason for these results is the previously mentioned mortar and intermediate transition zone.

The water cement ratio (w/c) is reverse reciprocal with an increase in the RCA content. As shown in Fig. 4, with an increase in w/c ratio, there is a decrease in strength. Which means that a higher proportion of RCA requires bigger amount of cement (lower w/c ratio) to achieve the same strength as in a mixture without RCA. This is confirmed by the fact that the highest compressive strength was recorded for RCA concrete with the lowest w/c ratio, and the largest decrease in compressive strength (19%) was recorded for concrete with 100% RCA content and the highest w/c ratio. With the increase in the water content, a transition zone of inferior quality develops in the RCA and the strength decreases. While the strength growth by increasing the proportion of cement may be attributed to a stronger interfacial transition zone and an improvement in the properties of the hydrated cement paste as a result of the increase in cement content [19].

2.1.2.2. Splitting tensile strength

Splitting tensile strength is generally also reduced by increasing the percentage of replaced aggregate. As shown on **Fig. 5** concrete mixtures with 25% replaced RCA can have a reduction in tensile strength by splitting about 2-8%, and those with a 100% cut have about 7–19% [19]. The largest decrease was recorded in the mix with the highest RCA content (100%) and the highest w/c ratio (0.5). The highest compressive splitting strength was recorded in the reverse case (25% RCA and w/c=0.40). The reason is the same as for compressive strength because the influence of water and cement on the transition zone with the existing mortar is the same.

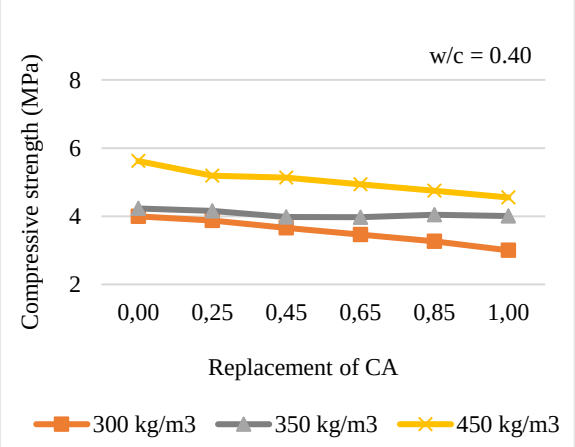

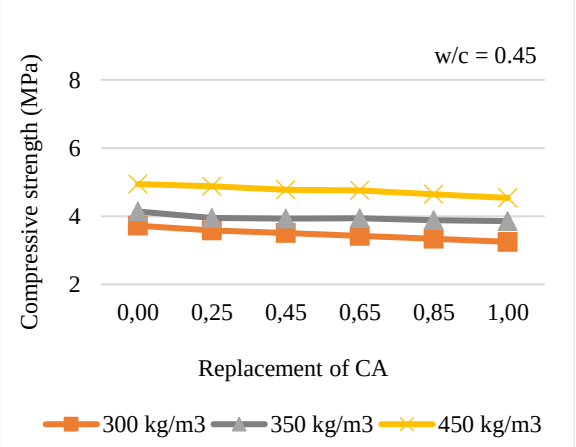

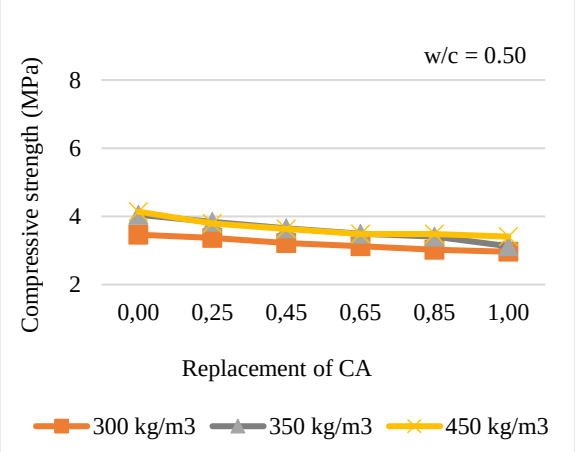

Fig. 5. Effect of aggregate replacement on splitting tensile strength of concrete. Data from [19].

2.1.3. Practical application of RCA concrete on a large scale

As already described in previous chapters, RCA due to adhered mortar has inferior properties than NA. Hence concrete made of RCA has if not additionally improved poorer properties, specifically, described compressive and tensile strength. It is a barrier to the practical application on a large scale of RCA concrete by only replacing NA with RCA. To overcome this barrier, there are several potential solutions.

The first possible solution is to adjust the w/c or water/binder (w/b) ratio. By reducing the w/c ratio for the same proportions of RCA, increase in the strength of concrete occurs. However, a reduced w/c ratio would mean the need for large amounts of cement. This solution is not sustainable and thus unacceptable on a large scale because it would mean a renewed increase in environmental pollution due to cement production. If factors such as processing methods and transport distances were added to this, the use of RCA for concrete production could initially be more expensive than the use of natural aggregate. Initial costs could deter some projects from considering the RCA concrete.

Second solution is the addition of mineral additives. Mineral additives such as fly ash or silica have smaller particle size than cement. Due to the large specific surface, they increase the volume around the cement particles and improve therefore the adhesion in the transition zone By hydration, they create hydrates that bridge the space between hydration products of cement and aggregate grains. This increases strength and reduces permeability by thickening the matrix [20]. However, for large-scale applications, the use of mineral supplements has some negative effects and challenges that need to be carefully considered.

While the use of mineral admixtures like fly ash and slag can reduce the carbon footprint of concrete production, there can be concerns related to the sourcing and production of these materials. For

example, the mining and processing of some mineral admixtures can have their own environmental impacts. Also, some mineral admixtures can be expensive to procure.

Research and experience have shown that well-designed mixes with recycled materials and mineral admixtures can perform well [21], the long-term performance of such concrete might still have uncertainties, especially if the materials are not well-characterized or if the specific conditions are unique.

The third solution is carbonation. Carbonation of concrete is the chemical reaction between CO_2 in the air and calcium hydroxide and hydrated calcium silicate in the concrete to give mainly carbonates. After carbonation concrete achieves better strength due to the formation of limestone. This means that RCA that has already been carbonated has better properties and its application in the production of concrete could potentially improve the properties of RC concrete. However, this is a process that is slow in nature and it is not possible to achieve large quantities of already carbonated RCA. To overcome this problem, the use of forced carbonation technology of recycled concrete aggregate is necessary.

This option has the most favorable impact on the environment not only through the use of RCA but also through the sequestration of carbon dioxide. In this way, a realistic balance would be achieved between the pollution of the atmosphere in the production of cement and the permanent installation of carbon dioxide accelerated by the carbonization of RCA. The use of this technology is still new and requires a multitude of tests. However, the favorable effects on the environment it offers justify it. The following chapter describes possible forced carbonization methods that can improve the properties of RCA and thus the properties of RCA concrete.

2.2. Forced carbonation of RCA

Forced carbonation has provided a unique solution for reusing demolished concrete material. The idea is after recycling this concrete material, the resulting RCA is cured with CO_2. In this way, forced carbonation of concrete would take place and improve the parameters of RCA, and consequently of RC concrete. Additionally, sequestration of CO_2 and permanent installation in the newly formed concrete would reduce spread of this gas in the atmosphere.

In order to make the principle of forced carbonation and its technology completely clear the chemical carbonation processes known so far, the positive and negative effects of carbonation on concrete and the identification of the carbonation depth into concrete are first described.

2.2.1. Chemism

To explain the chemism of carbonation at all, it is necessary to explain where the compounds that enter the chemical reactions of carbonation come from. Carbonation begins to take place in the initial phase of concrete hardening and continues for years until it completely permeates the concrete body [5]. Given that, it is a process that follows on from cement hydration .

There are four types of mineral compounds in cement, namely: alite (C_3A), belite (C_2S), aluminate (C_3A) and ferrite phase or celite (C_4AF). When these minerals encounter water, hydration occurs, which results in the hardening of cement or concrete. As products of hydration calcium silicate hydrates (C-S-H or silica gel), calcium hydroxide ($Ca(OH)_2$), calcium aluminate hydrate and etringit occurs. C-S-H and $Ca(OH)_2$ further enter the carbonation process by reacting with carbon dioxide, CO_2 [5].

Global average atmospheric carbon dioxide was 417.06 parts per million in 2022, setting a new record high [22]. Hence, CO_2 is not only found in the air, but also in other forms in nature. Almost all rainwater contains dissolved CO_2 and becomes mild carbonic acid, as shown in Eq. (1). When such rainwater or air wets the concrete, CO_2 enters the pores of the concrete.

$$H_2O+CO_2 \rightarrow H_2CO_3 \quad (1)$$

The main mechanism for water and chloride absorption in the outer part of concrete is capillary diffusion, and deeper in the concrete the dominant transport mechanism becomes diffusion. Diffusion is the movement of water molecules from a place of greater thickness of the adsorbed layer to a place of less thickness [5]. Adsorbed water is a layer up to about 5 water molecules thick. The first layer is the most tightly bound by surface forces, and the other layers are weakly, which affects the rate of diffusion. The rate of diffusion is also affected by the difference in the concentration of some other

substance in the solution, the chemical potential. In this case, the chemical potential is represented by CO_2.

After the CO_2 diffuses into the pores of the concrete, carbonation occurs. In the first case, a reaction occurs with calcium hydroxide, $Ca(OH)_2$. Calcium hydroxide dissolves according to Eq. (2) and creates calcium (Ca^{2+}) and hydroxide ions (OH^-) [23].

$$Ca(OH)_2 \rightarrow Ca^{2+} + 2OH^- \quad (2)$$

At the same time, the protolysis of carbonic acid takes place in two steps, Eq. (3) and Eq. (4), thereby creating bicarbonate H_2CO_3(HCO_3-) and carbonate (CO_3^2-) ions [24].

$$H_2CO_3 + OH^- \leftrightarrow HCO_3^- + H_2O \quad (3)$$

$$HCO_3^- + OH \leftrightarrow CO_3^{2-} + H_2O \text{ (at high pH, in uncarbonated concrete)} \quad (4)$$

In this case, Ca^{2+} and CO_3^{2-} are formed and can react and precipitate as limestone ($CaCO_3$) in concrete, Eq. (5) [5].

$$Ca^{2+} + CO_3^{2-} \rightarrow CaCO_3 \quad (5)$$

From these chemical reactions, the general chemical carbonation reactions result, as shown by Eq. (6) and (7) [5].

$$Ca(OH)_2 + H_2CO_3 \rightarrow CaCO_3 + 2H_2O \quad (6)$$

$$Ca(OH)_2 + CO_2 \rightarrow CaCO_3 + H_2O \quad (7)$$

In the second case, carbonic acid reacts with silica gel, C-S-H, and causes its decomposition into calcium carbonate ($CaCO_3$) and hydrated silicon dioxide (SiO_2), as shown in Eq. (8).

$$C-S-H + H_2CO_3 \rightarrow CaCO_3 + SiO_2(gel) + H_2O \quad (8)$$

Additionally, unhydrated cement clinkers from cementitious materials, such as tricalcium silicate or alite (C_3S) and dicalcium silicate or belite (C_2S), can also react with CO_2 gas, as shown in Eq. (9) and (10) [5].

$$3CaO{\cdot}SiO_2 + 3CO_2 + \mu H_2O \rightarrow SiO_2{\cdot}\mu H_2O + 3CaCO_3 \quad (9)$$

$$2CaO{\cdot}SiO_2 + 2CO_2 + \mu H_2O \rightarrow SiO_2{\cdot}\mu H_2O + 2CaCO_3 \quad (10)$$

Due to the removal of a certain amount of dissolved alkali metal hydroxides from the pore solution and incorporation of their cations into hydrated SiO_2, the pH value of the exposed concrete surface decreases. In this step, the negative influence of carbonation, which is described in the following chapter, becomes apparent.

In all these cases the result is the same, solid calcium carbonate ($CaCO_3$). It is a thermodynamically stable mineral called limestone. The obtained $CaCO_3$ has a different crystal structure, smaller volume than the original [5]. Hence the volume concentration of capillary pores in concrete increases and causes water loss. With the loss of water, the capillary forces increase and the concrete shrinks. In addition, CO_2 is permanently incorporated by these chemical processes. All mentioned chemical processes, whether with calcium hydroxide, silica gel or un-hydrated cement clinkers of cementitious materials, in which carbonates are produced, represent carbonation.

2.2.2. Effects of carbonation on hardened concrete

Carbonation creates a domino effect of negative effects on hardened concrete (see **Fig. 6**). First, the natural alkalinity of concrete is reduced from pH 13 to pH 8. Lowering the pH results in the destruction of the passivation layer around the steel. In this way, reinforcement is exposed to water and air and towards to corrosion, i.e., the steel rust. The steel that succumbs to rust expands and thereby puts pressure on the surrounding concrete. The internal pressure in the concrete element eventually results in the cracking of the concrete surface [25]. An example of such a rupture is shown in **Fig. 7**. Cracking concrete leads to weakening of the structure and a decrease of stiffness and finally also of the durability of the structure on an exponential rate. The negative impact of carbonation on steel corrosion can be further enhanced if chloride ions (salts) are penetrated by diffusion to reinforcement [25]. Due to the already mentioned different crystal structure of $CaCO_3$, the volume concentration of pores in concrete increases and causes water loss and increase in capillary forces in cement paste, and then shrinkage of concrete.

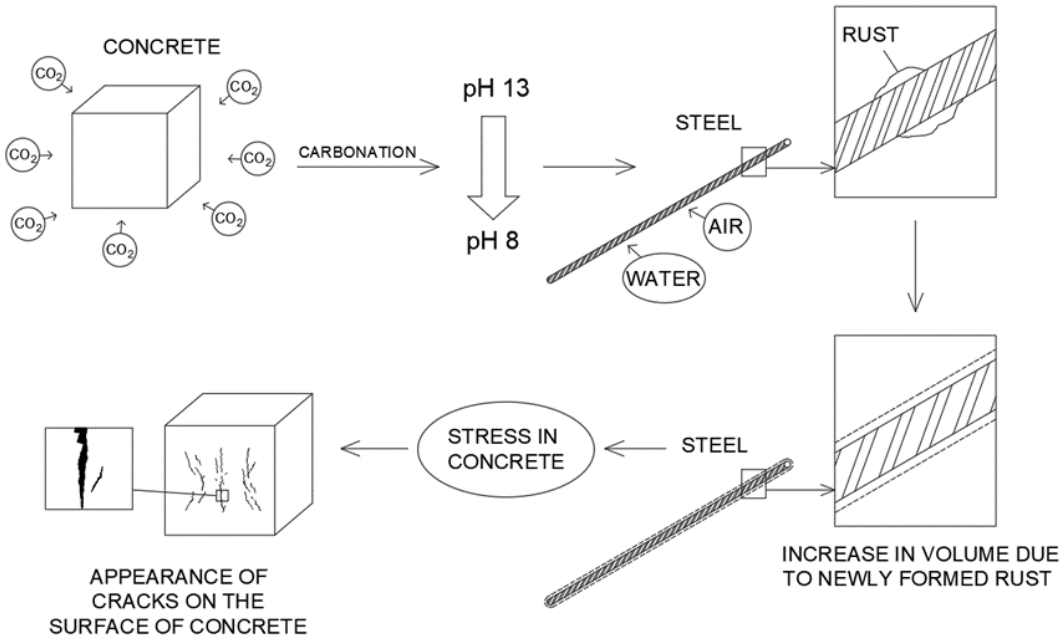

Fig. 6. Scheme of the negative effect of carbonation on concrete (own figure)

Slowing down or preventing this effect is possible with an anti-carbonation coating. The procedure goes by first cleaning the surface of the concrete and then applying a coating. In this way, CO_2 is prevented from entering the concrete. Depending on type of anti-carbonation coating this method ensures the prevention of carbonation for up to about 5 years [26]. However, this method is not always possible because sometimes some places of structures are hard to reach.

Positive side of the existence of carbonation is increasing the compressive and tensile strength of concrete. Increase in strength occurs because $CaCO_3$ has a higher hardness and solid-phase volume than $Ca(OH)_2$ [6]. That is why carbonation products increase the strength of the cement paste rapidly in the initial phase of carbonation, and a slight increase in strength occurs in the later period of carbonation reaction. This advantage of carbonation is one of the main reasons for the application of forced carbonation technology of RC concrete materials.

Fig. 7. Cracks on the concrete surface [27]

Likewise, carbonation makes ordinary concrete more durable because it reduces its overall porosity (see chapter 2.2.5.8.). By the progression of carbonation an increase in density is caused. With greater deposition of $CaCO_3$ in concrete, the permeability of concrete can be reduced, thus reducing the access of CO_2 to the interior of the concrete. This leads to a decrease in the rate of carbonation [28]. In general, it can be said that carbonation prolongs the durability of unreinforced concrete. However, it is not the same case with reinforced concrete precisely because of the previously described process of pH drop, cracks in concrete and consequently declining structural stability. Which means that natural carbonation of concrete structures has the safest and most effective positive effect when it comes to concrete elements without reinforcement. The same goes for RCA. Given that it is free from reinforcement, all the positive properties achieved by carbonation on non-reinforced concrete will also be achieved on RCA.

2.2.3. The depth of carbonation

The CO_2 volume is approximately 0,04% of the air, and the CO_2 diffusion coefficient of concrete is approximately 10^{-8} cm^2s^{-1} [29]. Thus, the natural carbonation reaction is quite slow. On **Fig. 8** is shown an identification of concrete carbonation using pH indicator (phenolphthalein). The structure of phenolphthalein id dynamic. It changes color depending on the pH of the environment. Specifically, there are 3 states of phenolphthalein:

(1) Increasing the Ph and becoming slightly basic, the solution becomes colorless.
(2) In anionic form, after the loss of the second proton, a dislocation occurs in the solution from colorless to purple re, which is due to an increase in pH between 8,0 and 9,9.
(3) In a strongly basic medium (pH > 13), colorless appearance [30].

This behavior allows the use of phenolphthalein as an indicator of concrete carbonation, which changes pH to a value between 8.5 and 9. Purple part is an uncarbonated part of concrete and a part without a change of color represents carbonated layer of concrete. Due to **Fig. 8**, it can be concluded that carbonation in concrete takes place from the surface to the inside and forms carbonated layer of concrete. This coincides with the already described method of carbonization and the fact that carbonization takes place in the presence of CO2, which enters the concrete through pores on the surface of the concrete.

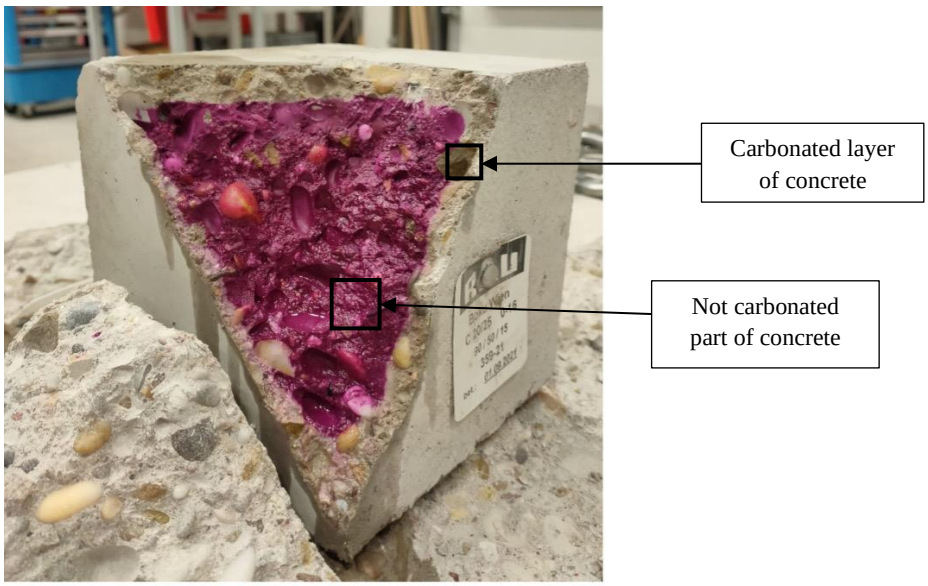

Fig. 8. Identification of concrete carbonation using pH indicator.

Identification of concrete carbonation using the pH indicator, as shown on **Fig. 9**, is called the phenolphthalein test. That is the easiest way to identify carbonation. The test is performed by the solution of phenolphthalein indicator. This testing metho according to the Austrian Standard ÖNORM EN 14630:2006 [31], works usually with 1 g of phenolphthalein in 70 ml of ethyl alcohol and diluted

in 100 ml ofml of distilled or deionized water. Other alcohols such as isopropylene can also be used. Samples should be prepared according to ENV 1504-9 [32]. Tests should be done as soon as possible after splitting the concrete. The solution applies to a freshly seceded concrete surface. Results are recorded within 30 seconds of solution application on the surface.

Fig. 9. Recycled concrete aggregate before carbonation (left) and after carbonation (right).

Measuring the depth of carbonation is done using a caliper or ruler. The depth of carbonation at any given point is the distance (measured in mm) from the external surface of the concrete to the edge of the red-purple colored region [31]. Carbonation depth is determined by carbonation front. It is irregular so both values mean $d_{x,mean}$ (A) and maximum $d_{x,max}$ (B) should be measured to the nearest mm (**Fig. 10**).

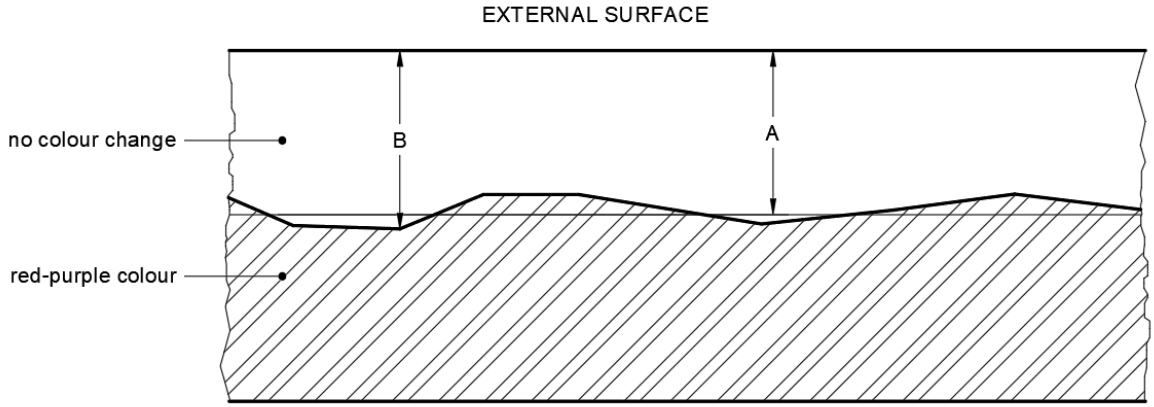

Fig. 10. Carbonation front [31]

In the case of isolated pockets of deeper carbonation, $d_{k,max}$ should not be included in the calculation of $d_{x,mean}$, (see **Fig. 11**).

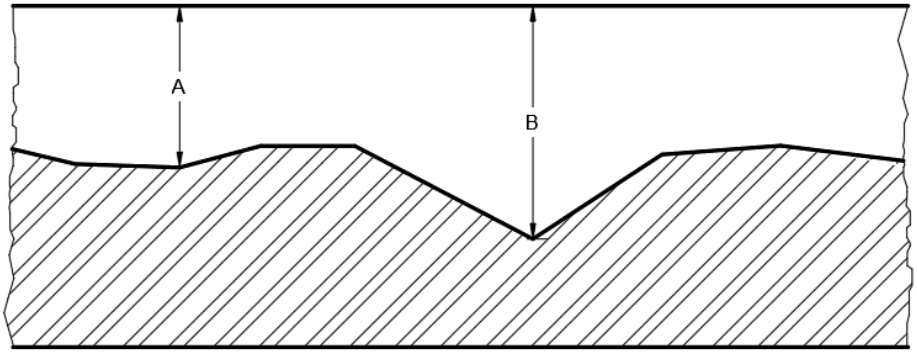

Fig. 11. Isolated pockets of deeper carbonation [31]

The depth of the carbonated layer as well as the rate of spread of carbonation depends on environmental conditions and quality of concrete, primarily pore structure (porosity and permeability) as described in chapter 2.2.5.8. It was found that the neutralization depth exists in the partly - carbonated zone of concrete where both $CaCO_3$ and $Ca(OH)_2$ are observed, and that carbonation front depth from which $CaCO_3$ is not detected, exists much deeper in concrete. Further, it was confirmed that the neutralization depth is about half of the carbonation front depth [33].

Except visually, spreading of carbonation is most easily described by the degree of carbonation, DoC. It is a value that is defined as the ratio of the amount of introduced CO_2 and the maximum intake of CO_2 into the carbonated volume of concrete [34], as shown in Eq. (11).

$$\mathrm{DoC} = \frac{\mathrm{CO_2\ in\ the\ carbonated\ zone}}{\mathrm{Maximum\ CO_2 uptake}} \tag{11}$$

The maximum CO_2 intake can often be equated with the CO_2 emissions from calcination extracted from the material. Blunt carbonation is defined only within an area that is considered carbonated and this area is defined as an area that shows a discoloration with a phenolphthalein test [34].

According to a conducted study by [35] carbonation can move at rate from 1-5 mm per year due to the different conditions and durability of concrete. Another study [29] showed that the natural carbonation depth of concrete after 20 years and 80 years were only 10 mm and 20 mm. These values may vary depending on the composition and properties of concrete as well as the exposure class of the structure.

2.2.4. Forced carbonation technology

Since there is a good correlation between natural and accelerated carbonation of concrete, accelerated or forced carbonation technology has developed in recent years [36]. Developed forced carbonation technology can ensure that RA is rapidly carbonated within several hours [37]. There are four main methods of RA carbonation curing:

- standard carbonation method,
- pressurized carbonation method,
- flow-through CO_2 curing method,
- water-CO_2 cooperative curing method.

All these methods are developed by increasing the CO_2 concentration, temperature, relative humidity, etc. [6]. They differ from each other according to carbonation efficiency and energy consumption. In practice, the standard carbonation method and the pressurized carbonation method are most used due to the simplicity of the required equipment compared to other methods.

In the following, all methods are described according to the studies that conducted their research in this way, and the methods are compared with each other according to efficiency.

2.2.4.1. Standard carbonation method

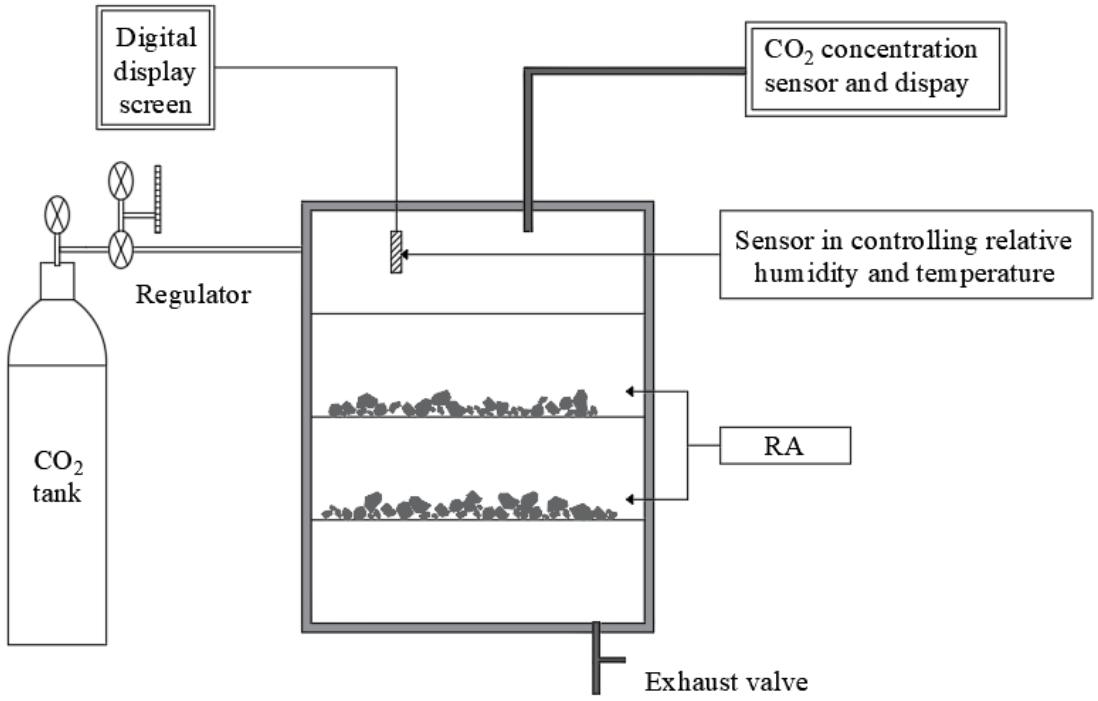

Fig. 12. Schematic view of standard carbonation equipment [6]

The equipment required for this method is shown on **Fig. 12**. RA samples are placed in a chamber which must be completely airtight. Then the gas is released until the desired CO_2 concentration is reached. Inside the tank are installed sensors connected with displays to monitor CO_2 concentration, relative humidity and temperature.

This standard carbonation test was used on the RA in accordance with Chinese standard GB/T 50082-2009 [38]. Shi et al.[39] as well as Zhang et al. [40] placed RA samples in a carbonation chamber under certain conditions. The temperature in the chamber was 20±2°C, RH was 60±5% and concentration of CO_2 was 20±2%. The CO_2 was maintained at ambient pressure. In both studies, CO_2 penetration into RA was low. This resulted in poor carbonation efficiency and the necessity for an time extension of CO2 curing [6].

2.2.4.2. Pressurized carbonation method

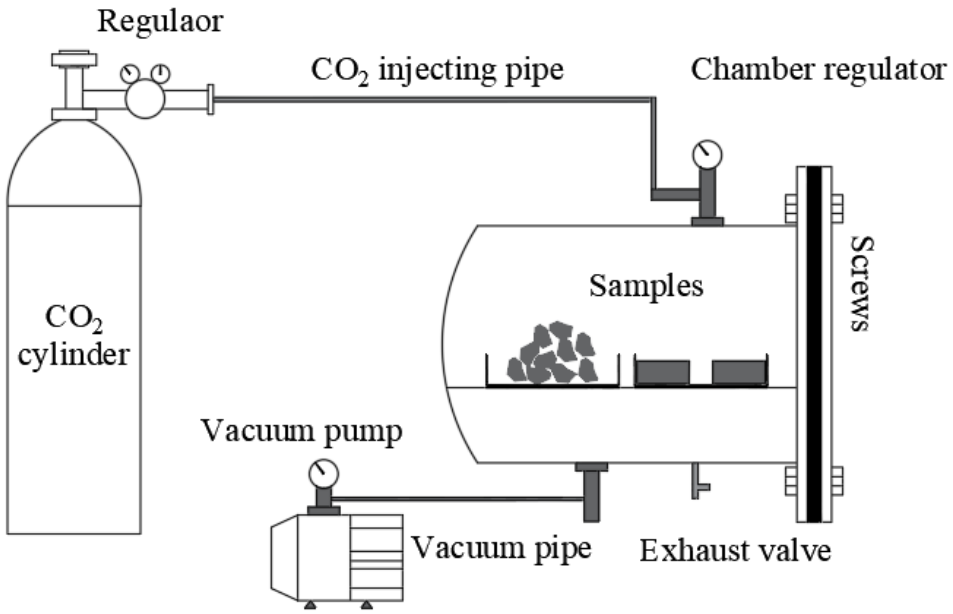

Fig. 13. Schematic view of pressurized carbonation equipment [6]

The pressurized carbonation method has emerged as a solution to improve the efficiency of RA carbonation compared to the standard carbonation method. The technology is based on increasing the pressure of CO_2 gas inside the chamber. The equipment required for testing this method is shown on **Fig. 13**. Kou et al. [41] conducted pressurized carbonation method in their study. An airtight steel cylindrical vessel was used as a curing chamber. RA was first dried and then placed in a chamber where the RH was 50±5% and temperature 25±3 °C. Before injecting CO_2 gas, a vacuum pump was used to reduce the pressure in the chamber to -0.5 bar, and CO_2 pressure in the chamber was controlled by a

gas regulator and maintained at a constant level. A sufficient amount of silica gel was placed at the bottom of the chamber to prevent unfavorable influence of high humidity. Silica gel can absorb evaporated water inside the chamber. As a result, this method has shown better efficiency than the standard carbonation method [41].

2.2.4.3. Flow-through CO_2 curing method

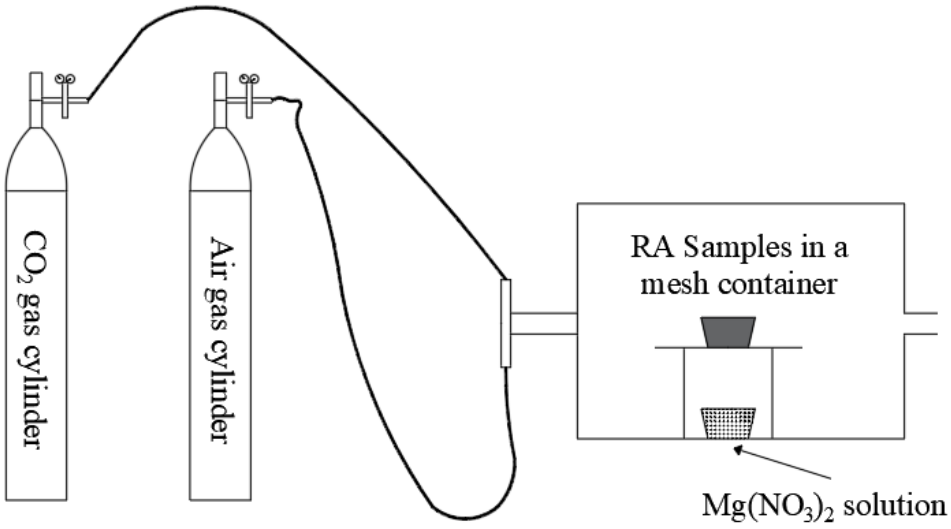

Fig. 14. Schematic view of flow-through CO_2 curing equipment [42]

The flow-through CO_2 curing method has also been developed to improve the efficiency of carbonation of RA. The equipment required for testing this method is shown on **Fig. 14**. Fang et al. [42] conducted flow-through CO_2 curing method in their study. Mixtures of air and CO_2 gas were first injected on one side into the chamber made of steel. The gas flow rate (a mixture of pure CO_2 and air) is controlled from 1.0 to 10 L/min. The RH in the chamber was controlled at 50±5% using a saturated solution of $Mg(NO_3)_2$, and the temperature was at room temperature (~25 °C).

This flow-through method is designed to test the effects of relative humidity, CO_2 concentration and gas flow rate. The results showed that the flow-through CO_2 curing method has lower energy consumption and higher carbonation efficiency than the standard carbonation method [6].

2.2.4.4. Water-CO_2 cooperative curing method

On the basis that the carbonation reaction between CO_2 and Ca^{2+} gas in the water-CO_2 mixture is more complete than that of a single CO_2 gas, this method uses water and CO_2 treatment [43]. It is suitable for fine aggregate and powder. On **Fig. 15** is shown a schematic diagram of set-up for water-CO_2

cooperative curing method. Pasquier et al. [44] conducted water-CO_2 cooperative curing method in their study.

All reactions of this test take place in a reactor with a stirrer. First, the required amount of solid is weighed and added to the reactor. Then distilled water is added and the pH is measured. Then the reactor is closed and mixing is started. A gas mixture composed of O_2 and CO_2 balanced with N_2 is also injected rapidly. When the desired pressure inside the reactor is reached, all valves are closed.

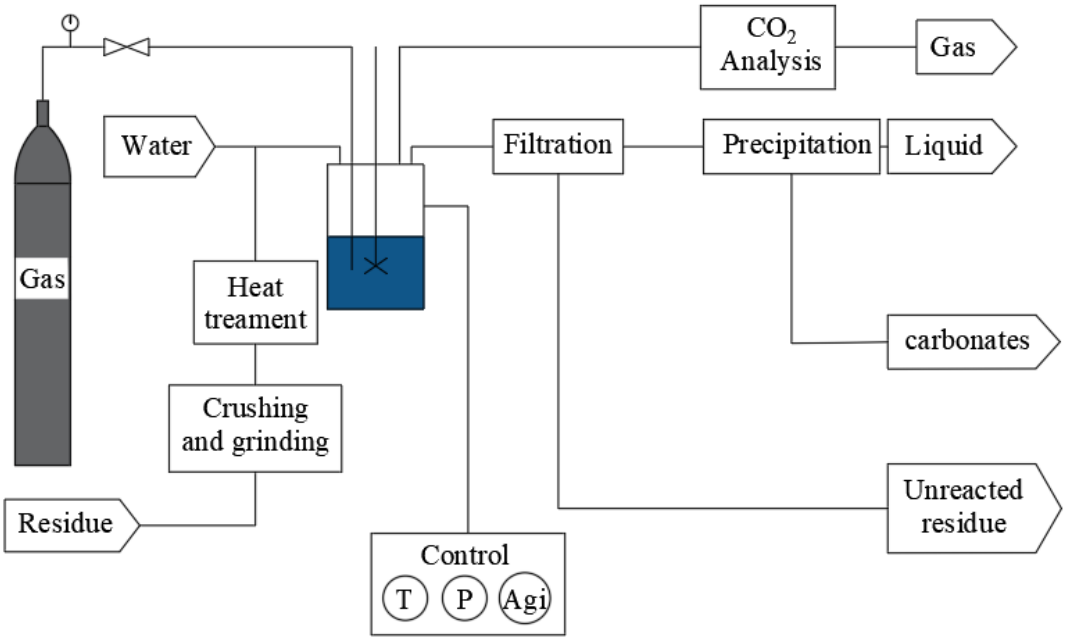

Fig. 15. Schematic diagram of set-up for water-CO_2 cooperative curing method [44]

Temperature, pressure and mixing speed were controlled during the experiment. The temperature was maintained at 22±3°C to maximize the solubility of CO_2 in the aqueous phase. The total pressure was maintained at 10.5 bar to maintain enough gas in the reactor. Upon completion, the gas was released. This gas was passed through the cold trap to condense the water and fill the sampling bag. Shaking was maintained during gas sampling. CO_2 concentration was measured using an infrared CO_2 analyzer. The rest of the reactor content went through filtration where the unreacted and reacted part was separated. The reacted part was separated into carbonates and the remaining liquid by precipitation.

In this method carbonation efficiency has increased compared to standard carbonation method. The reason for such a result is nano-bubbles of CO_2 that can be mixed with water and thus increase the efficiency of CO_2 curing [6].

2.2.5. Impact factors of forced carbonation

2.2.5.1. Effect of properties of the source material

The source material, in this case concrete used to prepare RCA, has a significant impact on the properties of RCA and carbonated RCA. In general, better properties of the source material result in better properties of carbonated RCA [14]. Thus, concrete of higher strength used for the preparation of RCA has a greater amount of hydration products that can be carbonated. This results in improvement of the RCA and RAC properties. Likewise, the high strength of the source material can lead to an increased density of adhered mortar on RCA and reduce the rate of CO_2 penetration and the carbonation efficiency of RCA. That assumption would not be useful for carbonation. That is why studies were conducted and the properties of RA and carbonated RA (CRA), which were prepared from concrete of different strengths, were compared.

Table 1. Properties of RA and CRA obtained from various strengths of concrete. Data from [45].

Parent material	Aggregate type	Apparent density (kg/m3)	Water absorption (%)
Concrete with C30 strength	RA	2639	6,58
	CRA	2619	5,25
Concrete with C45 strength	RA	2623	5,98
	CRA	2606	4,71
Concrete with C60 strength	RA	2620	5,95
	CRA	2670	4,61
Concrete with C80 strength	RA	2602	5,81
	CRA	2661	4,41

Table 1 shows the properties of RA and CRA obtained from different strengths of concrete. RA prepared from parent materials (concrete) with higher strengths show better properties after carbonation than those with lower strengths. In addition to the study shown in **Table 2** [45], two other studies have confirmed these results with various strengths of mortar [41; 46].

2.2.5.2. Effect of pretreatment methods

To achieve more thorough carbonation, the idea for the pretreatment of RA developed. It was found that pre-soaking in different solutions can improve CRA properties. The goal is to create an additional source of Ca^{2+} with these solutions that would result in an increase in carbonation percentage. Table 2 shows research results with $Ca(OH)_2$, $Ca(NO_3)_2$ and $CaCl_2$ pre-soaking. It is found that the CRA with

$Ca(OH)_2$ pre-soaking had the lowest powder content, and the CRA with $Ca(NO_3)_2$ pre-soaking had the lowest crushing value and water absorption, and the CRA with $CaCl_2$ pre-soaking had the highest compressive strength [47].

Table 2. Properties of CRA with various pre-treatment methods. Data from [47]

Pretreatment method	Crushing value (%)	Water absorption (%)	Compressive strength ratio
Without pretreatment	18	4,35	0,95
Presoak by $CaCl_2$	11	1,77	1,10
Presoak by $Ca(OH)_2$	13	1,65	1,04
Presoak by $Ca(NO_3)_2$	10	1,53	1,02

Another study [48] also showed that the properties of CRA with $Ca(OH)_2$ pre-soaking were better than those of the control group without $Ca(OH)_2$ pre-soaking. Also, a higher concentration of $Ca(OH)_2$ results in higher water absorption of CRA (see **Table 3**). There are two reasons that would explain this phenomenon:

(1) an insufficient amount of CO2 penetrated the RAs to react with all the free Ca2+ ions in the pore solution;
(2) the RAs became denser after carbonation, which hindered the further infiltration of CO_2 into them.

Regardless of the increase in water absorption, the increase in other factors was beneficial for increasing the compressive strength of concrete made of CRA. Therefore, a moderate CH concentration is desirable to improve CRA properties [48].

Table 3. Properties of CRA with various concentrations of $Ca(OH)_2$ in pre-treatment method. Data from [48].

Pretreatment method	Crushing value (%)	Water absorption (%)
Without pretreatment	19	3,75
0.01 mol/kg $Ca(OH)_2$	13	1,65
0.05 mol/kg $Ca(OH)_2$	14	2,00
0.25 mol/kg $Ca(OH)_2$	16	2,35

CRA properties were also tested by increasing the presoaking cycles with $Ca(OH)_2$ solution (see **Table 4**). As a result, an improvement in properties was obtained with each soaking cycle.

Table 4. Properties of CRA with increasing cycles of $Ca(OH)_2$ pretreatment. Data from [45].

Pretreatment method	Water absorption (%)
Without pretreatment	8,35
Presoak by $Ca(OH)_2$ - 1 cycle	6,52
Presoak by $Ca(OH)_2$ - 2 cycle	5,06
Presoak by $Ca(OH)_2$ - 3 cycle	4,29

2.2.5.3. Effect of particle size of RCA

Particle size plays a major role in the absorption of CO_2. The reduction of the particle size of RCA increases the specific surface area that is exposed to the absorption of CO_2. This results in an increase in CO_2 absorption and thus an increase in the rate of carbonation [49]. Which means when carbonated in the same conditions, smaller particles will absorb more CO_2 and the carbonation rate will be higher. Also, with the reduction of particles, there is an increase in the proportion of glued mortar, but also a decrease in its thickness, which allows easier CO_2 penetration, but also increases the amount of hydration products from mortar that can be easily carbonated.

Table 5. Water absorption of RA and CRA with various particle sizes. Data from [50–52].

	Aggregate types		Reference
Particle size (mm)	**RA**	**CRA**	
0,63-1,25	9,37	6,27	
1,25-2,5	7,79	5,57	[51]
2,5-5,0	7,12	5,25	
5,0-10,0	7,20	6,10	[50]
10,0-20,0	6,78	4,52	[52]

These results from **Table 5** were confirmed by various studies [49; 50; 53] that have come up with similar results. In all studies, it was confirmed that reducing the particle size increased the carbonation effect by showing better properties such as density and water absorption with smaller particle sizes [6].

For example, Xuan et al. [50] for RA with particle size of 5 mm got a value of 2,15% of CO_2 absorption, and with particle size of 5 to 10 mm only 0.81%.

2.2.5.4. Effect of CO_2 concentration

CO_2 concentration is also a key factor for concrete carbonation. Global average atmospheric carbon dioxide was 417.06 parts per million ("ppm" for short) in 2022, setting a new record high [54]. By increasing the concentration of CO_2 in the atmosphere the concentration of CO_2 in carbon rainwater increases. With the entry of such rainwater into concrete, the concentration of carbon dioxide in the pores of concrete increases. Consequently, the carbonation process is enhanced. Which means, by simply increasing the concentration of carbon dioxide in concrete, the desired efficiency of carbonation can be achieved. When it comes to carbonation of recycled concrete, there is an optimal value of CO_2 concentration [6]. When the CO_2 concentration is below the optimal value, the carbonation efficiency can be increased by further increasing the CO_2 concentration. Although, when the concentration exceeds this value, no further acceleration of carbonation will occur. Different studies [55; 56] showed that increased CO_2 concentration has a lower impact on concrete carbonation percentages when the CO_2 concentration is greater than 20%. Fang et al. [57] have shown that the percentage of carbonation RA with a concentration of CO_2 of 100% was only 9.1% higher than that with a CO_2 concentration of 10% after 24 hours of carbonation.

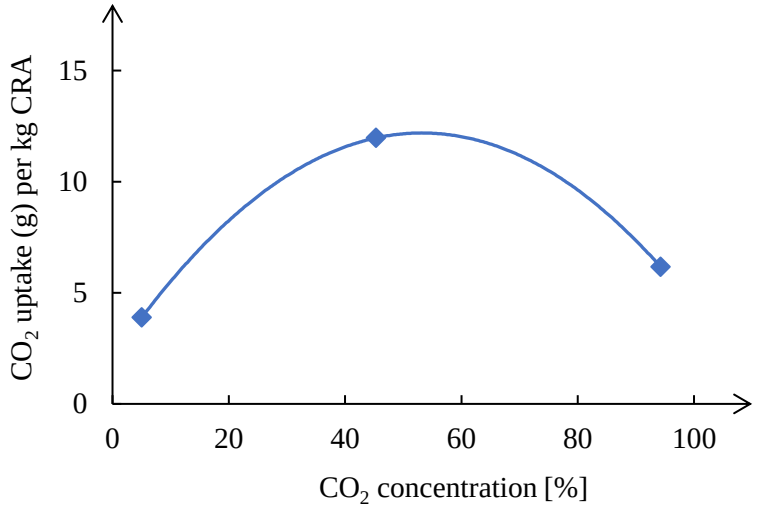

Fig. 16. Effect of CO_2 concentration on the carbonation efficiency of CRA. Data from [6].

The reason for these results may lie in the fact that the percentage of carbonation is controlled by the rate of dissolution of hydration products. Produced $CaCO_3$ can prevent the penetration of CO_2 into the recycled concrete aggregate [56]. This means that excessive concentration of CO_2 gas will not achieve an increase in the percentage of carbonation of RCA. A high concentration of CO_2 results in a dense

microstructure of cement materials and thus reduces CO_2 diffusion, a CO_2 concentration of up to approximately 50% often leads to a relatively high carbonization efficiency [58]. **Fig. 16** shows the effect of CO_2 concentration on RA carbonization efficiency, and the results emphasize that the optimal concentration of CO_2 used in CO_2 curing RA is 40-60% [6].

2.2.5.5. Effect of relative humidity and water content

Carbonation is a process that progresses more rapidly when concrete is exposed to alternating wetting and drying. The more concrete is soaked, the more water or rainwater enters the pores of the concrete. Drying is most pronounced on the concrete surface because these surfaces are exposed to the sun. Due to this connection between drying and carbonation, the greatest damage to the structures is always on the southwest side of the structures, and the smallest on the north side of the structures [5]. According to this knowledge of natural exposure, generally water and humidity are important factors that affect the carbonation of concrete.

Although expected the increase in relative humidity (RH) is not linearly related to the increase in carbonation rate. In the case of high RH, CO_2 diffusion into the concrete slows down. The reason is in the capillary condensation of water in the pores. In contrast, low RH slows down the dissolution of CO_2 and the dissolution of hydrates due to the drying of the capillary pores. There is a certain interval for optimal carbonation. Liang et al. [6] have shown that the interval is from 40% to 70%. Kabashi et al. [59] have shown in their study an interval from 50% to 90% (see **Fig. 17**). Which means, if:

- RH < 50 %, CO_2 cannot be dissolved,
- RH > 90%, CO_2 cannot enter the concrete because the diffusion of carbon dioxide is inhibited by the water that fills the pores of the concrete.

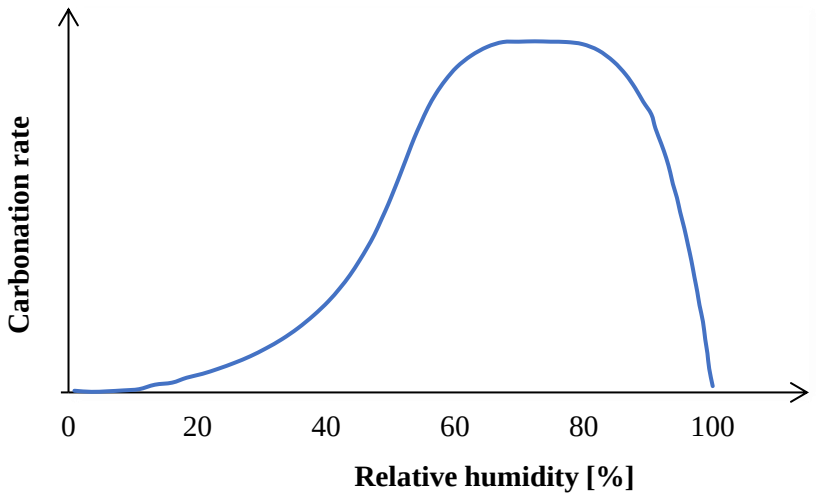

Fig. 17. Schematic representation of the rate of carbonation of concrete depending on the relative humidity of the environment Data from [59].

This is the range where the necessary water for carbonation is present, but the pores are not filled to inhibit the diffusion of CO_2. Also, optimal RH has led to rapid carbonation along with the production of amorphous calcium carbonate and monohydrocalcyte, while relatively low RH has led to slower carbonation with the production of portlandite and vaterite in cement materials [60].

The water content of RA plays a leading role in its carbonation efficiency because water dissolves the CO_2 and Ca^{2+} gas contained in RA and promotes the carbonation reaction [6]. Water content is closely related to RH, so there is an optimal water content in RA. When the water content of RA falls below the optimum moisture content, insufficient water participates in the carbonation reaction, while excess water content also hinders the penetration of CO_2 and reduces the carbonation efficiency of RA. Pan et al. [48] found that carbonated RA water absorption decreases when RA water content increases from 2.5% to 5.0%, while carbonated RA water absorption increases when RA water content reaches 7.5%. Zhan et al. [61] suggested that the optimal water content of RA is in the range of 4% to 6.5%.

2.2.5.6. Effect of temperature

Temperature has a complicated effect on carbonation. It can result in positive and negative effects on physical properties. Increased temperature generally leads to an improvement in physical properties. With a higher temperature, the leaching of Ca^{2+} ions from the silicates improves. So with an increase in the curing temperature from 25°C to 75°C, a decrease in w/b factor from 0.95 to 0.93 was observed, as well as an increase in compressive strength [62]. A similar result was obtained Zhan et al. [61], rates of carbonation of RA increased from 52.6 % to 55.0 % when temperatures ranged from 20°C to 80°C.

However, relatively high temperatures can have a counter effect. There may be an increase in the ratio of loss of consistency and thus a shortening of the hardening time. Chen et al. [63] reported that the strength at 28 d declined from 11.9 MPa to 11.4 MPa as the temperature increased from 25°C to 50°C, then increased to 12.1 MPa when the temperature further increased to 75°C. The reason is the reduction of solubility of CO2, leading to a high pH of water and a lower dissolution rate of Ca^{2+} [47]. From all the above, it can be concluded that the influence of the positive in relation to the negative effect is unpredictable and leads to unpredictable results.

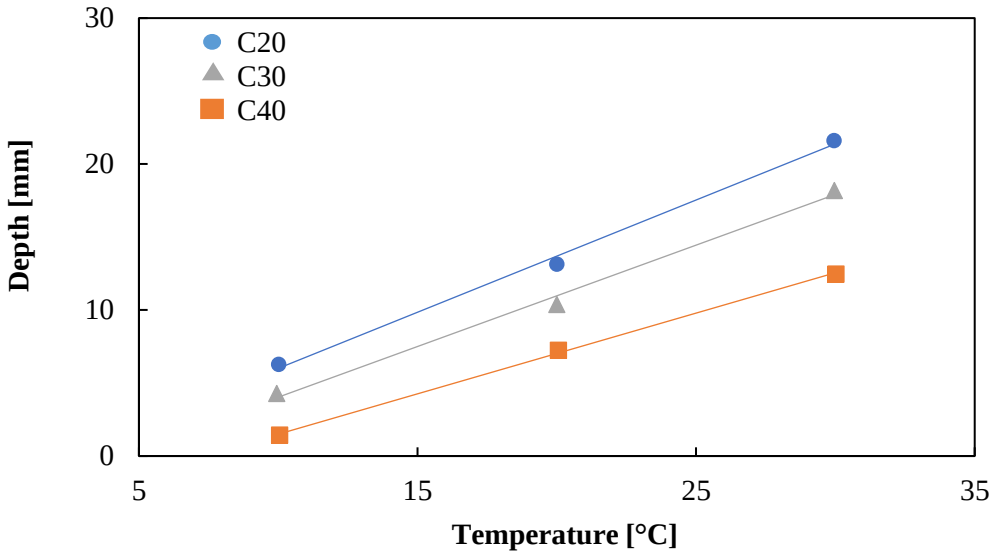

Fig. 18. Relation curve between the carbonation depth of concrete and temperature. Data from [63].

On **Fig. 18** are shown relation curves for different concrete mixtures between concrete carbonation depth and temperature [63]. Relative humidity was maintained at 70% and CO_2 concentration at 20%. It is clearly visible that with the increase in temperature there is an increase in the carbonation depth of concrete at temperatures up to 30 °C. Which means that carbonation reaction should be maintained at relative low temperature to form the more stable calcite [6].

2.2.5.7. Effect of time

The carbonation percentage increases with the increase of CO_2 curing time until the moment when RA is completely carbonated [6]. The greatest growth is achieved within the first two hours of carbonation, and then it decreases. Zhan et al. [53] reported that carbonation percentage on samples with a particle size of 10 to 14 mm after first 2 hours was 25.06%, and in the next two there was an increase of only 3.41%.

Fig. 19 shows the influence of CO_2 curing on the improvement in percentage of carbonation. In addition to the carbonation percentage, the apparent density increases and the water absorption and crushing value of carbonated RCA decreases [64]. These physical properties, as well as the carbonation percentage, achieve the greatest improvement within the first 2 hours. It is important to note that RA of different particle sizes will not have the same effect of carbonation cycles. With smaller particle sizes, the effect will be more obvious [41].

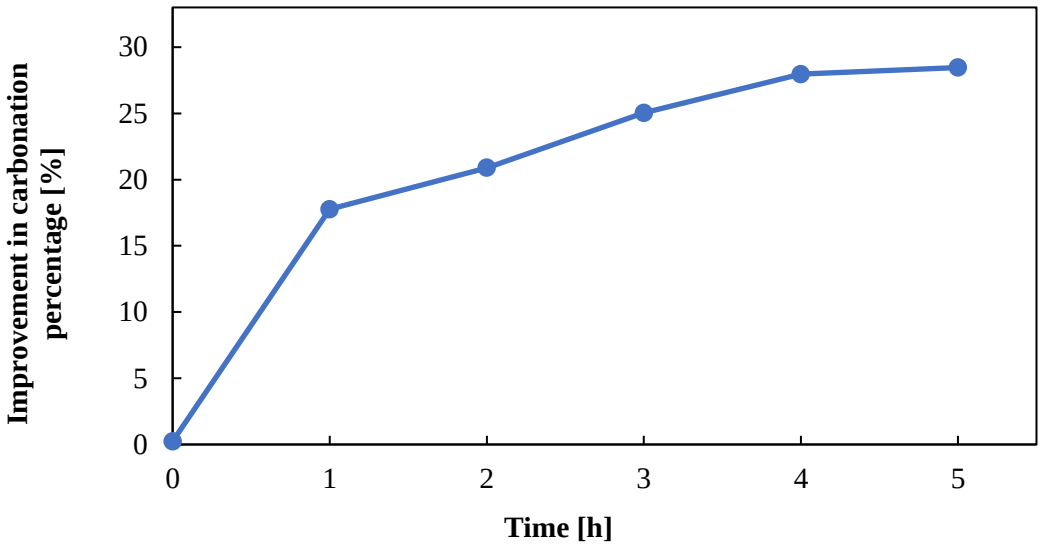

Fig. 19. Effects of CO_2 curing time on the improvement in carbonation percentage. Data from [64].

2.2.5.8. Effect of porosity and permeability

Porosity is the amount of space in the material concrete, and permeability is material's ability to pass liquids or gasses [5]. That are factors related to the structure of concrete. These two related properties have a close relationship with the water-binder ratio (w/b). The water binding factor is the volume ratio and can be expressed as the weight ratio of the components, as shown in Eq. (12).

$$w/b = \upsilon_w/\upsilon_b \cdot \frac{\rho_w}{\rho_b} \tag{12}$$

The members of υ_w and υ_b represent the volume concentrations of water and binders, and ρ_w and ρ_b densities. *W/b* directly determines the pore system of concrete and the degree of hydration. The higher w/b ratio, the higher permeability of the concrete. Consequently, a considerable amount of free water remains in the concrete after hydration is complete and increases the carbonation. Conversely, after the end of carbonation, the porosity of the hardened paste decreases [5]. The cause is the deposition of limestone in the concrete, which occupies a place in the pores of concrete. It reduces the permeability and at the same time reduces the access of CO_2 to the interior of the concrete, as described in chapter 2.2.1. The result is a decrease in the dissolution of $Ca(OH)_2$. In this case, higher density of concretes is preferred [5]. Higher concrete density reduces permeability and porosity, which delays the effect of carbonation. Also, various studies have shown that concrete made from RA that has undergone the carbonization process has higher water resistance and lower gas permeability [28]. The reason for this observation was that the RA carbonization treatment eliminated larger pores larger than 200 nm in size and reduced the amounts of medium pores in size 50–200 nm, which led to a decrease in the porosity of RA [6].

2.2.6. CO_2 uptake

During the entire lifetime of a concrete structure, only a certain amount of CO_2 gas can be absorbed by the carbonization reaction of the structural concrete. In general, the CO_2 uptake rate and amount increase with decreasing RCA particle size. As such, the amount of CO_2 uptake of RCA with a particle size of 5-10 mm is approximately 50% greater than that with a particle size of 14-20 mm [58]; moreover, the amount of absorbed CO_2 in RCA with an average particle size of 1.18 mm is about 100% higher than that with an average particle size of 7.5 mm [57], as shown on **Fig. 20**

This observation is attributed to the fact that RCA with a smaller particle size results in more cement participating in the carbonation reaction [68]. In addition, pressurized CO_2 curing and presoak treatment can further increase CO_2 uptake in RCA [45; 56].

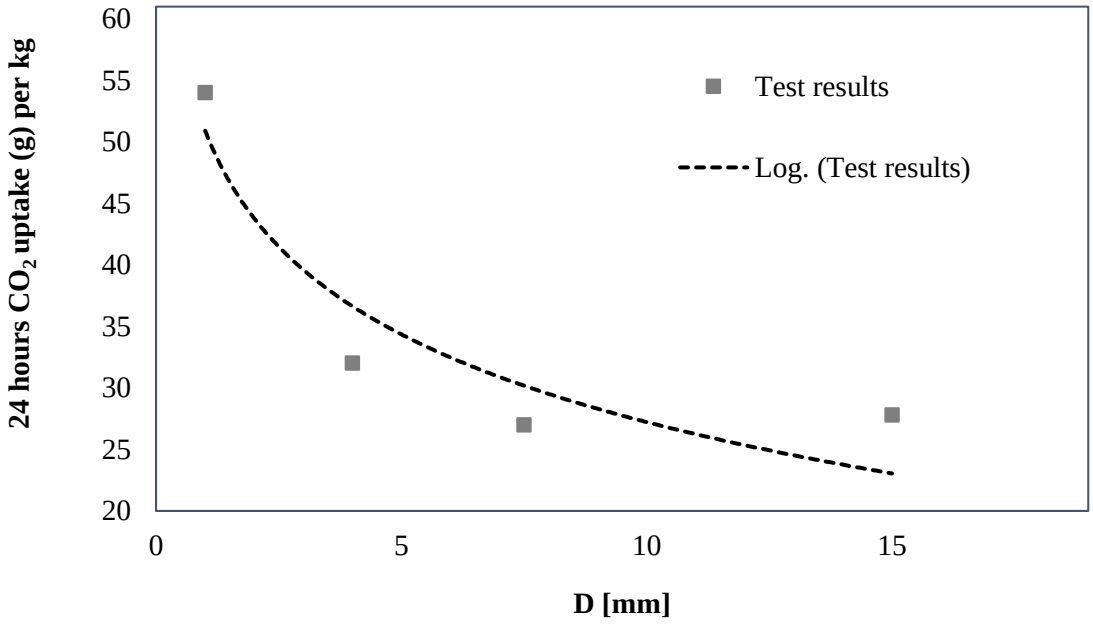

Fig. 20. Effect of particle size of RCAs on CO_2 uptake rate. Data from [57].

3. Experimental program

3.1. Preparation of RCA

To obtain RCA, precast concrete slabs from the tramway infrastructure of Vienna were used for research purpose. The owner of the slabs is the Vienna public transport company Wiener Linien (see **Fig. 21**). The slabs with an age between 10 and 20 years were removed (most of them around 15 years). In **Table 6**. the exposure conditions for the slabs are shown.

Table 6. Properties of recycled concrete during production (according to Wiener Linien)

Type of concrete:	**C50/60/B7/XM2/GK11**	
	C50/60	Compressive strength
	B7	XC4/XD3/XF4/XA1L/SB
	XC4	Exposure class (hydraulic structures and dense concrete structures exposed to high water pressure, water pressure > 10 m).
	XD3	Components that are exposed to increased exposure to chloride, e.g. parking decks, road surfaces, salt storage.
	XF4	High water saturation with de-icing agent. Vertical and horizontal concrete surfaces exposed to spray water containing de-icing agent (zone up to approx. 3 m above the road) and are exposed to frost.
	XA1L	Mildly chemically aggressive environment
	SB	Exposed concrete
		Mean centric tensile strength at least 4.1 N/mm^2 Equivalent resistance to frost class XF4 according to ÖNORM 23303.
	XM2	Concrete corrosion due to wear and tear according to ÖNORM B4710-1 (ÖNORM EN14157 (Böhme dry) and ÖNORM B3303 section 7.5)
	GK11	Maximum grain size
The strength at handover must be at least 28N/mm^2.		
The abrasion loss < = 15 cm^3/50 cm^2.		
The concrete cover should be 4.0 cm for the top and 2.5 cm for the bottom.		

Fig. 21. On the left are panels in the usage phase in the tramway infrastructure, and on the right are the same panels after deconstruction ready for recycling

All RC is crushed in the jaw crusher for concrete (see **Fig. 22**).

Fig. 22. Used jaw crusher with the swing jaw fixed at the upper position

For crushing, setting B was used to obtain a grading curve as shown in the **Fig. 23**.

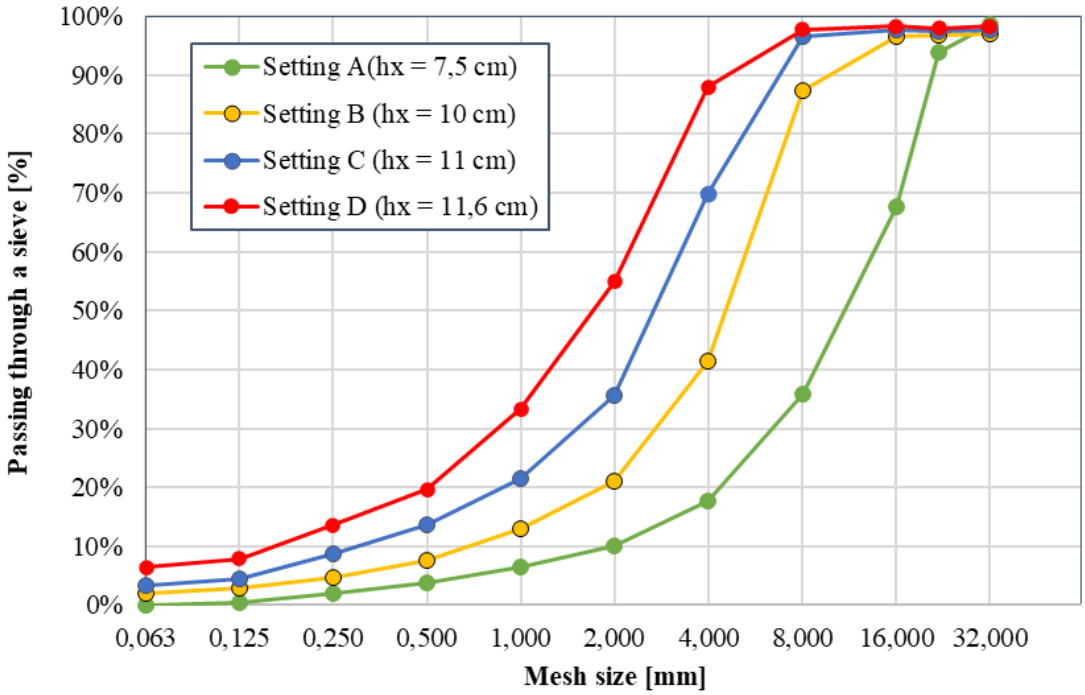

Fig. 23. Grading curves

Then, the material was sieved using a vibrating sieve machine (see **Fig. 24**). The duration of the vibration was about 15 minutes. Then the material from each drawer of the machine was carefully separated.

Fig. 24. Vibrating sieve machine

The following fractions were obtained: 0-0.25 mm, 0.25–0.5 mm, 0.5-1 mm, 1-2 mm, 2-4 mm, 4-8 mm, 8-16 mm, 16-22 mm (see

Fig. 25).

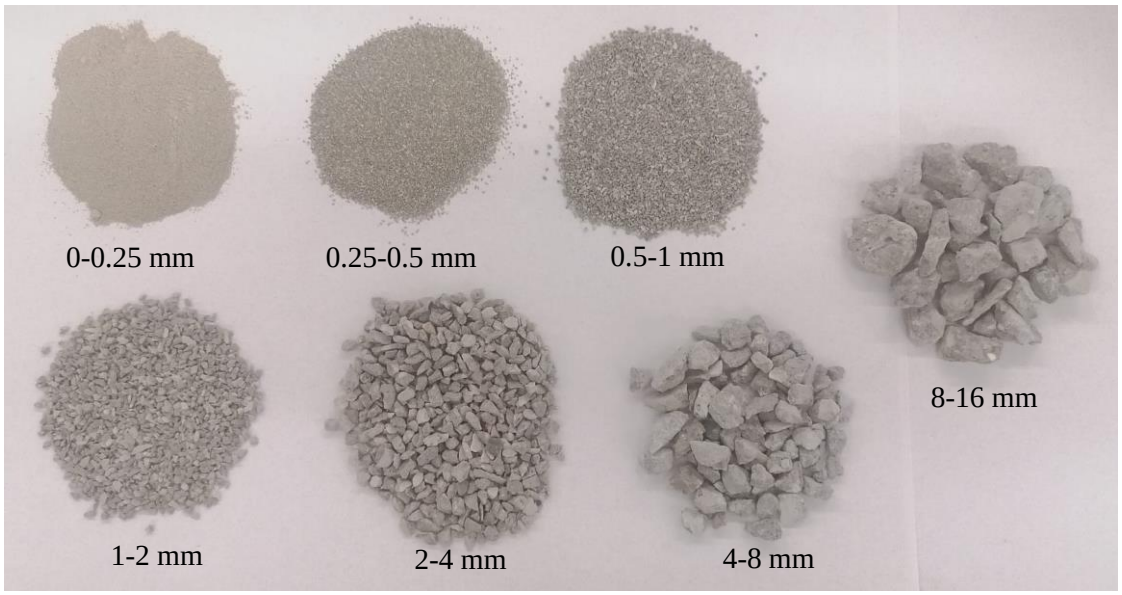

Fig. 25. Fractions of tested RCA

After crushing and sieving, the mass of RCA and the moisture content were measured and the phenolphthalein test was performed. The same measurements were made after the CO_2 curing in order to compare the properties of RCA before and after CO_2 curing. After the measurement, and before CO_2 curing, the RCA was placed in polypropylene boxes adapted to the passage of gas through them. A filter material was placed on the bottom for coarse RCA and on the edges for aggregates of fine RCA (see **Fig. 26** and **Fig. 27**). The role of the filter material was to prevent aggregate loss during transfer from the CO_2 curing site to the test site. Two experiments were performed for each group.

Fig. 26. Box with filter material

Fig. 27. RCA prepared for CO_2 curing.

The amount of material inside one box was approximately 3 kg to achieve easier penetration of CO_2 into all RCA. In each experiment, 4 boxes of RCA (~12 kg) were placed according to the scheme shown on (see **Fig. 28**).

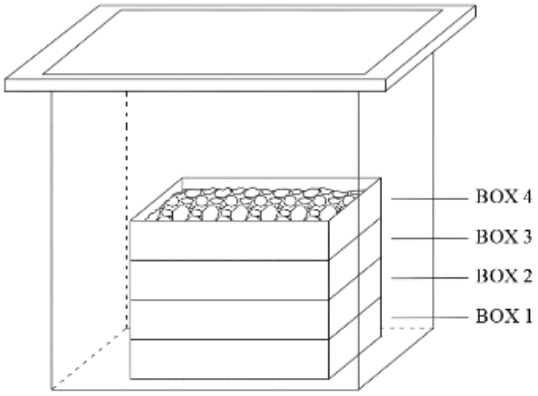

Fig. 28. Schematic representation of the order of stacking the boxes

3.2. CO_2 curing process

For CO2 curing process a combination of standard carbonation method and flow-through CO2 curing method was used at the laboratory of the Institute of Structural Engineering, Vienna (IKI-lab) (see chapter 2.2.4.1. and 2.2.4.3.). An airtight chamber was made for testing. Inside the chamber were installed three sensors. Schematic representation of sensor arrangement as well as the equipment used for CO_2 curing are shown on **Fig. 29** and **Fig. 30**.

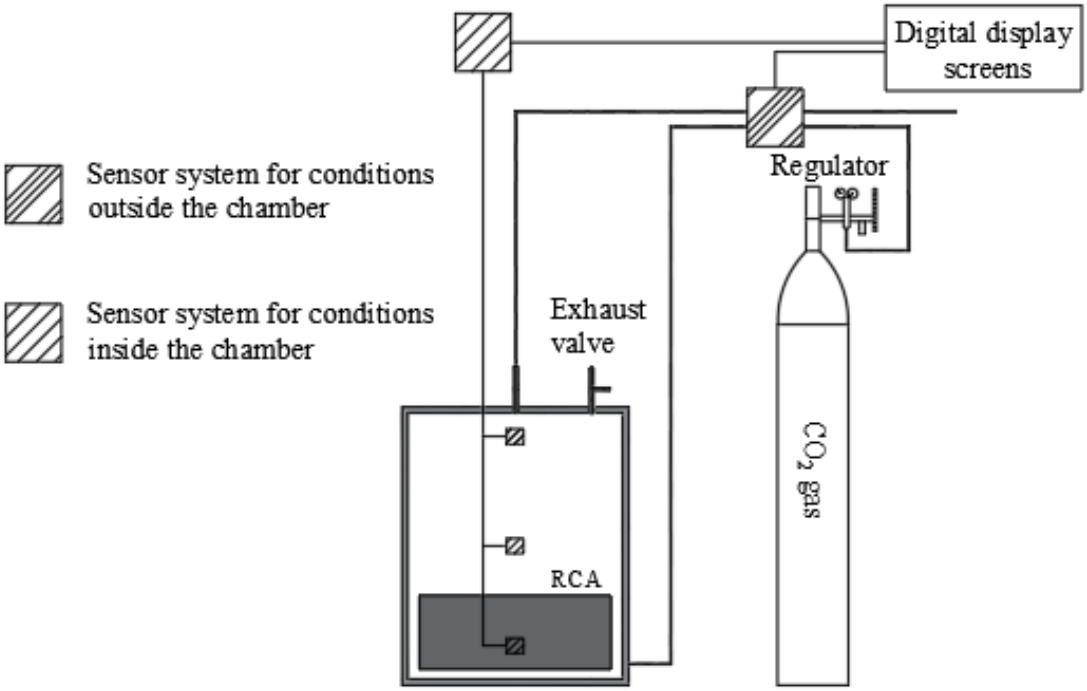

Fig. 29. Schematic representation of equipment used for CO_2 curing

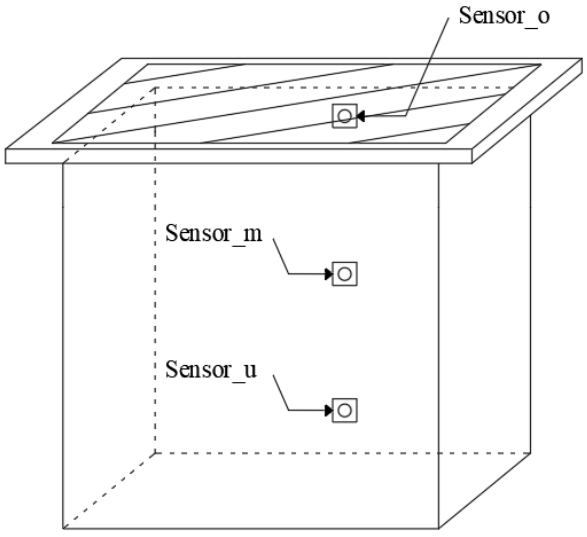

Fig. 30. Schematic representation of sensor arrangement inside chamber

The equipment used for CO_2 curing as well as the appearance of the sensor in reality is given on **Fig. 31** and **Fig. 32**.

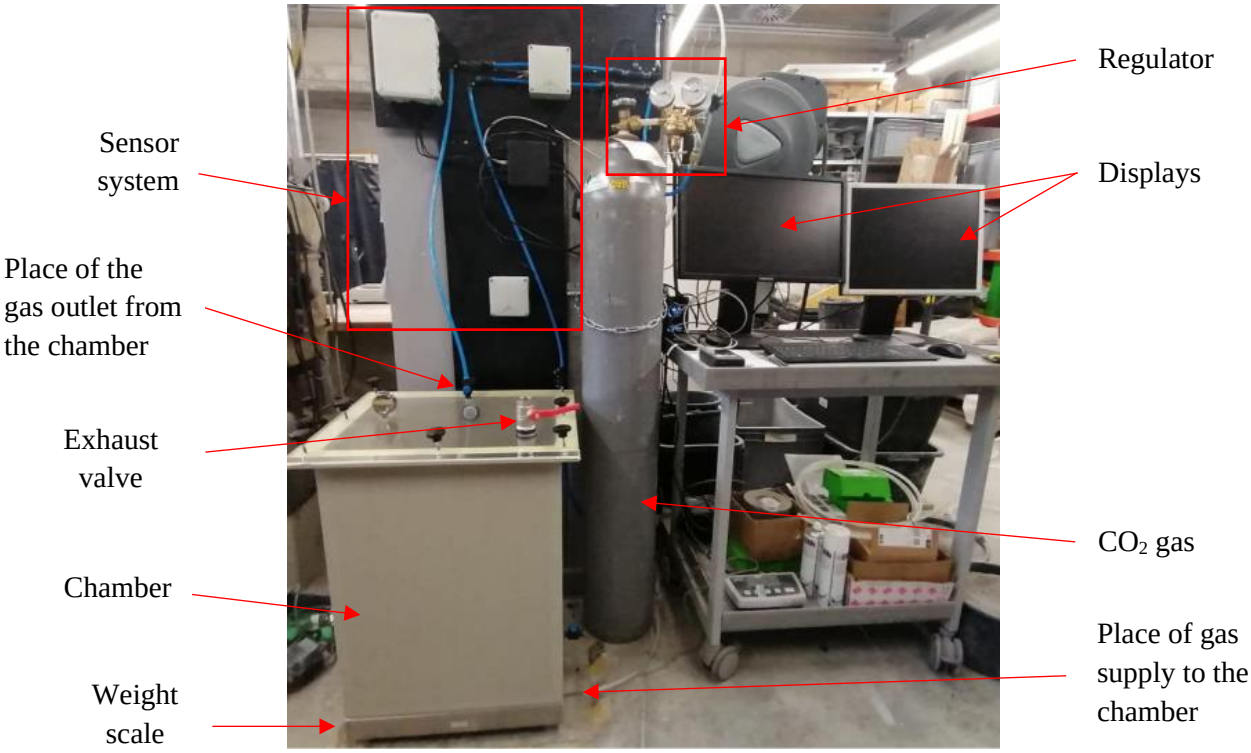

Fig. 31. Equipment at the IKI- laboratory used for CO_2 curing

In addition to inside, there were also sensors placed outside the chamber that monitored the flow of incoming and outgoing gas. Also, the chamber was placed on a weight scale that continuously measured changes in mass. All sensors, as well as the weight scale, were connected with display to monitor mass, CO_2 concentration, gas flow, relative humidity and temperature.

Fig. 32. Sensors inside chamber

The experiments began by placing boxes with RCA inside the chamber. Then the tank was closed and CO_2 gas was released. At the beginning of the experiment, the gas flow inside the chamber was kept high, ~7 slm (standard liter per minute), until a CO_2 concentration of approximately 100% was reached on the sensors inside the chamber. After that, the gas flow was reduced to ~ 1 slm to maintain the CO_2 concentration at 100% on all sensors until the end of the experiment. At the end of the test, the gas was immediately released through the exhausting valve and the RCA samples were taken out.

The sampling rate of CO_2 concentration and gas flow was 1 Hz, for relative humidity was 2 Hz and for mass 3 Hz. The software used during the test to obtain the values read by the sensors is SEK-Control Center 1.39.1.Name of the sensor for relative humidity is SHTC3_RH, for CO2 concentration is STC31_CO2, for input gas stream is Gasflow_in and for output gas stream is Gasflow_out. All these sensors also measured the temperature. The duration of the experiments was 4, 8 and 12 hours depending on the RCA fraction (see **Table 7**). The temperature in the chamber was 25±3°C. CO_2 was maintained at ambient pressure.

Table 7. Duration of the test due to fraction of RCA

Name of experiment	Fraction	Duration
WL20 WL26	8-16 mm	12 hours
WL13 WL15	4-8 mm	12 hours
WL16 WL17	2-4 mm	12 hours
WL18 WL21	1-2 mm	8 hours
WL24 WL27	0,5-1 mm	8 hours
WL23 WL25	0,25-0,5 mm	4 hours
WL19 WL22	0-0,25 mm	4 hours

3.3. Testing

3.3.1. Determination of the moisture content of the RCA

Moisture content (*MC*), along with the porosity, is the main characteristic of an RCA for this type of RCA testing. *MC* was measured by a simple test during which RCA was exposed to drying cycles in the microwave until the mass of RCA became constant (see **Fig. 33**). The first drying cycle lasted 8 minutes, and each subsequent drying cycle lasted 1.5 minutes. In experiments where multiple RCA boxes were tested simultaneously, the mass of all boxes was considered together. Therefore, the sample for MC was prepared in such a way that an approximately equal amount of RCA was taken from each box and mixed. *MC* (in %) was determined by Eq. (13):

$$MC = \frac{m_{wet} - m_{dried}}{m_{dried}} \times 100 \ [\%] \tag{13}$$

where m_{wet} is the mass of the RCA before drying and m_{dried} is the mass of the RCA after drying.

Fig. 33. Mass measurement during moisture content testing

3.3.2. Determination of carbonation

Determination of carbonation was carried out by phenolphthalein test before and after CO_2 curing in order to determine the condition of the samples (whether carbonation was performed or not). This test is for visual assessment only. It is not possible to determine the quantity of the carbonated part and it only shows the occurrence of carbonation on the surface of the CRA. For the purposes of the test, a

solution of phenolphthalein indicator according to the Austrian standard ÖNORM EN 14630:2006 was used, as described in chapter 2.2.3. The solution was applied by spraying on the sample until uniform saturation with the phenolphthalein solution was achieved over the entire surface of the sample. The purple-pink part of the sample was classified as the non-carbonated part, and the colorless part as the carbonated part of the sample.

Also, the thickness of the carbonated layer was measured on one group of samples. Carbonated RCA is cut in half and sprayed with phenolphthalein solution. Then the highest value of the depth of the carbonated layer $d_{x,max}$ was measured with a digital caliper and the depth of carbonated front $d_{x,mean\ WAS}$ determined.

3.3.3. Determination of CO_2 uptake by the RCA

To determine the CO_2 uptake of RCA, mass monitoring was carried out to identify the mass gain ($\Delta m_{balance}$) inside chamber during the CO_2 curing. Also, mass gain of RCA (Δm_{RCA}) was measured and gas change (Δm_{gas}) was calculated. The gas change was calculated by completely filling the chamber with CO_2 gas, and the control was calculated using the volume of the chamber and the difference in the density of air and CO_2 gas. In addition, the difference in water content, i.e. the mass of water in RCA (Δm_w), before and after forced carbonation was calculated using *MC* values. Based on all the above values, formulas for ΔM_{car_1} and ΔM_{car_2} are arrived at.

$$\Delta M_{car_1} = \Delta m_{balance} - \Delta m_{gas} + \Delta m_w \quad (14)$$

$$\Delta M_{car_2} = \Delta m_{RCA} + \Delta m_w \quad (15)$$

ΔM_{car_1} and ΔM_{car_2} represent the maximum experimental uptake of CO_2 according to which the increase in carbonization mass is calculated, as shown in Eq. (14) and (15). Next, CO_2 uptake is calculated as a ratio of ΔM_{car_2} and initial mass of RCA ($m\emptyset$) as shown in Eq. (16).

$$CO_{2_{uptake}} = \frac{\Delta M_{car_2}}{m_{\emptyset}} \quad (16)$$

3.4. Results

All data obtained during the test is presented in detail in the appendices at the end of this Master thesis, including the results of mass, relative humidity, phenolphthalein test and diagrams for each experiment based on the obtained data. Labels inside the graphs _u, _m, _o, _in and _out refer to the location of the sensor that recorded the data. Given that the tests were carried out in the laboratory of the Institute of Structures at BOKU University in Vienna, German names for locations were used, such as “u” means bottom (ger. unten), “m” means middle (ger. mitten), “o” means above (ger. oben), as shown on . The labels “in” and “out” refer to the sensors that recorded data in the input and output gas streams.

3.4.1. Visual evaluation of carbonation using the phenolphthalein test

By conducting a phenolphthalein test after the CO_2 curing process, it was determined whether and to what extent carbonation of RCA occurred. Thus, it was observed that in the experiments with the RCA fraction of 8-16 mm, complete carbonation did not occur, especially in the lowest box in the chamber (see Appendix). For this reason, it is necessary to extend the CO_2 curing time for this RCA fraction. In fractions 4-8, 2-4 and 1-2 mm, complete carbonation at the surface occurred in all boxes except for the box at the bottom of the chamber. There, purple color can be seen on individual grains, which indicate the absence of carbonation as shown on **Fig. 34**.

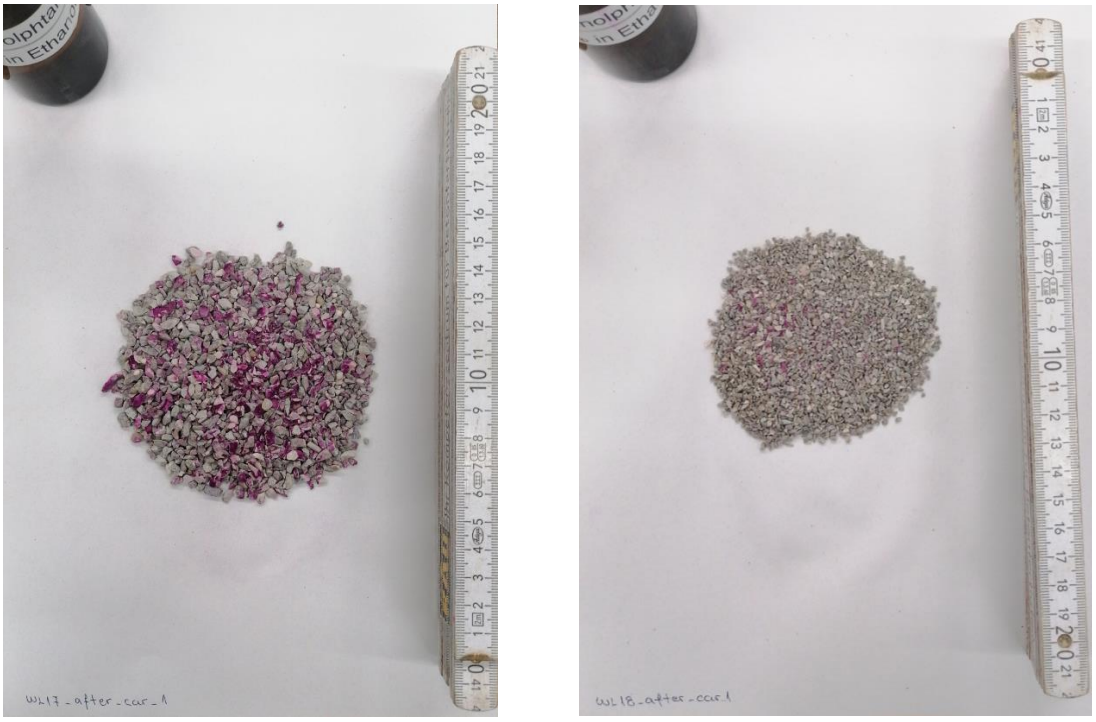

Fig. 34. Phenolphthalein test results for boxes in the bottom of the chamber for experiments WL17 (left) and WL18 (right).

The purple color, i.e., the non-carbonized part, was more pronounced the higher the fraction. Other fractions of RCA 0.5-1, 0.25-0.5 and 0-0.25 mm did not show a color change, indicating that complete carbonation of RCA surface had occurred.

3.4.2. Depth of carbonation layer

RCA which is cured with CO_2 for 23 hours was used for this test. The depths of the carbonate layers for 4 grains randomly taken from the sample are shown in **Table 8.** Thickness of carbonated layers of RCA. This means that the average thickness of the carbonated layer for RCA that was CO_2 cured for 23 hours is about 0.6 mm. Grain size of RCA was from 18 to 22 mm. **Fig. 35** shows carbonated layers (colorless parts of RCA) on cut off pieces of RCA.

Table 8. Thickness of carbonated layers of RCA

No.	**Thickness of layer (mm)** **(**Mean value)
1	0.87
2	0.46
3	0.93
4	0.12

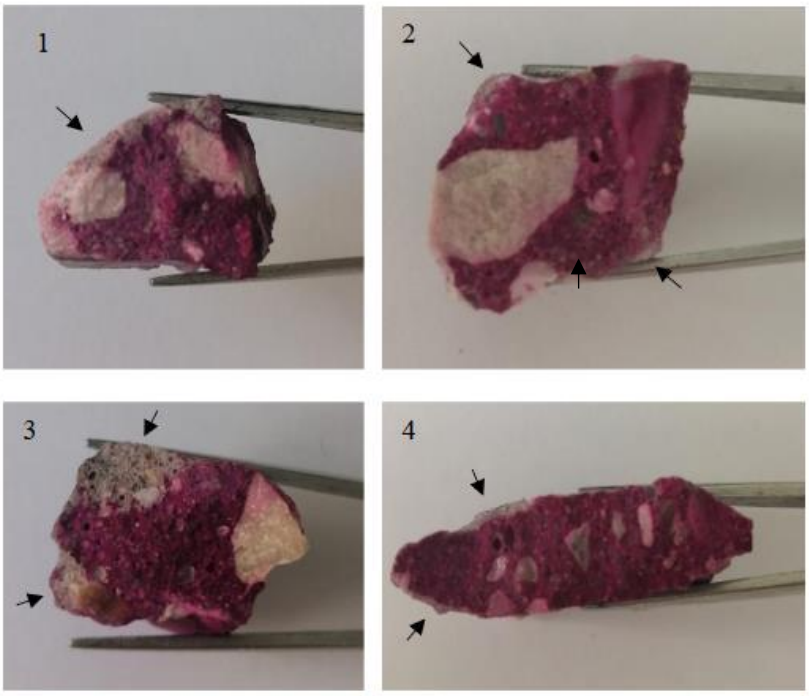

Fig. 35. Carbonated layers on cut off pieces of RCA

3.4.3. Impact of forced carbonation on the mass change of RCA

If we consider the average value of the change in the RCA mass in relation to the RCA grain size, this results in the graph shown on **Fig. 36**. After the CO_2 curing process there was an increase in the RCA mass. Also, by reducing the grain size of the RCA, there was a greater increase in the mass of the RCA. Therefore, the largest increase was recorded for the fraction of 0–0.25 mm (2.7%), and the smallest for the fraction of 8–16 mm (0.3%). Likewise, the biggest difference between individual fractions was recorded between the 0-0.25 mm and 0.25-0.5 mm fractions (1.3%).

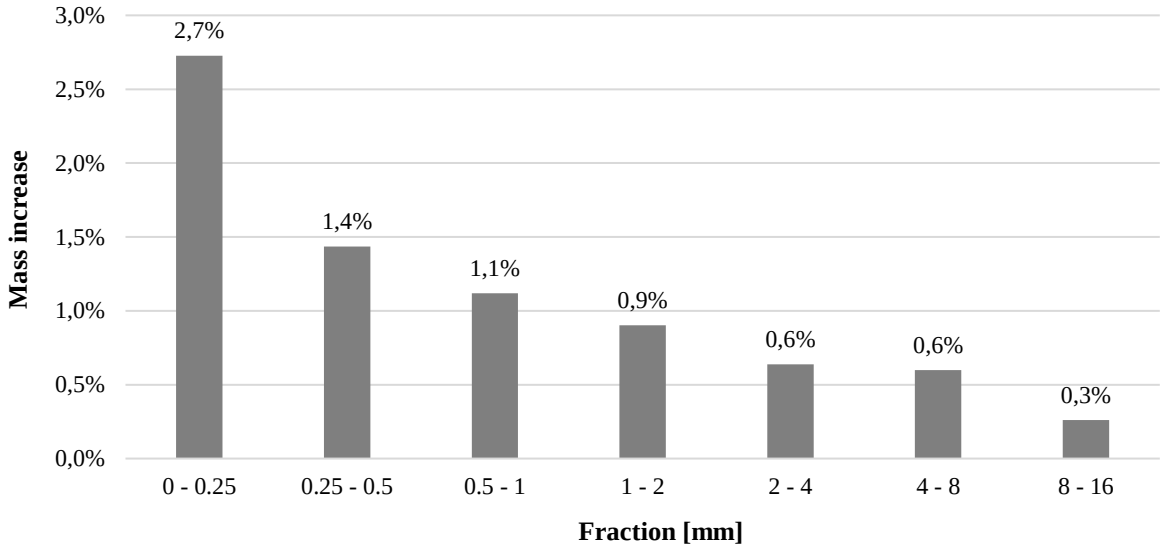

Fig. 36. RCA mass change due to fraction of RCA

3.4.4. Impact of forced carbonation on temperature of RCA

During CO_2 curing, the temperature on the sensors inside the chamber showed a maximum of 25°C, except for fractions 0-0.25 and 0.25-0.5 mm. For these fractions, the temperature was between 25 and 30°C. After CO_2 curing, it was noticed that the RCA was heated. The increase in temperature was especially pronounced in the central part of the boxes, where the CO_2 gas flow is greatest. Also, the greatest heating of the RCA was recorded in the lowest box in the chamber, which corresponds to the recorded temperature values on the sensors inside the chamber (Temp_u). **Fig. 37** shows a diagram of the temperature change during CO_2 curing for the fraction of 4-8 mm where RCA heating did not occur, and on **Fig. 38** for the fraction of 0-0.25 mm where RCA heating occurred.

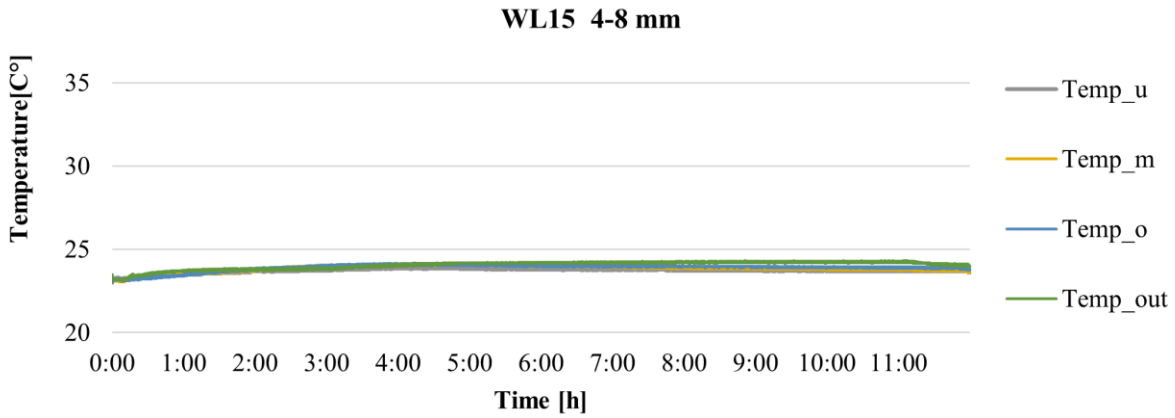

Fig. 37. Temperature change over time for experiment WL15.

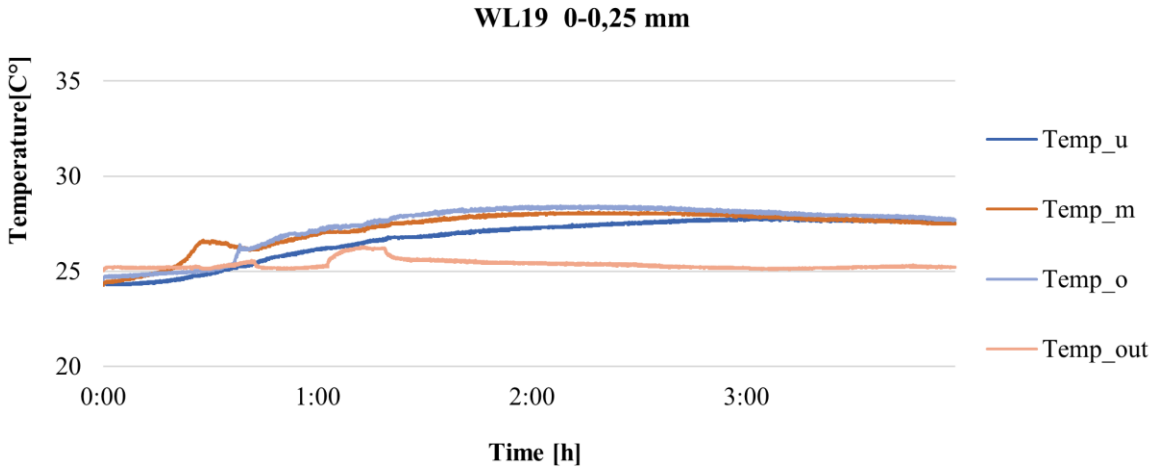

Fig. 38. Temperature change over time for experiment WL19.

Fine aggregate has a larger specific surface area, so a larger surface reacts with CO_2. This is also confirmed by the higher gas consumption in experiments with smaller RCA grains. More precisely, it took a longer time to reach a CO_2 concentration of 100% inside the chamber.

Lekakh et al. [62] claim that an increase in temperature leads to an increase in the melting of Ca^{2+} ions from silicates. This assumption coincides with the obtained results, because in the experiments where the increase in temperature inside the chamber was recorded, the highest CO_2 uptake was recorded at the same time. Likewise, the increase in temperature inside the chamber for the smallest RCA grains led to the greatest increase in RCA mass (2.7%).

The reason why the temperature inside the chamber increased in the first place may be hidden behind the thermoactivated effect caused by the collision of so many small aggregate particles reacting with CO_2 and releasing energy as the reactions take place.

This increase in temperature had no effect on the relative humidity of the RCA. Both in the case of fine and coarse grain of RCA, the difference in moisture content before and after CO_2 curing was ~0.35%. At such low temperature values, there was no negative effect of temperature by increasing the pH of water and decreasing the dissolution rate of Ca^{2+}, which confirms the statements of Zhan et al. [61].

3.4.5. Impact of forced carbonation on relative humidity inside chamber

The behavior of the relative humidity inside the chamber was very different for each individual experiment and it is easiest to compare them if they are divided into 2 cases depending on the part of the chamber.

In the upper and middle part of the chamber (labels RH_o and RH_m), relative humidity would generally drop at the very beginning until the CO_2 concentration inside the chamber stabilized. Then the RH curve is continuous in a slight increase or decrease until the end of the experiment (see **Fig. 39**). The only significant deviation occurred in the WL20 and WL26 (8-16 mm) experiments, where a relative humidity of approximately 100% was recorded at the beginning of the experiment. After that, there was a sharp drop below 60%. By the end of the experiments, the value did not reach a value higher than 60% (see **Fig. 40** and **Fig. 41**). This experiment showed slightly higher values of mass increase than RCA and CO_2 uptake (see Appendix 3).

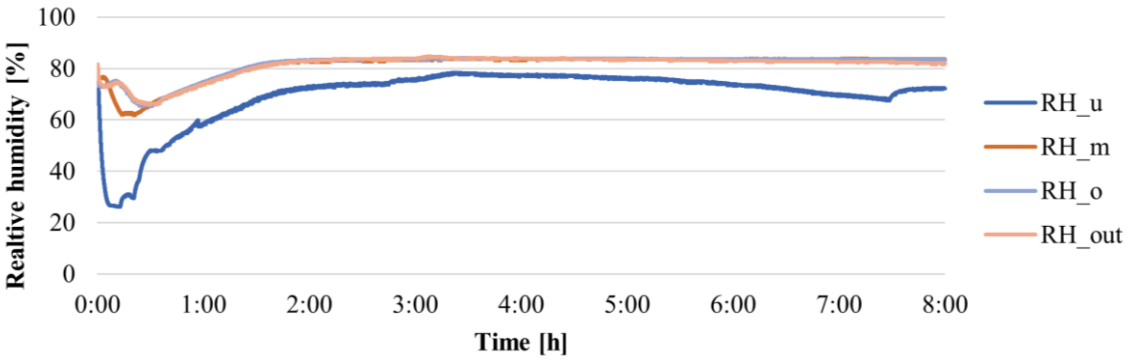

Fig. 39. Relative humidity over time for experiment WL18 (1-2 mm).

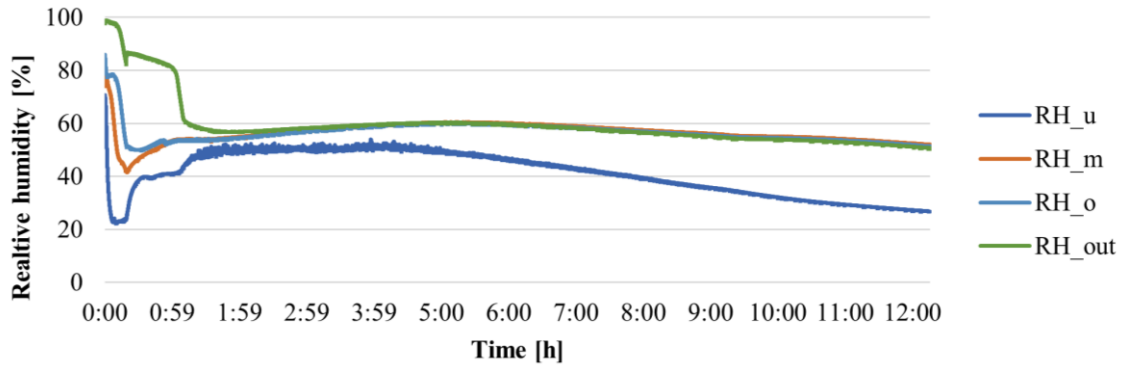

Fig. 40. Relative humidity over time for experiment WL20 (8-16 mm).

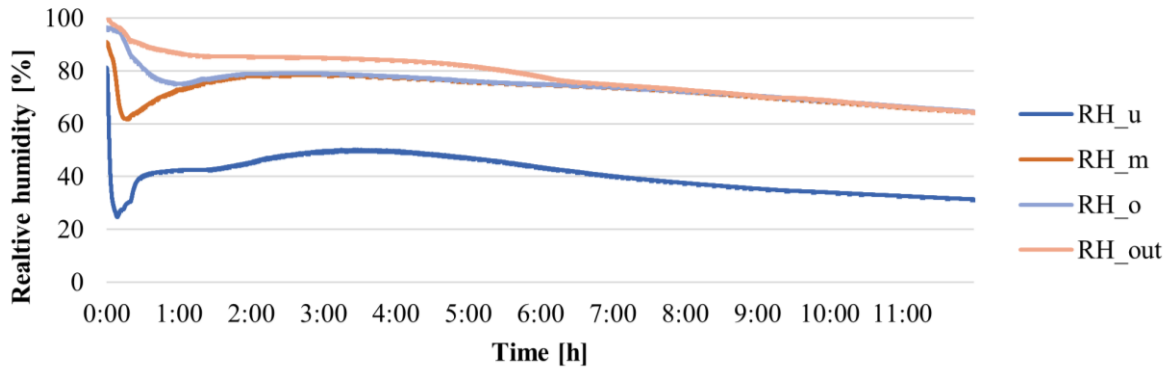

Fig. 41. Relative humidity over time for experiment WL26 (8-16 mm).

In the lower part of the chamber (on the RH_u sensor), the relative humidity behavior is unpredictable. In the case of very large fractions (8-16 mm) and very small fractions (<1 mm), the drop in RH at the beginning of the experiment is significantly more pronounced compared to the middle and upper part of the chamber (see **Fig. 41** and **Fig. 42**).

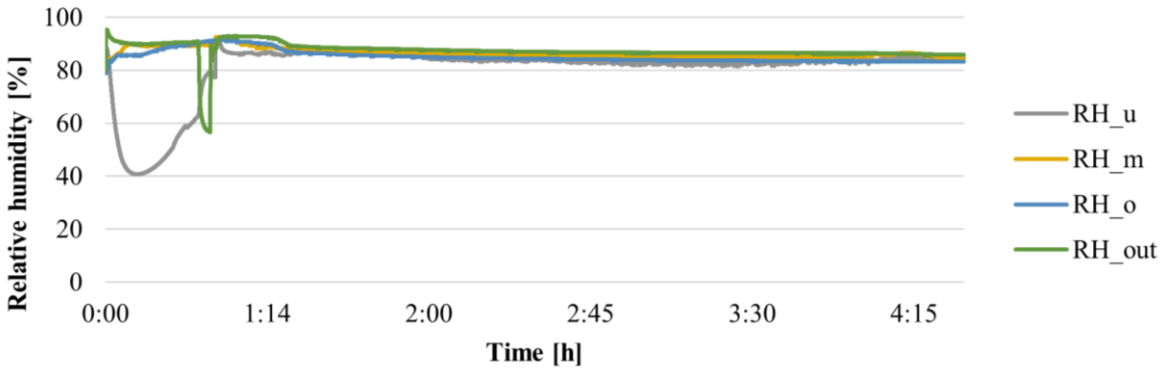

Fig. 42. Relative humidity over time for experiment WL22 (0-0,25 mm).

Also, after reaching 100% of CO_2 concentration inside the chamber in the case of larger RCA fractions, there was no significant increase in the value in the lower part of the chamber and the difference compared to the other parts of the chamber remained until the end (see **Fig. 41**). On the contrary, in the case of fractions of smaller aggregate grains, the value in the lower part of the chamber (after reaching 100% CO_2 concentration) reached the same value as in the other parts of the chamber (see **Fig. 41**).

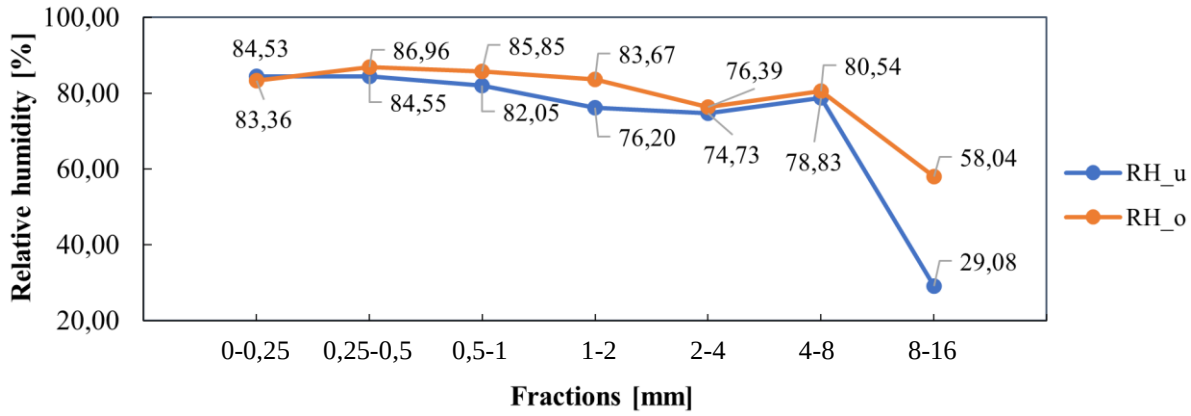

Fig. 43. Change of relative humidity due to fractions of RCA on sensors on bottom and top of the chamber.

Specific RH values for the lower and upper part of the chamber are shown on **Fig. 43**. For each fraction, the mean RH value at the end of the experiment was taken. For the largest fraction there is a sharp decline in RH. Especially in the lower part of the chamber where the difference is ~30%.

It is important to note that for 0-0.25 mm RCA condensation occurred inside the chamber during CO_2 curing. At the end of the test, the entire chamber was dewed as shown on **Fig. 44**.

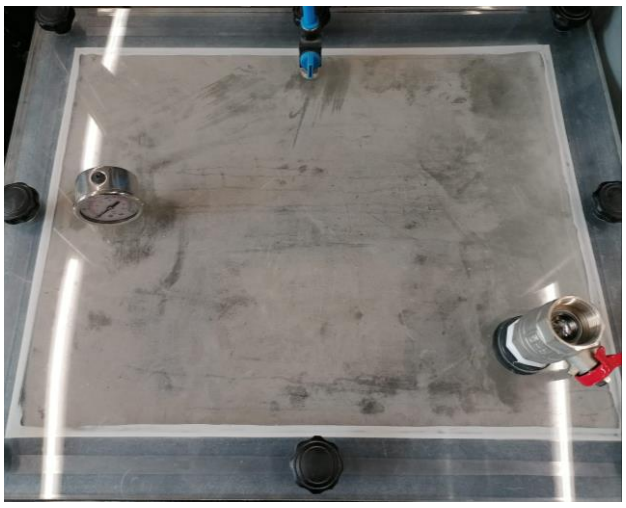

Fig. 44. Condensation inside the chamber

This phenomenon can be related to the temperature inside the chamber and the heating of the material. This led to condensation inside the chamber and wetting of the material, which consequently showed a smaller difference in moisture content before and after CO_2 curing (**Fig. 45**). This also affected the relationship between the RH and MC. A decrease in RH value was achieved in fine RCA with increasing grain size. At coarse RCA (4-16 mm) the decline has stopped. MC assumed approximately the same values (**Fig. 45**).

3.4.6. Impact of forced carbonation on moisture content of RCA

Fig. 45 shows that after CO_2 curing there was mostly an increase in the value of MC. In cases where there was no increase, the decrease was negligible. The only deviation occurred for the fraction of 4 - 8 mm where the average value of MC is significantly lower after CO_2 curing (~0,25 %).

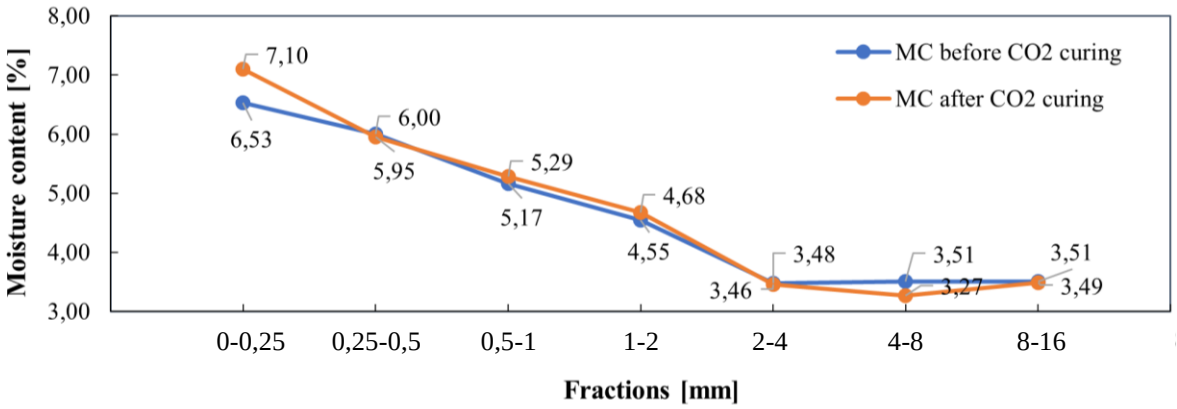

Fig. 45. Impact of CO2 curing on moisture content of RCA.

Also, the effect of the initial value of moisture content on CO_2 uptake is visible (see **Table 9).** Experiments in the same fractions showed higher values of CO_2 uptake when the initial value of moisture content in RCA was higher. Deviations occurred in fractions 0.5-1 mm and 8-16 mm. However, given that there are only two experiments for each fraction, this deviation would need to be proven by a larger number of experiments. Therefore, an increase in the MC value is accompanied by an increase in CO_2 uptake (**Fig. 46**).

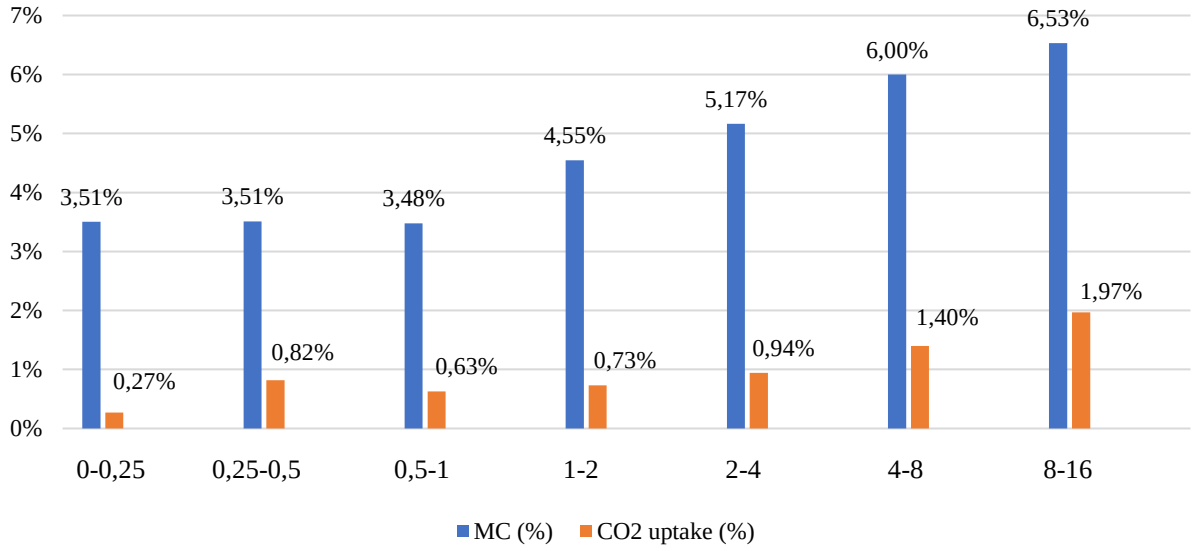

Fig. 46. Relationship between moisture content and CO_2 uptake

Table 9. Values of moisture content and CO_2 uptake

Name of experiment	Fraction	MC (%)	CO_2 uptake (%)
WL20	8-16 mm	3,33%	0,34%
WL26		3,68%	0,20%
WL13	4-8 mm	3,79%	0,94%
WL15		3,23%	0,70%
WL16	2-4 mm	3,26%	0,55%
WL17		3,69%	0,71%
WL18	1-2 mm	4,57%	0,77%
WL21		4,52%	0,69%
WL24	0,5-1 mm	5,08%	1,05%
WL27		5,25%	0,83%
WL23	0,25-0,5 mm	5,75%	1,22%
WL25		6,25%	1,58%
WL19	0-0,25 mm	6,32%	1,87%
WL22		6,74%	2,07%

3.4.7. Effect of the RCA grain size on the CO_2 uptake

There was a visible increase in the value of CO2 uptake with a decrease in the RCA grain size (see **Fig. 47**). The increase in values was continued for all fractions except for the 4-8 mm fraction where there was an unexpected increase in both experiments. The highest CO_2 uptake value obtained is 2.07% (0-0.25 mm), and the smallest 0.20% (8-16 mm). The difference between individual fractions is more pronounced in the case of smaller aggregates (< 1 mm) where it amounts to ~0.5%. Furthermore, with an increase in grain size, the decrease in CO_2 uptake is smaller.

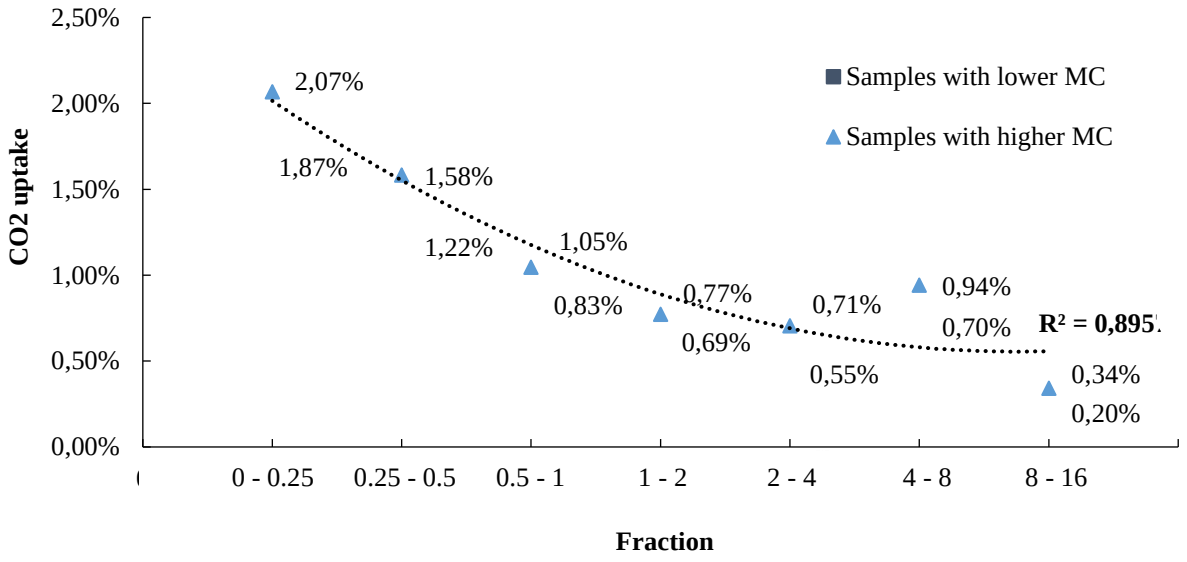

Fig. 47. CO_2 uptake versus fractions of RCA

Therefore, it is concluded that fine RCA had a greater capacity to store CO_2 than the coarse RCA. This confirmed the assumption from the literature according to Kikuchi et al. [49] and Fang et al [57]. First, this difference can be explained by the physical effect of CO_2 diffusion in the 1–4 mm RCA, which depends on the diameter of the RCA particles. The diffusion time of CO_2 in a fine RCA is lower than in a coarse RCA. Furthermore, the distribution of the phases able to be carbonated differs in the two fractions. The formation of calcium carbonates at the surface of a coarse RCA can hinder the diffusion of CO_2 more than in a fine RCA, where the total volume is carbonated uniformly.

2.5. Conclusion

The use of RCA accelerated carbonation technology is still a novelty. The aim of this work was to investigate the potential of accelerated carbonation of recycled concrete aggregate according to different aggregate fractions. For these needs, a combination of the standard carbonation method and the pressurized carbonation method was used at the Laboratory of the Institute for Structural Engineering, Vienna. The RCA was placed in an airtight chamber and treated with carbon dioxide. The conditions inside and outside the chamber are monitored by sensors. To detect carbonation, the phenolphthalein test was applied, with the help of which the depth of carbonation was also measured. The following results were obtained by constant measurement of CO_2 concentration, relative humidity, temperature, gas flow and mass.

By conducting a phenolphthalein test after the CO_2 curing process, it was observed that in the experiments with the RCA fraction of 8-16 mm, complete carbonation did not occur, especially in the lowest box in the chamber. In fractions 1-4 mm, complete carbonation at the surface occurred in all boxes except for the box at the bottom of the chamber. Other fractions of RCA 0-0.5 mm did not show a color change, indicating that complete carbonation of RCA surface had occurred. Due to these results the estimated time of CO_2 curing was insufficient for larger fractions of the RCA.

The average thickness of the carbonated layer for 16-22 mm RCA that was CO_2 cured for 23 hours is about 0,6 mm. Given the age of concrete and grain size, these values indicated the effectiveness of this process. Due to these results, it was confirmed that not only the surface carbonation of the grain carbonated, but there was a deeper penetration of carbonation into the grain of RCA.

The results also showed that after the CO_2 curing process there was an increase in the RCA mass. By reducing in the grain size of the RCA, there was a greater increase in the mass of the RCA. The largest increase was recorded for fine RCA (2,7%), and the smallest for coarse RCA (0,3%). These values indicate an extremely good increase in mass.

Additionally, the greatest increase in RCA mass (2.7%) for fine RCA can relate to temperature. After CO_2 curing, it was noticed that the fine RCA was heated. The increase in temperature was especially pronounced in the central part of the boxes, where the CO_2 gas flow is greatest. Also, the greatest heating of the RCA was recorded in the lowest box in the chamber. The reason why the temperature inside the chamber increased in the first place may be hidden behind the thermoactivated effect caused by the collision of so many small aggregate particles reacting with CO_2 and releasing energy as the reactions take place.

Also, for fine RCA condensation occurred inside the chamber during CO_2 curing. This phenomenon further led to observation of relative humidity behavior during CO_2 curing. In the lower part of the

chamber, the relative humidity behavior is unpredictable. In the case of coarse RCA (8-16 mm) and small fractions (<1 mm), the drop in relative humidity at the beginning of the experiment is significantly more pronounced compared to the middle and upper part of the chamber. In the upper and middle part of the chamber, relative humidity would generally drop at the very beginning until the CO_2 concentration inside the chamber stabilized. Then the RH curve is continuous in a slight increase or decrease until the end of the experiment. The only significant deviation occurred in the case of coarse RCA where a relative humidity of approximately 100% was recorded at the beginning of the experiment. After that, there was a sharp drop below 60%. By the end of the experiments, the value did not reach a value higher than 60%. This resulted with a sharp decline in RH values between lower and upper part of chamber (~30%).

All of the above effected moisture content. After CO_2 curing there was mostly an increase in the value of MC which confirmed predictions from the theoretical part. In cases where there was no increase, the decrease was negligible. The only deviation occurred for the fraction of 4-8 mm where the average value of MC is significantly lower after CO_2 curing (~0,25 %).

Finally, it is concluded that fine RCA had a greater capacity to store CO_2 than the coarse RCA. This confirmed the assumption from the literature. There was a visible increase in the value of CO_2 uptake with a decrease in the RCA grain size. The highest CO_2 uptake value obtained is 2.07% (0-0.25 mm), and the smallest 0.20% (8-16 mm).

These results confirmed the effectiveness of this method as well as the assumptions of other studies on the increase of CO_2 uptake and the mass of carbonized RCA with the reduction of the fraction. Other conditions that were monitored gave a clearer picture of the possibilities of applying this technology in further research.

Referring to the 3 research questions at the beginning of this thesis, the following answers have been elaborated:

- Treating recycled aggregate with accelerated carbonation is still a novel technology, but has a high potential.
- Combining the standard carbonation method with the pressurized method is a very promising technology to store CO2 within recycled aggregates.

List of tables

List of tables in appendices

List of figures

List of figures in appendices

Literature

[1] Buck, A. D. (1977) *Recycled Concrete as a Source of Aggregate* in: ACI Journal Proceedings 74, H. 5, S. 212–219. https://doi.org/10.14359/11004

[2] Baojian, Z.; Chisun, P.; Caijun, S. (2013) *CO2 curing for improving the properties of concrete blocks containing recycled aggregates* in: Cement and Concrete Composites 42, S. 1–8. https://doi.org/10.1016/j.cemconcomp.2013.04.013

[3] Jerga, J. (2004) *Physico-mechanical properties of carbonated concrete* in: Construction and Building Materials 18, H. 9, S. 645–652. https://doi.org/10.1016/j.conbuildmat.2004.04.029

[4] Chang, C.; Chen, J. (2005) *Strength and elastic modulus of carbonated concrete*, 102(5):315-321.

[5] Krstulović, P. (2000) *Svojstva i tehnologija betona*. Split: Faculty of Civil Engineering, Architecure and Geodesy and IGH Institute.

[6] Liang, C. et al. (2020) *Utilization of CO2 curing to enhance the properties of recycled aggregate and prepared concrete: A review* in: Cement and Concrete Composites 105, S. 103446. https://doi.org/10.1016/j.cemconcomp.2019.103446

[7] McNeil, K.; Kang, T. H.-K. (2013) *Recycled Concrete Aggregates: A Review* in: International Journal of Concrete Structures and Materials 7, H. 1, S. 61–69. https://doi.org/10.1007/s40069-013-0032-5

[8] Oikonomou, N. (2005) *Recycled concrete aggregates* in: Cement and Concrete Composites 27, H. 2, S. 315–318. https://doi.org/10.1016/j.cemconcomp.2004.02.020

[9] Jang, H.; Kim, J.; Sicakova, A. (2021) *Effect of Aggregate Size on Recycled Aggregate Concrete under Equivalent Mortar Volume Mix Design* in: Applied Sciences 11, H. 23, S. 11274. https://doi.org/10.3390/app112311274

[10] Bonifazi, G.; Palmieri, R.; Serranti, S. (2018) *Evaluation of attached mortar on recycled concrete aggregates by hyperspectral imaging* in: Construction and Building Materials 169, S. 835–842. https://doi.org/10.1016/j.conbuildmat.2018.03.048

[11] Limbachiya, M. C.; Leelawat, T.; Dhir, R. K. (2000) *Use of recycled concrete aggregate in high-strength concrete* in: Materials and Structures 33, H. 9, S. 574–580. https://doi.org/10.1007/BF02480538

[12] Sagoe-Crentsil, K. K.; Brown, T.; Taylor, A. H. (2001) *Performance of concrete made with commercially produced coarse recycled concrete aggregate* in: Cement and Concrete Research 31, H. 5, S. 707–712. https://doi.org/10.1016/S0008-8846(00)00476-2

[13] AShayan, A.; Xu, A. (2003) *Performance and Properties of Structural Concrete Made with Recycled Concrete Aggregate* in: ACI Materials Journal 100, H. 5. https://doi.org/10.14359/12812

[14] Etxeberria, M. et al. (2007) *Influence of amount of recycled coarse aggregates and production process on properties of recycled aggregate concrete* in: Cement and Concrete Research 37, H. 5, S. 735–742. https://doi.org/10.1016/j.cemconres.2007.02.002

[15] Matias, D. et al. (2013) *Mechanical properties of concrete produced with recycled coarse aggregates – Influence of the use of superplasticizers* in: Construction and Building Materials 44, S. 101–109. https://doi.org/10.1016/j.conbuildmat.2013.03.011

[16] Lindstedt, S.; Bolander, A. (2015) *Automation and Optimization of Primary Gyratory Crusher Performance for Increased Productivity* [Masters thesis]. Luleå University of Technology.

[17] Tavakoli, M.; Soroushian, P. (1996) *Strengths of Recycled Aggregate Concrete Made Using Field-Demolished Concrete as Aggregate* in: ACI Materials Journal 93, H. 2. https://doi.org/10.14359/9802

[18] Tavakoli, M., Soroushlan, P. (1996) *Strengths of recycled aggregate concrete made using field-demolished concrete as aggregate*, H. 2, p. 182–190.

[19] Thomas, J.; Thaickavil, N. N.; Wilson, P. M. (2018) *Strength and durability of concrete containing recycled concrete aggregates* in: Journal of Building Engineering 19, S. 349–365. https://doi.org/10.1016/j.jobe.2018.05.007

[20] H.F.W. Taylor (1997) *Cement Chemistry 2nd Edition* in: Thomas Telford Publishing, Thomas Telford Services Ltd, 1 Heron.

[21] Zawal, D.; Grabiec, A. M. (2022) *Influence of selected mineral additives on properties of recycled aggregate concrete (RAC) considering eco-efficiency coefficients* in: Case Studies in Construction Materials 17, e01405. https://doi.org/10.1016/j.cscm.2022.e01405

[22] Lindsey, R. (2009) *Climate Change: Atmospheric Carbon Dioxide* [online]. https://www.climate.gov/news-features/understanding-climate/climate-change-atmospheric-carbon-dioxide#.

[23] Euler, W. B.; Kirschenbaum, L.; Ruekberg, B. (2000) *Determination of Ksp, ΔG°, ΔH°, and ΔS° for the Dissolution of Calcium Hydroxide in Water a General Chemistry Experiment*, S. 3–4.

[24] Britannica (2023) *Encyclopedia Britannica* [online]. https://www.britannica.com/science/carbonic-acid.

[25] Ikumapayi, C. M. et al. (2019) *Effects of Carbonation on the Properties of Concrete* in: Scientific Review, H. 512, S. 205–214. https://doi.org/10.32861/sr.512.205.214

[26] Merah, A. (2021) *Concrete anti-carbonation coatings: a review* in: Journal of Adhesion Science and Technology 35, H. 4, S. 337–356. https://doi.org/10.1080/01694243.2020.1803594

[27] *Concrete Crack Causes and Solutions* [online]. https://www.liftupconcrete.net/concrete-crack-solutions/.

[28] Xuan, D.; Zhan, B.; Poon, C. S. (2017) *Durability of recycled aggregate concrete prepared with carbonated recycled concrete aggregates* in: Cement and Concrete Composites 84, S. 214–221. https://doi.org/10.1016/j.cemconcomp.2017.09.015

[29] Lee, S.; Park, W.; Lee, H. (2013) *Life cycle CO2 assessment method for concrete using CO2 balance and suggestion to decrease LCCO2 of concrete in South-Korean apartment* in: Energy and Buildings 58, S. 93–102. https://doi.org/10.1016/j.enbuild.2012.11.034

[30] National Center for Biotechnology Information (2004) *PubChem Compound Summary for CID 4764, Phenolphthalein* [online]. https://pubchem.ncbi.nlm.nih.gov/compound/Phenolphthalein.

[31] (2006) *Products and systems for protection and repair of concrete structures - Test methods - Determination of carbonation depth in hardened concrete by the phenolphthalein method – EN 14630:2006 (E)*. Wien: ON Österreisches Normungsinstitut.

[32] (2006) *Products and systems for the protection and repair of concrete structures - Definitions, requirements, quality control and evaluation of conformity – EN 1504-6:2006*. Wien: ON Österreisches Normungsinstitut.

[33] Fukushima, T. et al. (1998) *Relationship Between Neutralization Depth and Concentration Distribution of CaCO3 -Ca(OH)2 in Carbonated Concrete* in: Austrian Standards Institute [Hrsg.] *SP-179: Fourth CANMET/ACI/JCI Conference: Advances in Concrete Technology*. American Concrete Institute.

[34] Andrade, C. (2020) *Evaluation of the degree of carbonation of concretes in three environments* 230, S. 116804. https://doi.org/10.1016/j.conbuildmat.2019.116804

[35] Construction Testing Solutions Ltd (16th November 2022) *Concrete deterioration and testing methods* [online]. https://www.constructiontesting.co.uk/cts-group-spotlight-on-concrete-deterioration-and-testing-methods/#.

[36] Neves, R.; Branco, F.; Brito, J. (2013) *Field assessment of the relationship between natural and accelerated concrete carbonation resistance* in: Cement and Concrete Composites 41, S. 9–15. https://doi.org/10.1016/j.cemconcomp.2013.04.006

[37] Dongxing, X.; Baojian, Z.; Poon, C. S. (2016) *Assessment of mechanical properties of concrete incorporating carbonated recycled concrete aggregates* in: Cement and Concrete Composites 65, S. 67–74. https://doi.org/10.1016/j.cemconcomp.2015.10.018

[38] GB/T 50082-2009 (2009) *Standard for test methods of long-term performance and durability of ordinary concrete*. China Architecture & Building Press.

[39] Shi, C. et al. (2018) *Performance of mortar prepared with recycled concrete aggregate enhanced by CO2 and pozzolan slurry* in: Cement and Concrete Composites 86, S. 130–138. https://doi.org/10.1016/j.cemconcomp.2017.10.013

[40] Zhang, J. et al. (2015) *Influence of carbonated recycled concrete aggregate on properties of cement mortar* in: Construction and Building Materials 98, S. 1–7. https://doi.org/10.1016/j.conbuildmat.2015.08.087

[41] Kou, S.-C.; Zhan, B.; Poon, C.-S. (2014) *Use of a CO2 curing step to improve the properties of concrete prepared with recycled aggregates* in: Cement and Concrete Composites 45, S. 22–28. https://doi.org/10.1016/j.cemconcomp.2013.09.008

[42] Fang, X.; Xuan, D.; Poon, C. S. (2017) *Empirical modelling of CO2 uptake by recycled concrete aggregates under accelerated carbonation conditions* in: Materials and Structures 50, H. 4. https://doi.org/10.1617/s11527-017-1066-y

[43] Lim, M. et al. (2010) *Environmental remediation and conversion of carbon dioxide (CO(2)) into useful green products by accelerated carbonation technology* in: International journal of environmental research and public health 7, Nr. 1, pp. 203–228. https://doi.org/10.3390/ijerph7010203

[44] Pasquier, L.-C. et al. (2014) *Parameters optimization for direct flue gas CO 2 capture and sequestration by aqueous mineral carbonation using activated serpentinite based mining residue* in: Applied Geochemistry 50, S. 66–73. https://doi.org/10.1016/j.apgeochem.2014.08.008

[45] Zhan, B. J.; Xuan, D. X.; Poon, C. S. (2018) *Enhancement of recycled aggregate properties by accelerated CO2 curing coupled with limewater soaking process* in: Cement and Concrete Composites 89, S. 230–237. https://doi.org/10.1016/j.cemconcomp.2018.03.011

[46] Li, L. et al. (2018) *Effect of carbonation of modeled recycled coarse aggregate on the mechanical properties of modeled recycled aggregate concrete* in: Cement and Concrete Composites 89, S. 169–180. https://doi.org/10.1016/j.cemconcomp.2018.02.018

[47] Zhan, M. et al. (2017) *Effect of presoak-accelerated carbonation factors on enhancing recycled aggregate mortars* in: Magazine of Concrete Research 69, H. 16, S. 838–849. https://doi.org/10.1680/jmacr.16.00468

[48] Pan, G. et al. (2017) *Effect of CO2 curing on demolition recycled fine aggregates enhanced by calcium hydroxide pre-soaking* in: Construction and Building Materials 154, S. 810–818. https://doi.org/10.1016/j.conbuildmat.2017.07.079

[49] Kikuchi, T.; Kuroda, Y. (2011) *Carbon Dioxide Uptake in Demolished and Crushed Concrete* in: Journal of Advanced Concrete Technology 9, H. 1, S. 115–124. https://doi.org/10.3151/jact.9.115

[50] Xuan, D.; Zhan, B.; Poon, C. S. (2016) *Development of a new generation of eco-friendly concrete blocks by accelerated mineral carbonation* in: Journal of Cleaner Production 133, S. 1235–1241. https://doi.org/10.1016/j.jclepro.2016.06.062

[51] Zhao, Z. F.; Jin, P. F.; Zhao, Q. Q. (2014) *Influence of Laboratory Accelerated Carbonation on the Properties of Recycled Concrete Aggregates* in: Advanced Materials Research 919-921, S. 1817–1820. https://doi.org/10.4028/www.scientific.net/AMR.919-921.1817

[52] Zhan, B. J. et al. (2019) *Carbonation treatment of recycled concrete aggregate: Effect on transport properties and steel corrosion of recycled aggregate concrete* in: Cement and Concrete Composites 104, S. 103360. https://doi.org/10.1016/j.cemconcomp.2019.103360

[53] Zhan, B. et al. (2014) *Experimental study on CO2 curing for enhancement of recycled aggregate properties* in: Construction and Building Materials 67, S. 3–7. https://doi.org/10.1016/j.conbuildmat.2013.09.008

[54] (2023) *Greenhouse gases continued to increase rapidly in 2022 – Carbon dioxide, methane and nitrous oxide rise further into uncharted levels* [online]. National Oceanic and Atmospheric Administration, U.S. Department of Commerce. https://www.noaa.gov/news-release/greenhouse-gases-continued-to-increase-rapidly-in-2022.

[55] Castellote, M. et al. (2009) *Chemical changes and phase analysis of OPC pastes carbonated at different CO2 concentrations*, S. 515–525.

[56] Kashef-Haghighi, S.; Shao, Y.; Ghoshal, S. (2015) *Mathematical modeling of CO 2 uptake by concrete during accelerated carbonation curing* in: Cement and Concrete Research 67, S. 1–10. https://doi.org/10.1016/j.cemconres.2014.07.020

[57] Fang, X. L.; Xuan, D. X.; Poon, S. C. (2017) *Empirical modelling of CO2 uptake by recycled concrete aggregates under accelerated carbonation conditions*, S. 200–212.

[58] Cui, H. et al. (2015) *Experimental study on effects of CO2 concentrations on concrete carbonation and diffusion mechanisms* in: Construction and Building Materials 93, S. 522–527. https://doi.org/10.1016/j.conbuildmat.2015.06.007

[59] Kabashi, N. et al. (2017) *Corrosion in concrete under sulphate and chloride attacks* [online]. Institute of Building Materials and Structures “IBMS”. https://www.researchgate.net/publication/316440930_CORROSION_IN_CONCRETE_UNDER_SULPHATE_AND_CHLORIDE_ATTACKS.

[60] Steiner, S. et al. (2020) *Effect of relative humidity on the carbonation rate of portlandite, calcium silicate hydrates and ettringite* in: Cement and Concrete Research 135, S. 106116. https://doi.org/10.1016/j.cemconres.2020.106116

[61] Zhan, B. J. et al. (2016) *Effect of curing parameters on CO2 curing of concrete blocks containing recycled aggregates* in: Cement and Concrete Composites 71, S. 122–130. https://doi.org/10.1016/j.cemconcomp.2016.05.002

[62] Lekakh, S. N. et al. (2008) *Kinetics of Aqueous Leaching and Carbonization of Steelmaking Slag* in: Metallurgical and Materials Transactions B 39, H. 1, S. 125–134. https://doi.org/10.1007/s11663-007-9112-8

[63] Chen, Y.; Liu, P.; Yu, Z. (2018) *Effects of Environmental Factors on Concrete Carbonation Depth and Compressive Strength* in: Materials (Basel, Switzerland) 11, Nr. 11. https://doi.org/10.3390/ma11112167

[64] Luo, S. et al. (2018) *Carbonated recycled coarse aggregate and uniaxial compressive stress-strain relation of recycled aggregate concrete* in: Construction and Building Materials 188, S. 956–965. https://doi.org/10.1016/j.conbuildmat.2018.08.159

[65] *Glock, Chr.; Haist, M.; Bergmeister, K.; Voit, K.; Beyer, D.; Heckmann, M.; Hondl, T.; Hron, J.; Pürgstaller, A.; Schack, T. (2023): Klima- und ressourcenschonendes Bauen mit Beton. Mit Urban Mining zum kreislauffähigen Betonbau* in:: Betonkalender 2024

[66] *Voit, K.; Hron, J.; Bergmeister, K. (2022) Das Potential rezyklierter Gesteinskörnung für einen nachhaltigen* Betonbau in: Österreichische Ingenieur- und Architektenzeitschrift 167

Appendix 1

Table 1. Results of experiments cured with CO_2 for 4 hours

	4 HOURS			
	(0,25-0,5 mm)		(0-0,25 mm)	
No.	WL23	WL25	WL19	WL22
Duration	4 h	4 h	4 h	4 h, 30 min
$m_{ø}$ [g]	11995,95	10009,15	12000,45	12005,30
m_1 [g]	12171,45	10150,00	12310,85	12349,70
Δm [g]	175,50	140,85	310,40	344,40
Δm_{gas} [g]	69,00	69,00	69,00	69,00
Δm_w [g]	-29,57	17,59	-86,10	-96,08
$\Delta m_{bal\ [g]}$	275,00	229,00	448,00	436,00
$\Delta M_{car.\ 1}$ [g]	176,43	177,59	292,90	270,92
$\Delta M_{car.\ 2}$ [g]	145,93	158,44	224,30	248,32
CO_2 uptake	1,22%	1,58%	1,87%	2,07%
MC before	5,75%	6,25%	6,32%	6,74%
MC after	5,91%	5,99%	6,86%	7,33%
m_{w0} [g]	689,77	625,57	758,43	809,16
m_{w1}[g]	719,33	607,99	844,52	905,23

Appendix 2

Table 2. Results of experiments cured with CO_2 for 8 hours

	8 HOURS			
	(1-2 mm)		(0,5-1 mm)	
No.	WL18	WL21	WL24	WL27
Duration	8 h	8 h	8 h	8 h
$m_{ø}$ [g]	12011,60	12007,35	11989,56	12068,25
m_1 [g]	12101,20	12134,35	12120,45	12206,55
Δm [g]	89,60	127,00	130,89	138,30
Δm_{gas} [g]	69,00	69,00	69,00	69,00
Δm_w [g]	3,17	-44,57	-5,44	-37,78
$\Delta m_{bal\ [g]}$	144,00	198,00	220,00	226,00
$\Delta M_{car.\ 1}$ [g]	78,17	84,43	145,56	119,22
$\Delta M_{car.\ 2}$ [g]	92,77	82,43	125,45	100,52
CO_2 uptake	0,77%	0,69%	1,05%	0,83%
MC before	4,57%	4,52%	5,08%	5,25%
MC after	4,51%	4,84%	5,07%	5,50%
m_{w0} [g]	548,93	542,73	609,07	633,58
m_{w1} [g]	545,76	587,30	614,51	671,36

Appendix 3

Table 3. Results of experiments cured with CO_2 for 12 hours

	12 HOURS					
	(8-16 mm)		(4-8 mm)		(2-4 mm)	
No.	WL20	WL26	WL13	WL15	WL16	WL17
Duration	12 h	12 h	12 h	12 h	12 h	12 h
$m_{ø}$ [g]	11978,30	12050,40	12066,90	12024,95	12044,20	12025,85
m_1 [g]	12015,80	12075,75	12122,95	12113,20	12132,10	12091,45
Δm [g]	37,50	25,35	56,05	88,25	87,90	65,60
Δm_{gas} [g]	69,00	69,00	69,00	69,00	69,00	69,00
Δm_w [g]	3,56	-1,05	57,52	-4,06	-21,06	19,34
$\Delta m_{bal\ [g]}$	84,00	80,00	181,00	163,00	127,00	89,00
$\Delta M_{car.\ 1}$ [g]	18,56	9,95	169,52	89,94	36,94	39,34
$\Delta M_{car.\ 2}$ [g]	41,06	24,30	113,57	84,19	66,84	84,94
CO_2 uptake	0,34%	0,20%	0,94%	0,70%	0,55%	0,71%
MC before	3,33%	3,68%	3,79%	3,23%	3,26%	3,69%
MC after	3,29%	3,68%	3,30%	3,24%	3,41%	3,51%
m_{w0} [g]	398,88	443,33	457,34	388,41	392,64	443,75
m_{w1} [g]	395,32	444,39	399,81	392,47	413,70	424,41

Appendix 4

Documentation of experiments:

1) Appendix 4.1 – WL13
2) Appendix 4.2 – WL15
3) Appendix 4.3 – WL16
4) Appendix 4.4 – WL17
5) Appendix 4.5 – WL18
6) Appendix 4.6 – WL19
7) Appendix 4.7 – WL20
8) Appendix 4.8 – WL21
9) Appendix 4.9 – WL22
10) Appendix 4.10 – WL23
11) Appendix 4.11 – WL24
12) Appendix 4.12 – WL25
13) Appendix 4.13 – WL26
14) Appendix 4.14 – WL27

Appendix 4.1

Code: **WL13** Fraction: **4-8 mm** Duration: **12h**

Notes: There was an unexplained jump in the mass between the 4th and 5th hour, but since the return jump occurred between 7 and 8 o'clock there was no effect on the result.

Table 4. Properties of the examined RCA before and after CO_2 curing for experiment WL13.

		$m_{ø}$ = 12066,90 g m_1 = 12122,95 g	Δm = 56,05 g
MC $_{before}$ = 3,79 % MC $_{after}$ = 3,30 %	→ →	m_{w_0} = 457,34 g m_{w_1} = 399,81 g	Δm_w = 57,52 g
			Δm_{bal} = 181,00 g Δm_{gas} = 69,00 g
$\Delta M_{car.\ 1}$ = 169,52 g		$\Delta M_{car.\ 2}$ = 113,57 g	CO_2 uptake = **0,94 %**

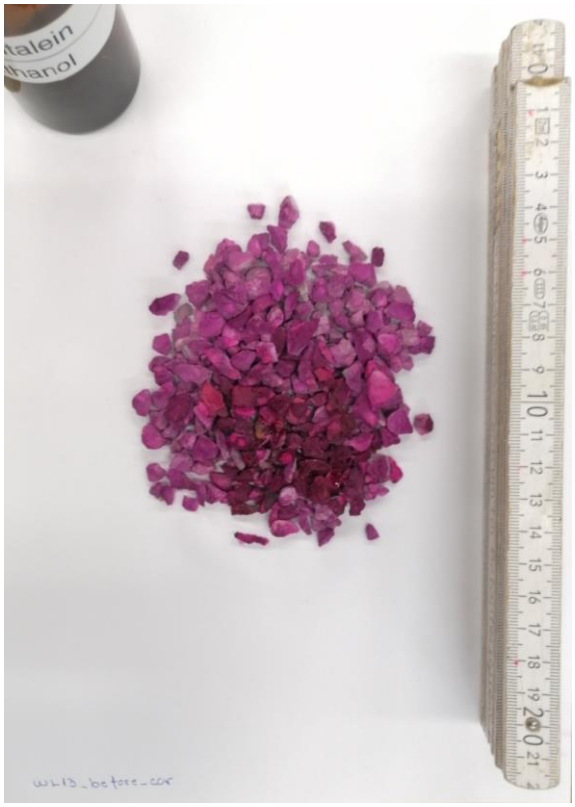

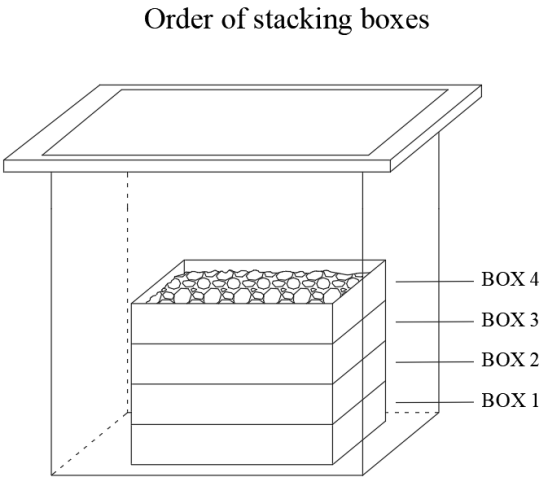

Fig. 1. Phenolphthalein test results before CO_2 curing for experiment WL13.

Box 1

Box 2

Box 3

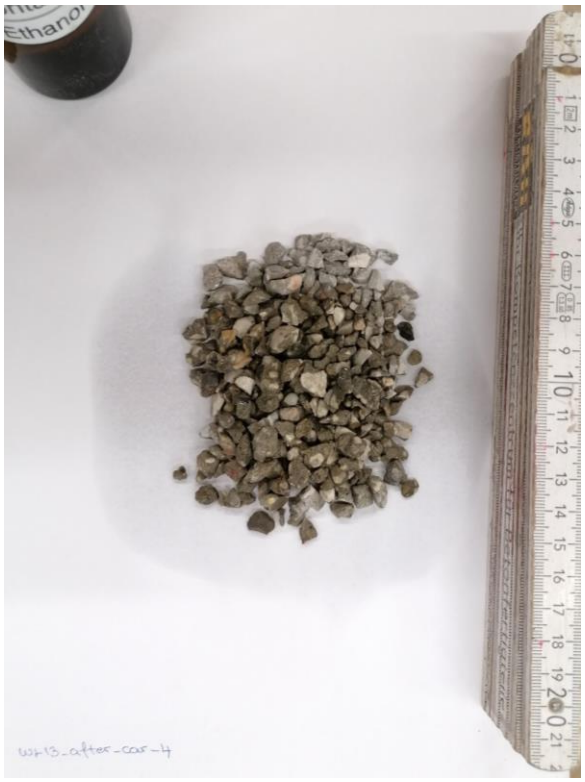

Box 4

Fig. 2. Phenolphthalein test results for each box of experiment WL13 after CO_2 curing.

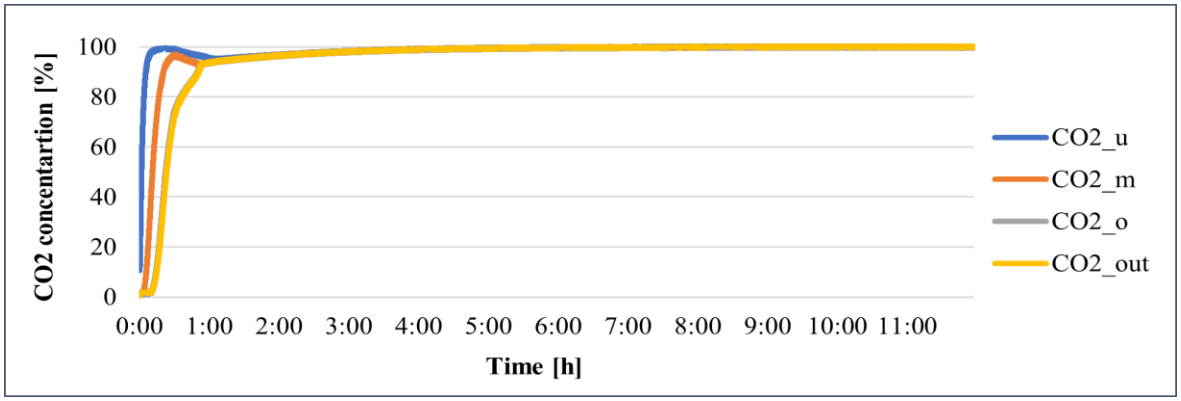

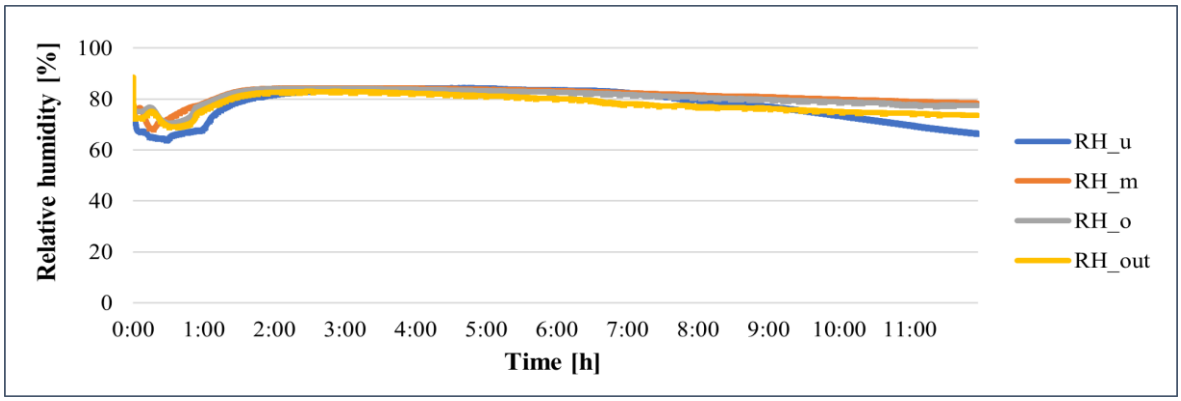

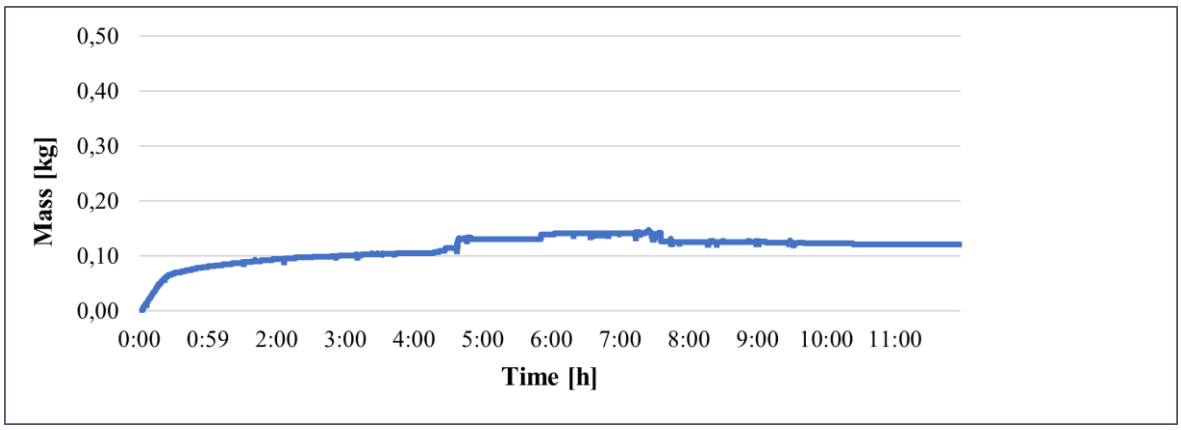

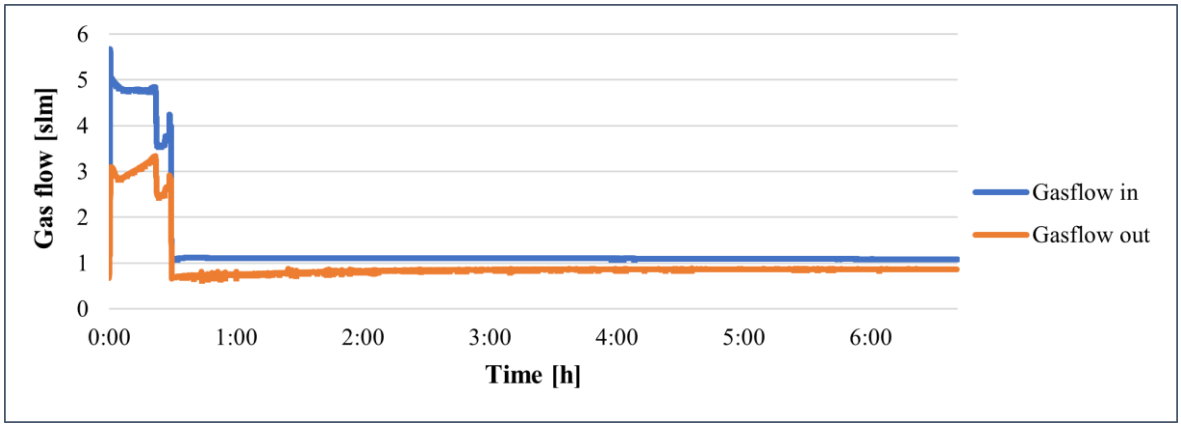

Fig. 3. The resulting diagrams for experiment WL15.

Appendix 4.2

Code: **WL15** Fraction: **4-8 mm** Duration: **12 h**

Table 5. Properties of the examined RCA before and after CO_2 curing for experiment WL15.

		$m_{ø}$ = 12024,95 g m_1 = 12113,20 g	Δm = 88,25 g
MC_{before} = 3,23 %	→	m_{w_0} = 388,41 g	Δm_w = -4,06 g
MC_{after} = 3,24 %	→	m_{w_1} = 392,64 g	
			Δm_{bal} = 163,00 g
			Δm_{gas} = 69,00 g
$\Delta M_{car.\ 1}$ = 89,94 g		$\Delta M_{car.\ 2}$ = 84,19 g	CO_2 uptake = **0,70 %**

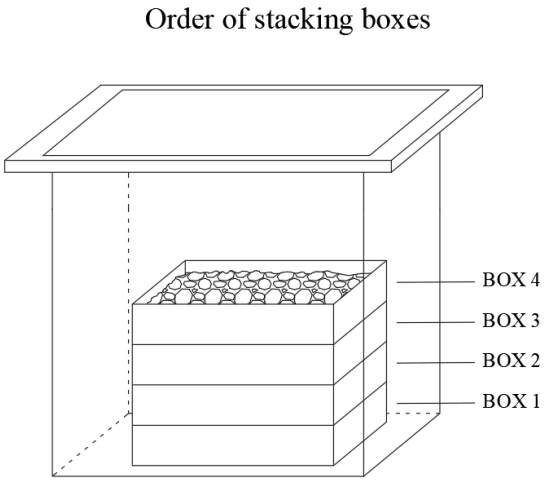

Fig. 4. Phenolphthalein test results before CO_2 curing for experiment WL15.

Box 1

Box 2

Box 3

Box 4

Fig. 5. Phenolphthalein test results for each box of experiment WL15 after CO_2 curing.

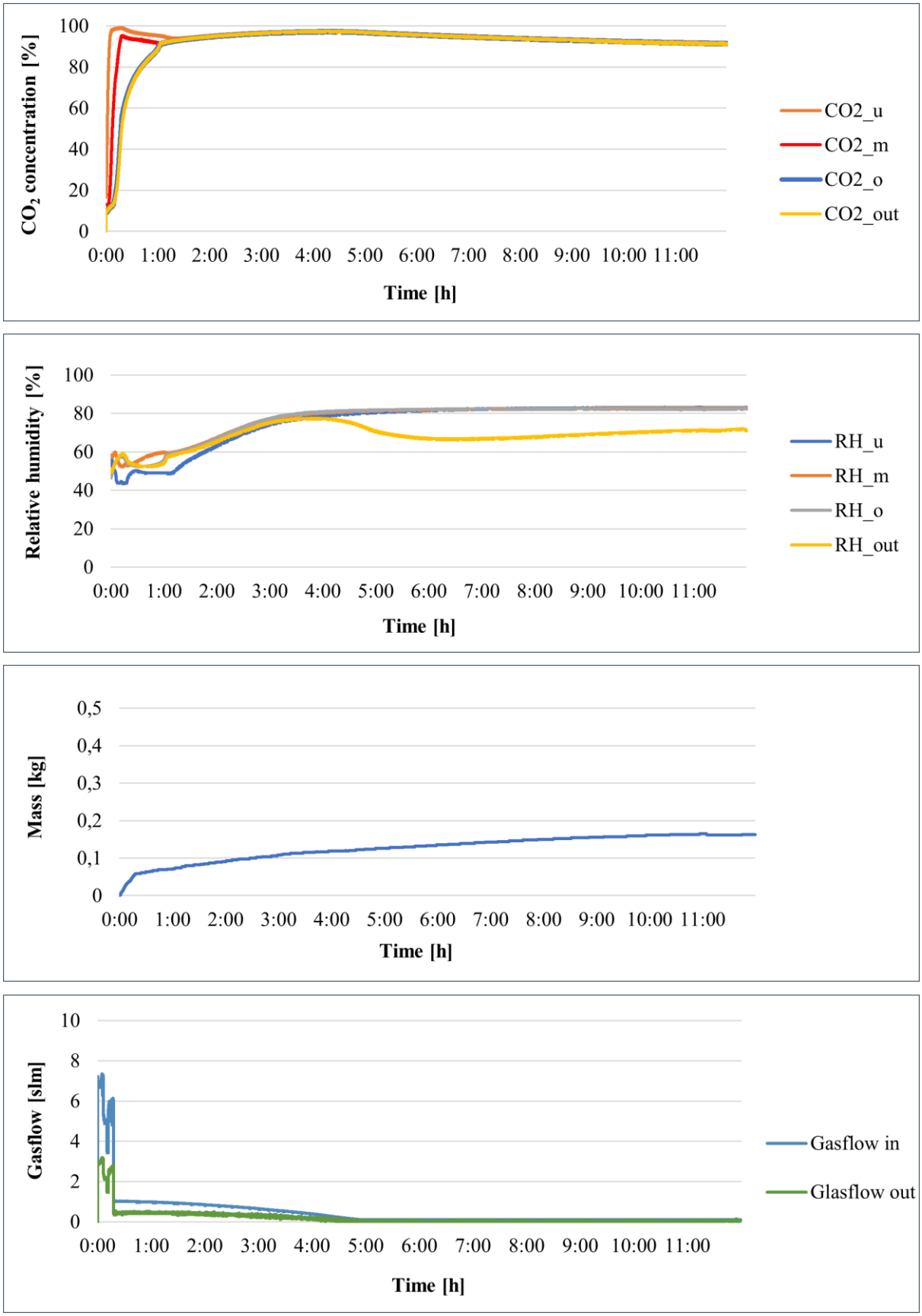

Fig. 6. The resulting diagrams for experiment WL15.

Appendix 4.3

Code: **WL16** Fraction: **2-4 mm** Duration: **12h**

Table 6. Properties of the examined RCA before and after CO_2 curing for experiment WL16.

		$m_{ø}$ = 12044,20 g m_1 = 12132,20 g	Δm = 87,90 g
MC_{before} = 3,26 %	→	m_{w_0} = 392,64 g	Δm_w = -21,06 g
MC_{after} = 3,41 %	→	m_{w_1} = 413,70 g	
			Δm_{bal} = 127,00 g Δm_{gas} = 69,00 g
$\Delta M_{car.\ 1}$ = 36,94 g		$\Delta M_{car.\ 2}$ = 66,84g	CO_2 uptake = **0,55 %**

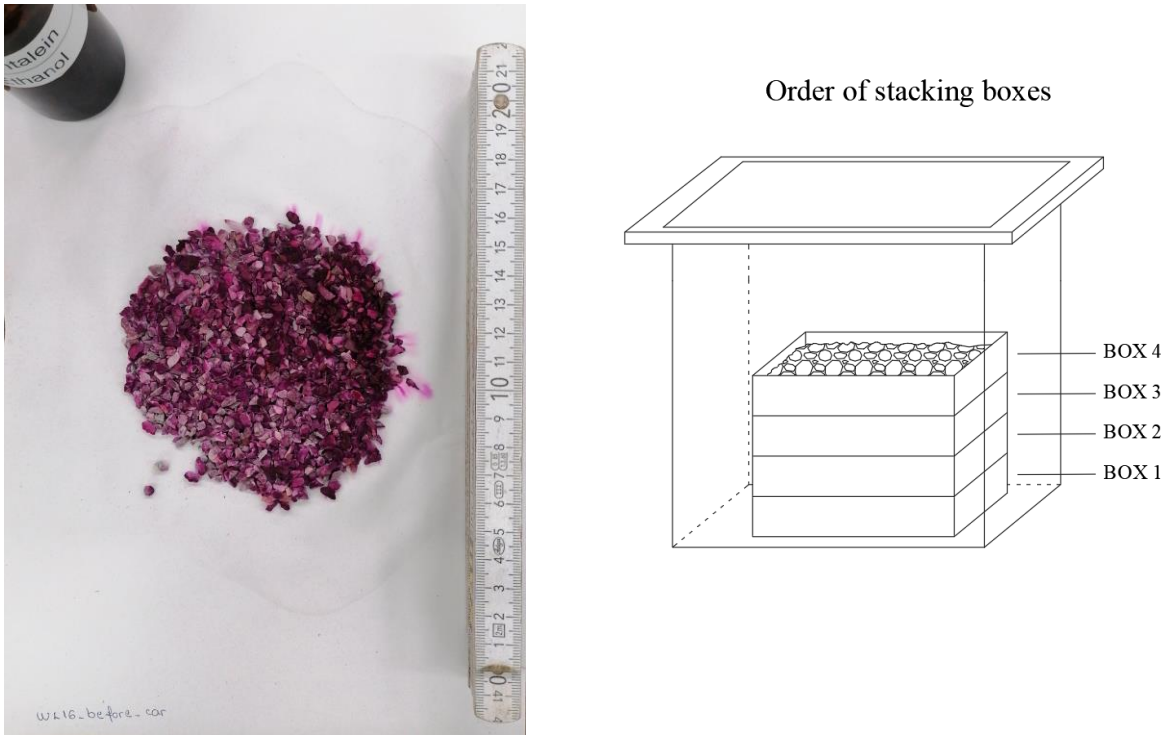

Fig. 7. Phenolphthalein test results before CO_2 curing for experiment WL16.

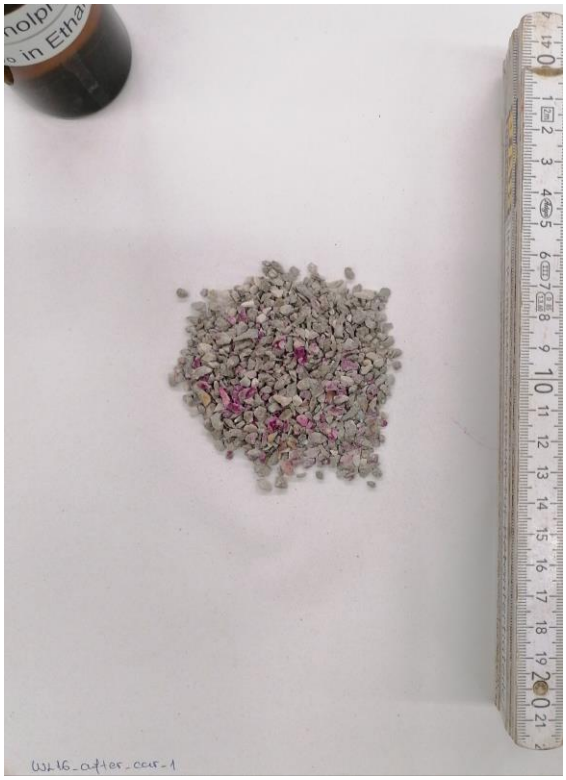

Box 1

Box 2

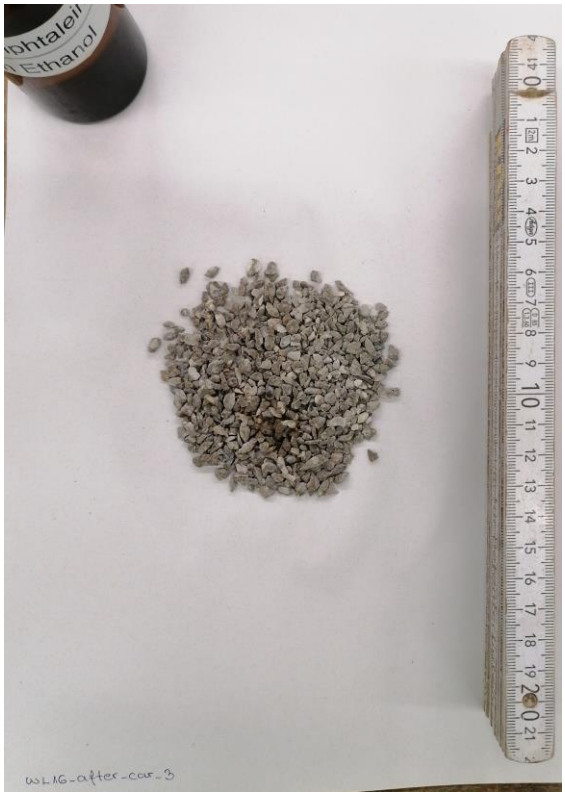

Box 3

Box 4

Fig. 8. Phenolphthalein test results for each box of experiment WL16 after CO_2 curing.

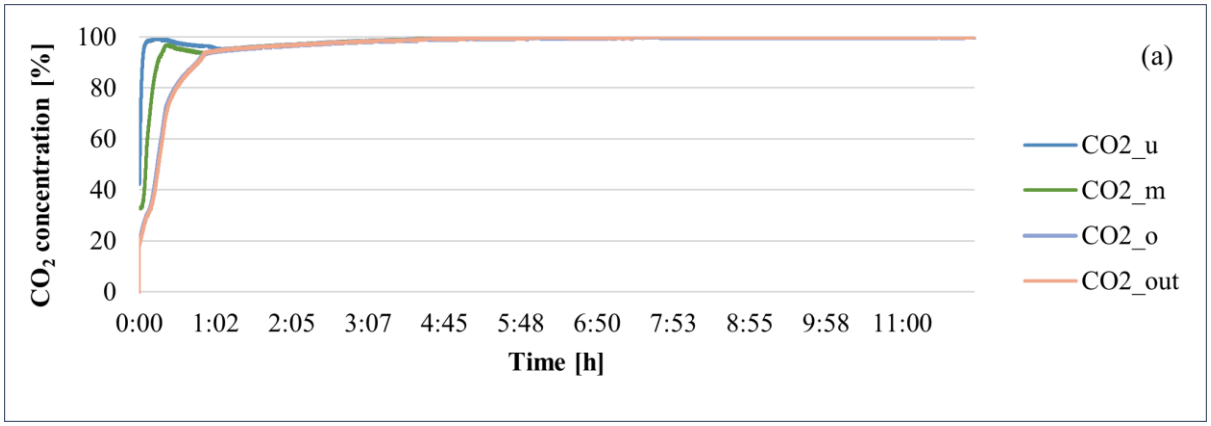

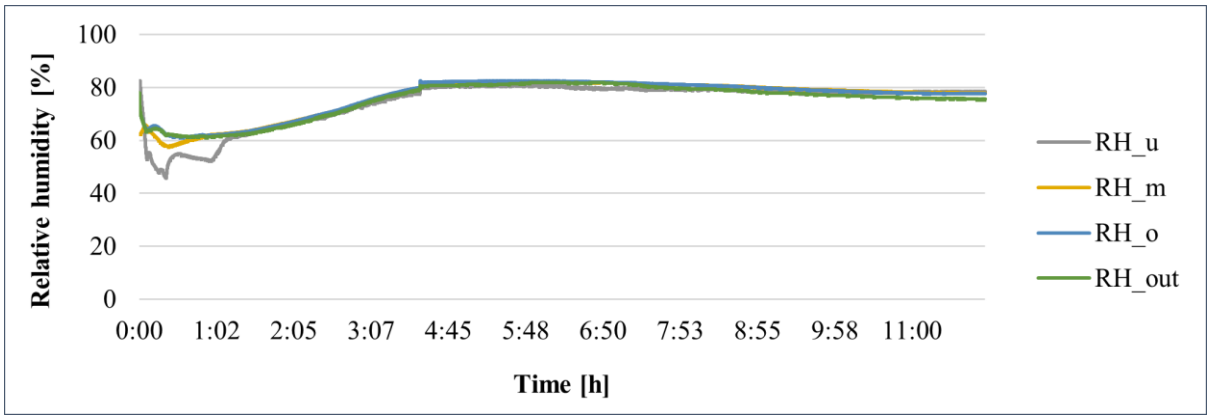

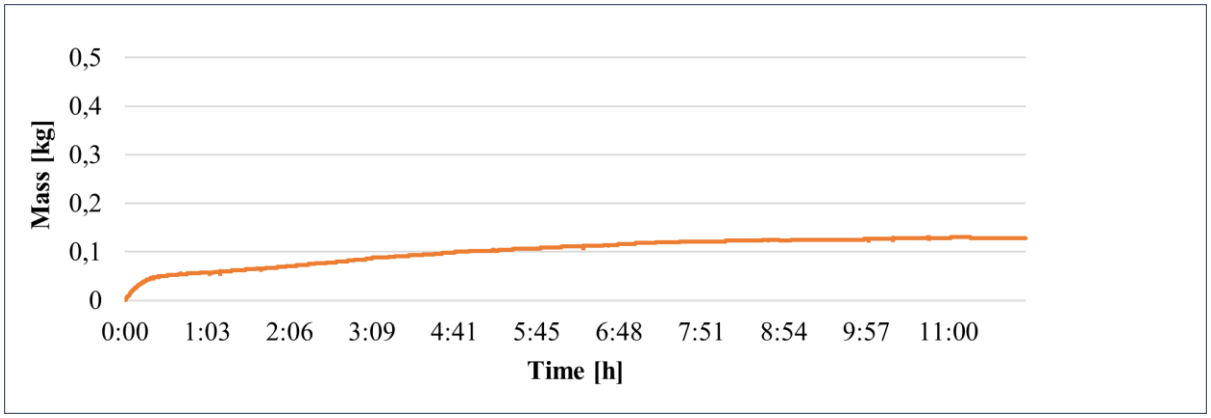

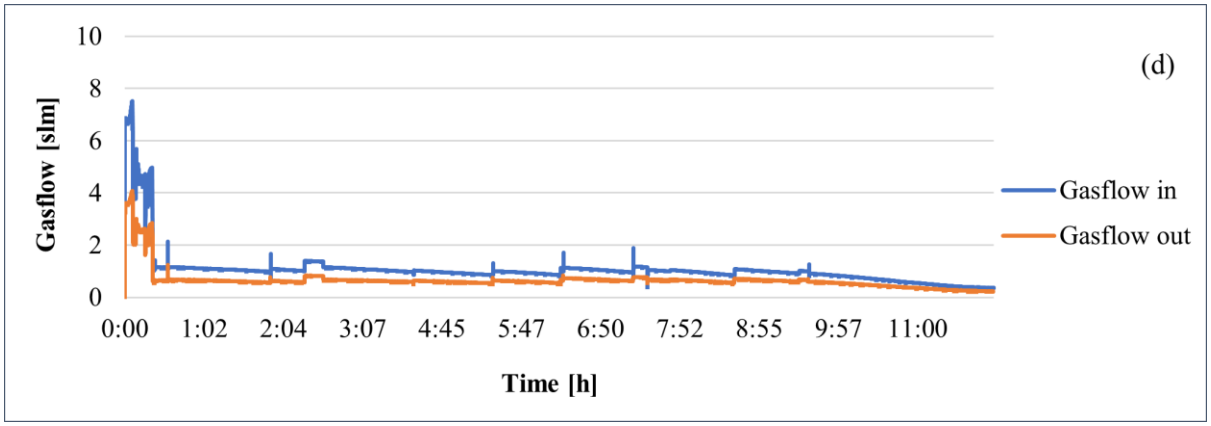

Fig. 9. The resulting diagrams for experiment WL16.

Appendix 4.4

Code: **WL17** Fraction: **2-4 mm** Duration: **12h**

Notes: RCA did not fully carbonized. The phenolphthalein test detected a non-carbonized part in the box at the bottom of the chamber.

Table 7. Properties of the examined RCA before and after CO_2 curing for experiment WL17.

		$m_{ø}$ = 12025,85 g m_1 = 12091,45 g	Δm = 65,60 g
MC $_{before}$ = 3,69 % MC $_{after}$ = 3,51 %	→ →	m_{w_0} = 443,75 g m_{w_1} = 424,41 g	Δm_w = 19,34 g
			Δm_{bal} = 89,00 g Δm_{gas} = 69,00 g
$\Delta M_{car.\ 1}$ = 39,34 g		$\Delta M_{car.\ 2}$ = 84,94g	CO_2 uptake = **0,71 %**

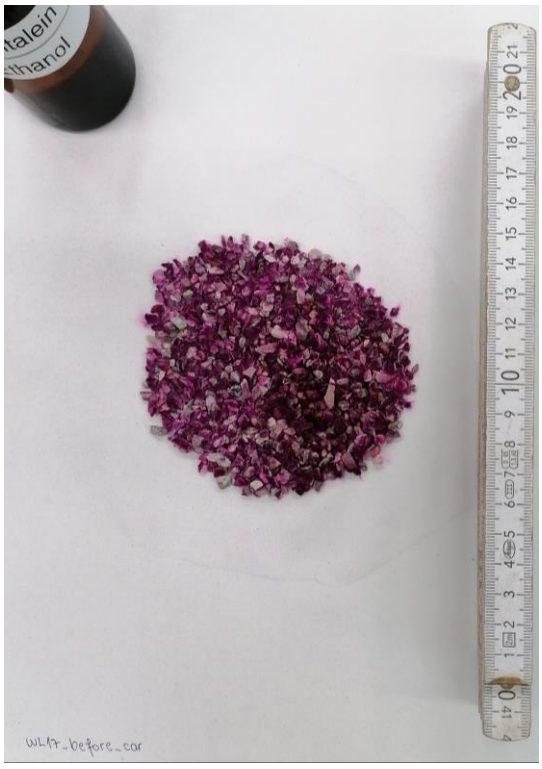

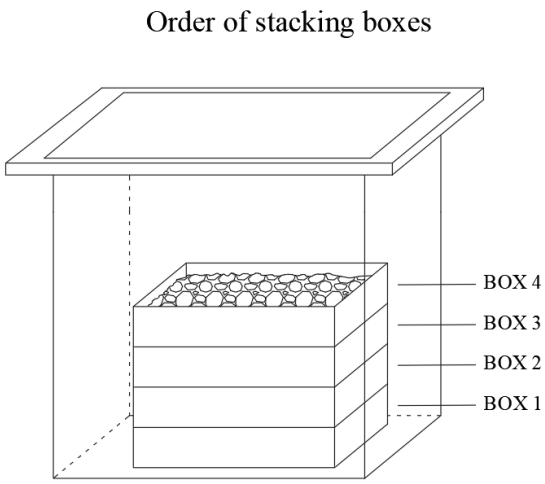

Fig. 10. Phenolphthalein test results before CO_2 curing for experiment WL17.

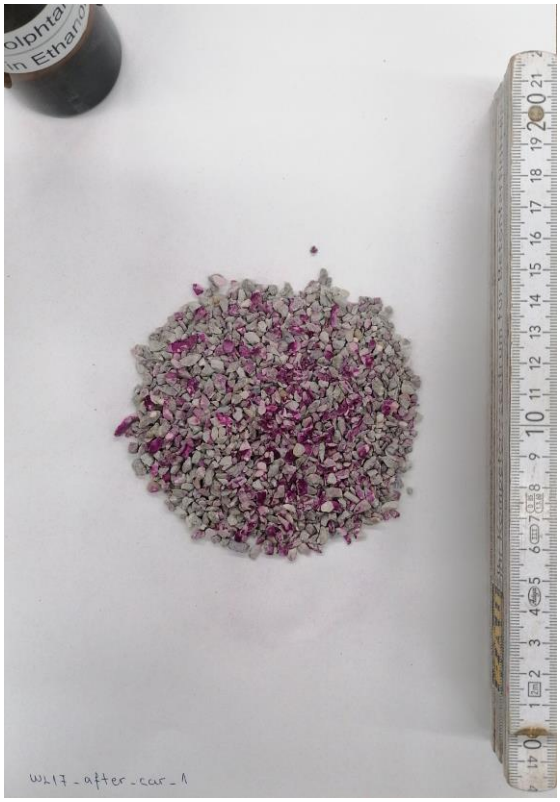

Box 1

Box 2

Box 3

Box 4

Fig. 11. Phenolphthalein test results for each box of experiment WL17 after CO_2 curing.

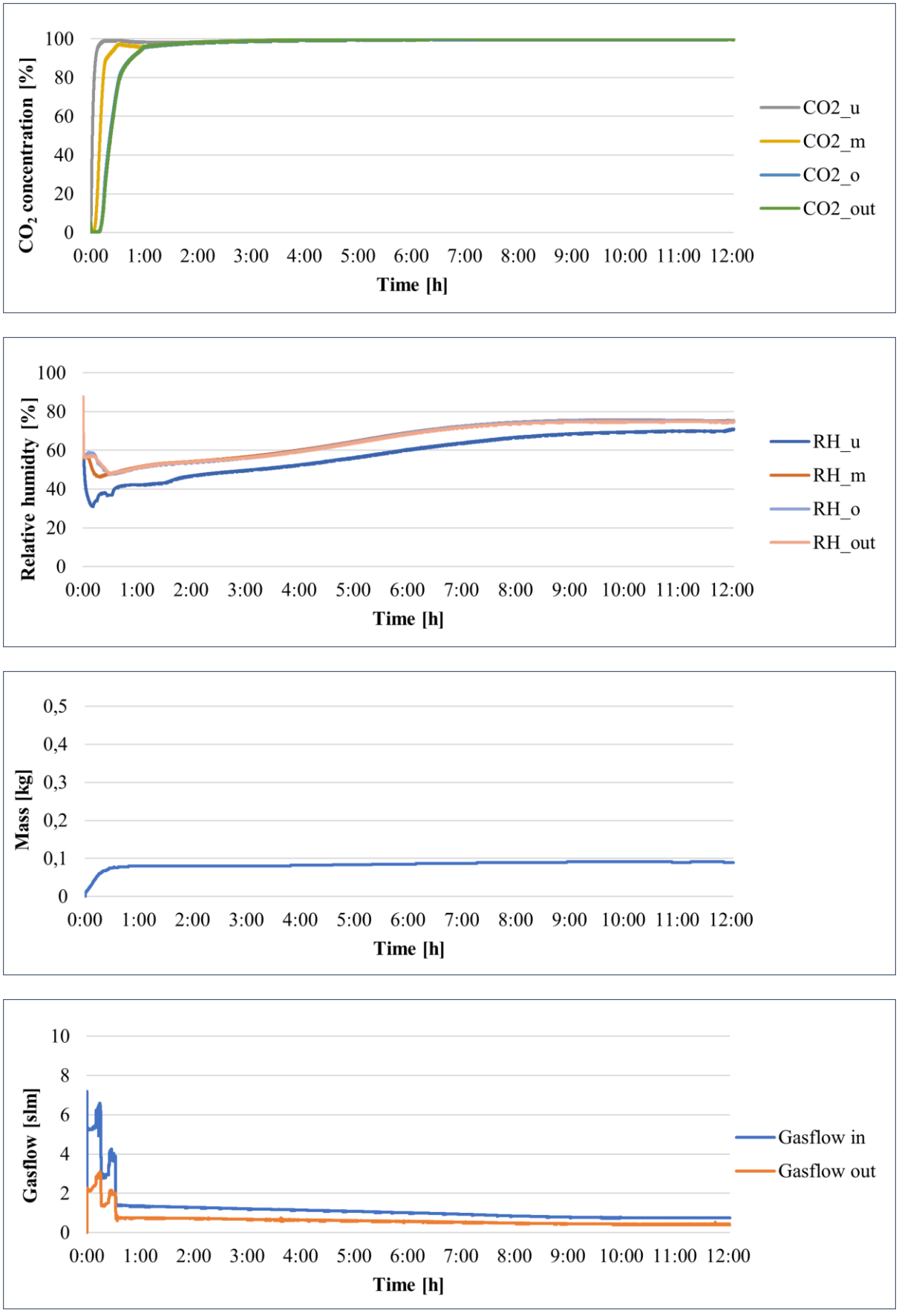

Fig. 12. The resulting diagrams for experiment WL17.

Appendix 4.5

Code: **WL18** Fraction: **1-2 mm** Duration: **8h**

Notes: There was a drop in the relative humidity value on the sensor RH_u (bottom of the chamber).

Table 8. Properties of the examined RCA before and after CO_2 curing for experiment WL18.

		$m_{ø}$ = 12011,60 g m_1 = 12101,20 g	Δm = 89,60 g
MC_{before} = 4,57 % MC_{after} = 4,51 %	→ →	m_{w_0} = 548,93 g m_{w_1} = 545,76 g	Δm_w = 3,17 g
			Δm_{bal} = 144,00 g Δm_{gas} = 69,00 g
$\Delta M_{car.\ 1}$ = 78,17 g		$\Delta M_{car.\ 2}$ = 92,77 g	CO_2 uptake = **0,77 %**

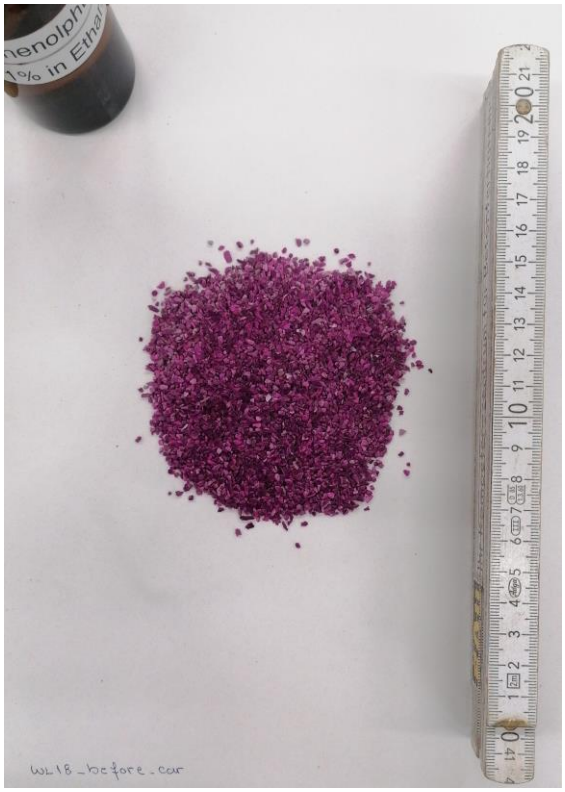

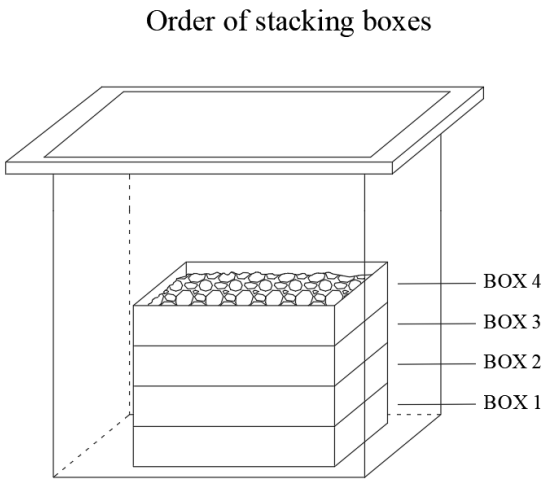

Fig. 13. Phenolphthalein test results before CO_2 curing for experiment WL18.

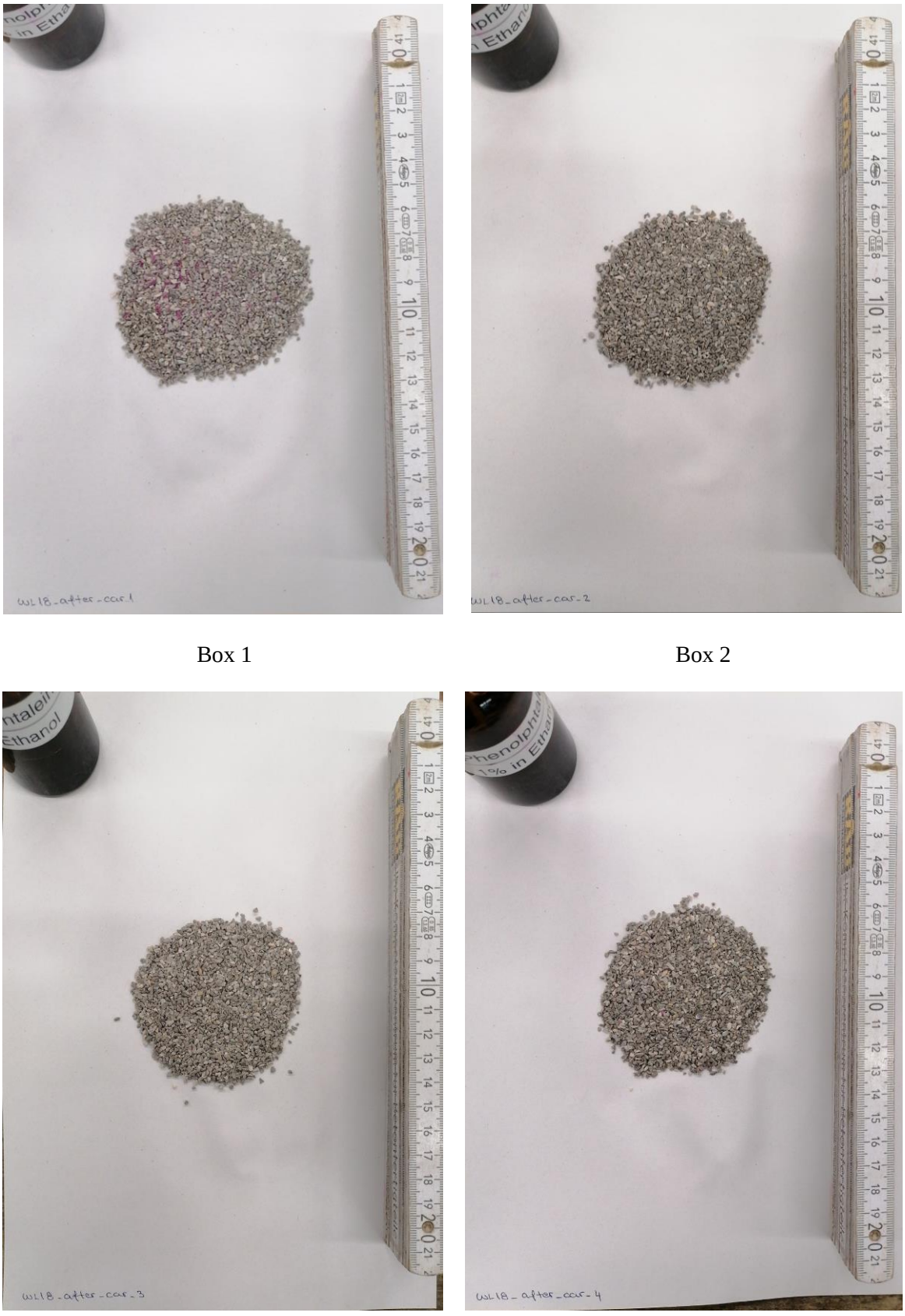

Box 1 Box 2

Box 3 Box 4

Fig. 14. Phenolphthalein test results for each box of experiment WL18 after CO_2 curing.

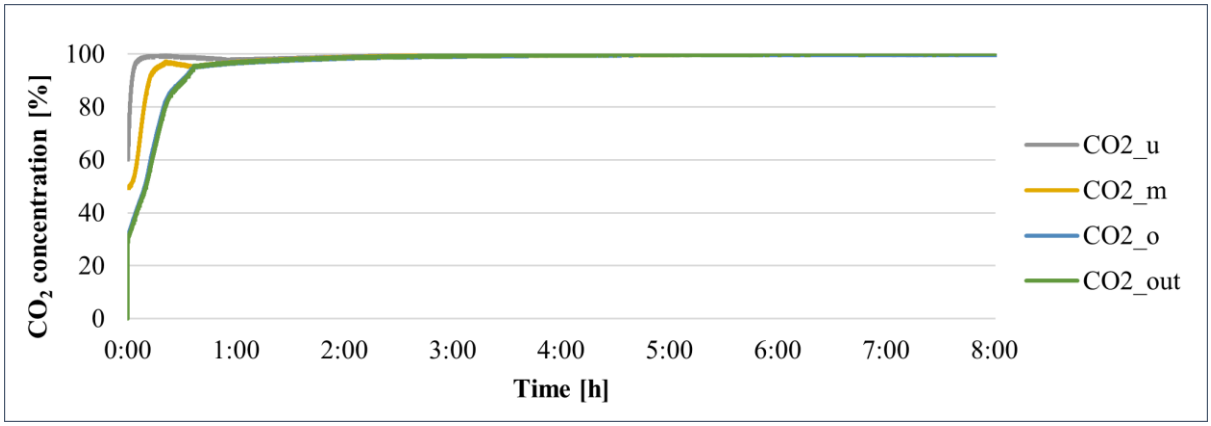

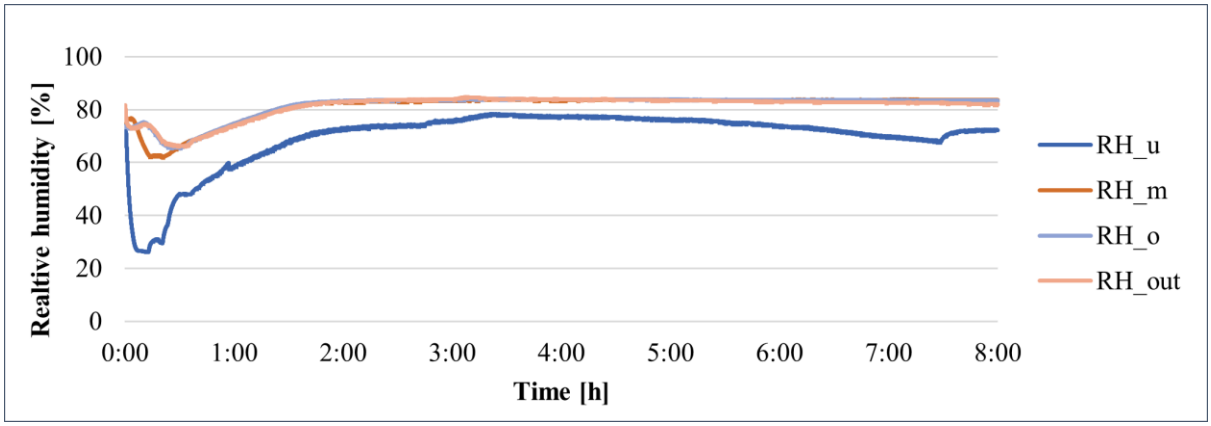

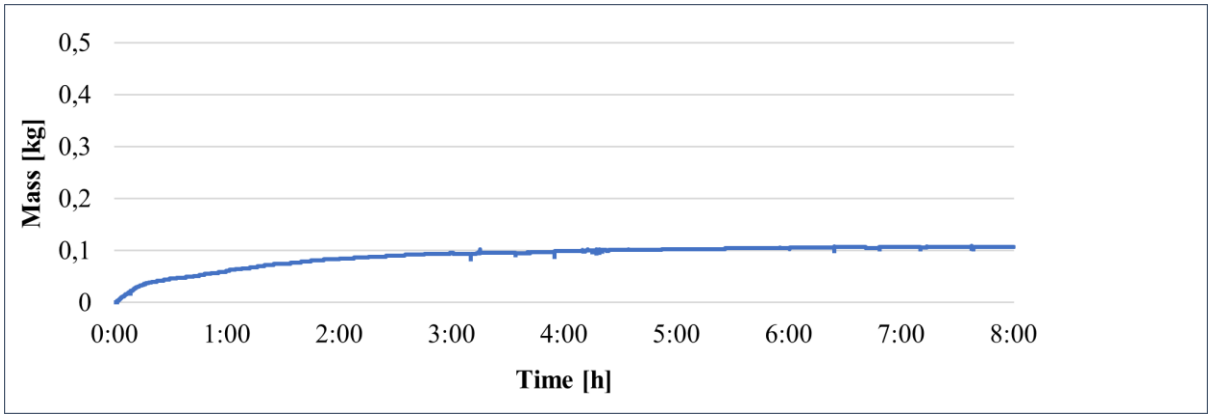

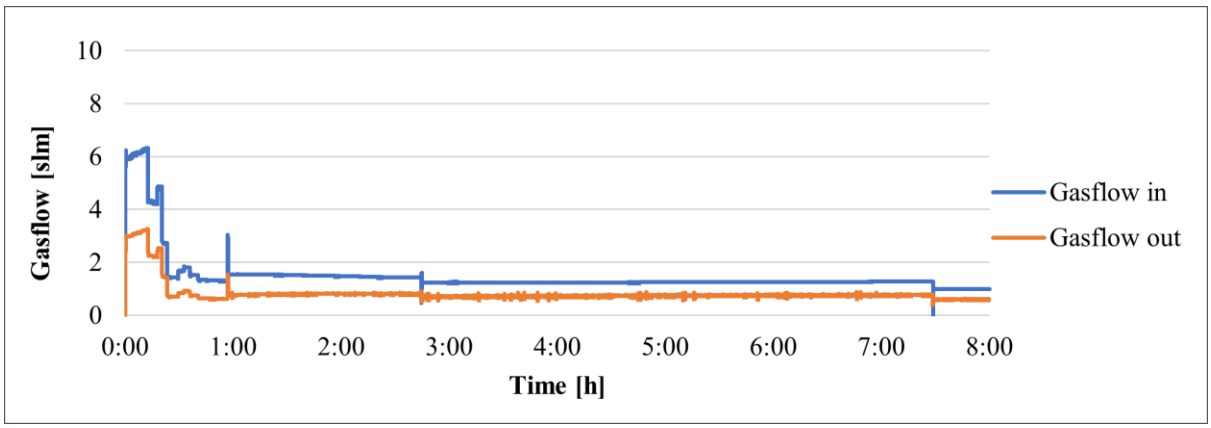

Fig. 15. The resulting diagrams for experiment WL18.

Appendix 4.6

Code: **WL19** Fraction: **0-0,25 mm** Duration: **4h**

Notes: At the end of the CO2 curing, the RCA was heated and moist. Dewing in the chamber was observed, especially in the lower part.

Table 9. Properties of the examined RCA before and after CO_2 curing for experiment WL19.

		$m_{ø}$ = 12000,45 g m_1 = 12310,85 g	Δm = 310,40 g
MC_{before} = 6,32 %	→	m_{w_0} = 758,43 g	Δm_w = -86,10 g
MC_{after} = 6,86 %	→	m_{w_1} = 844,52 g	
			Δm_{bal} = 448,00 g Δm_{gas} = 69,00 g
$\Delta M_{car.\ 1}$ = 292,90 g		$\Delta M_{car.\ 2}$ = 224,30 g	CO_2 uptake = **1,87 %**

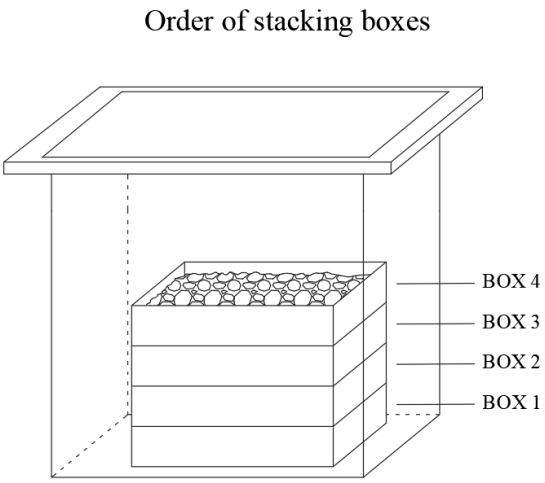

Fig. 16. Phenolphthalein test results before CO_2 curing for experiment WL19.

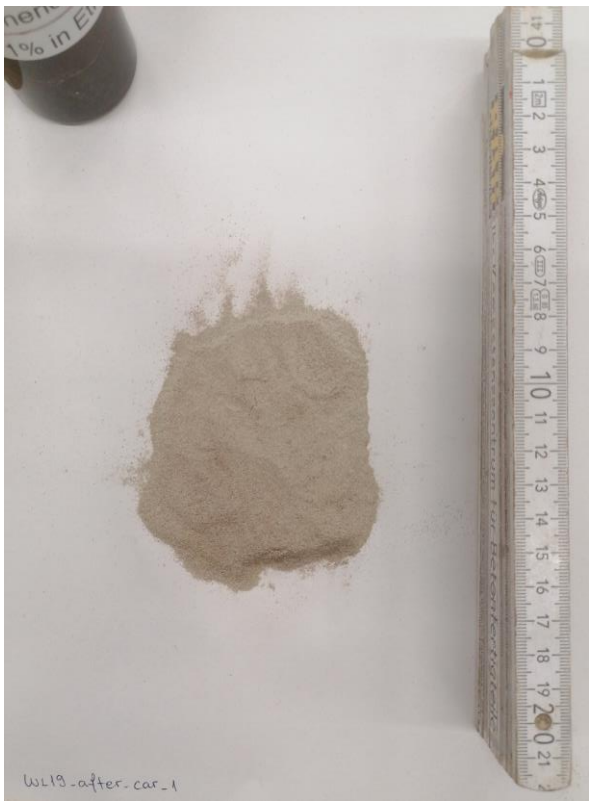

Box 1

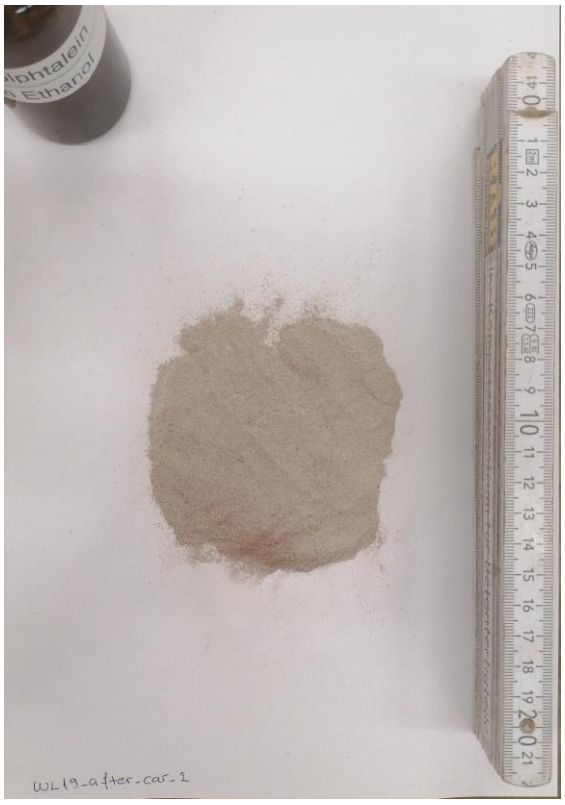

Box 2

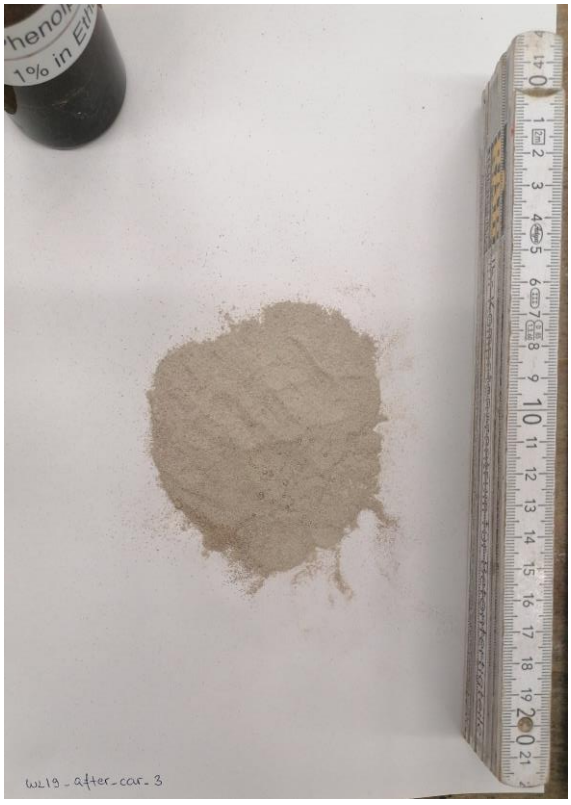

Box 3

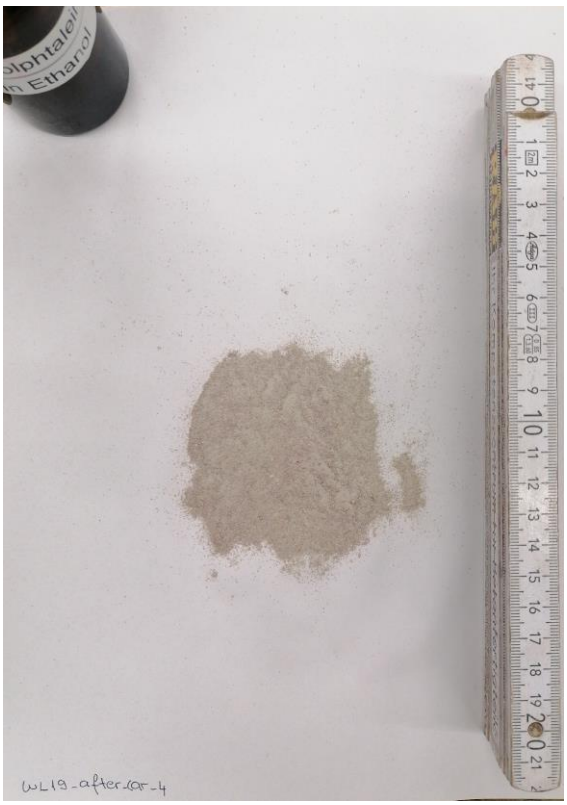

Box 4

Fig. 17. Phenolphthalein test results for each box of experiment WL19 after CO_2 curing.

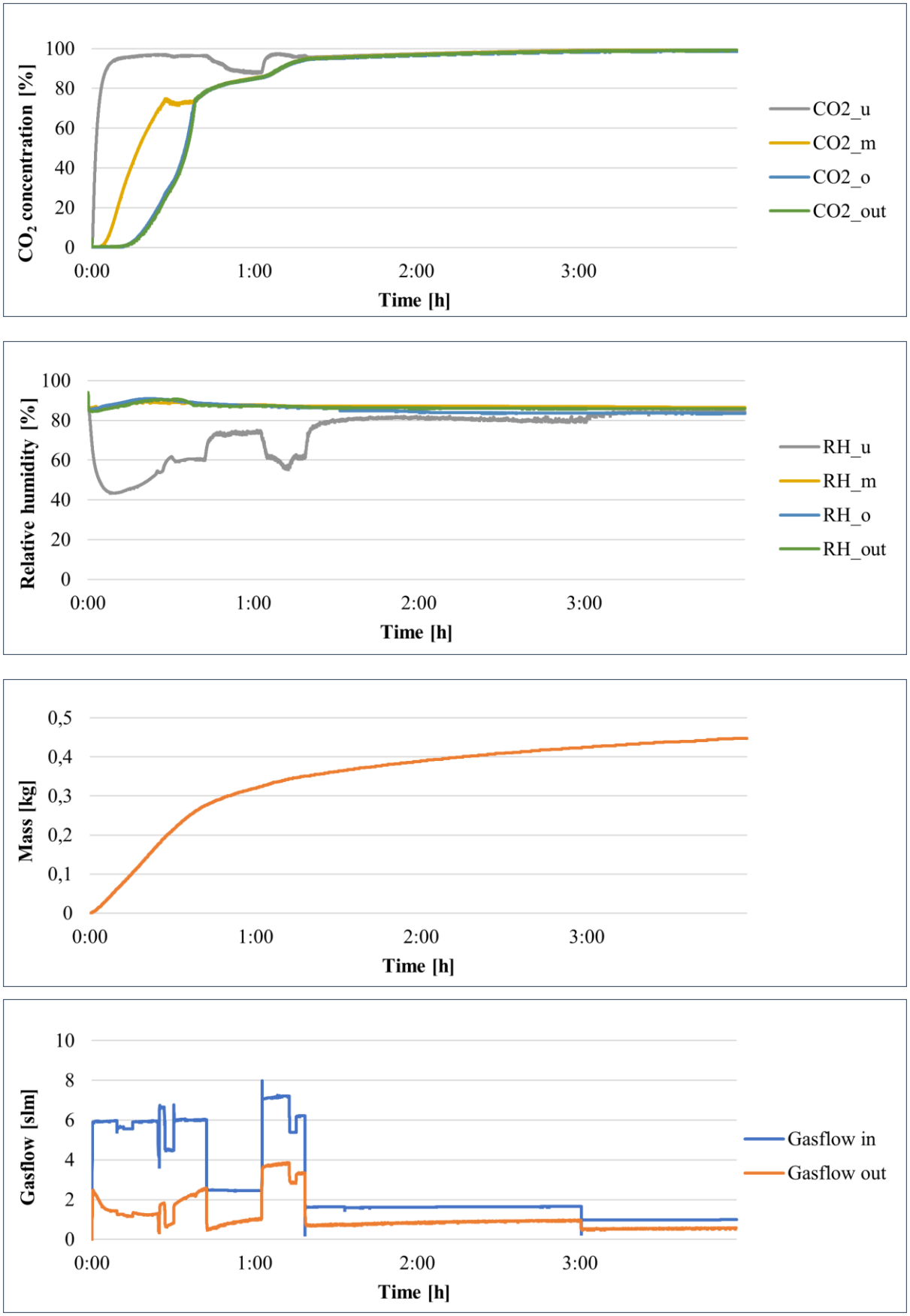

Fig. 18. The resulting diagrams for experiment WL19.

Appendix 4.7

Code: **WL20** Fraction: **8-16 mm** Duration: **12h**

Notes: Complete carbonation did not occur in all boxes, especially in the one at the bottom of the chamber. A significant drop in relative humidity was also observed.

Table 10. Properties of the examined RCA before and after CO_2 curing for experiment WL20.

		$m_{ø}$ = 11978,30 g m_1 = 12015,80 g	Δm = 37,50 g
MC_{before} = 3,33 %	→	m_{w_0} = 398,88 g	Δm_w = 3,56 g
MC_{after} = 3,29 %	→	m_{w_1} = 395,32 g	
			Δm_{bal} = 84,00 g Δm_{gas} = 69,00 g
$\Delta M_{car.\ 1}$ = 18,56 g		$\Delta M_{car.\ 2}$ = 41,06 g	CO_2 uptake = **0,34 %**

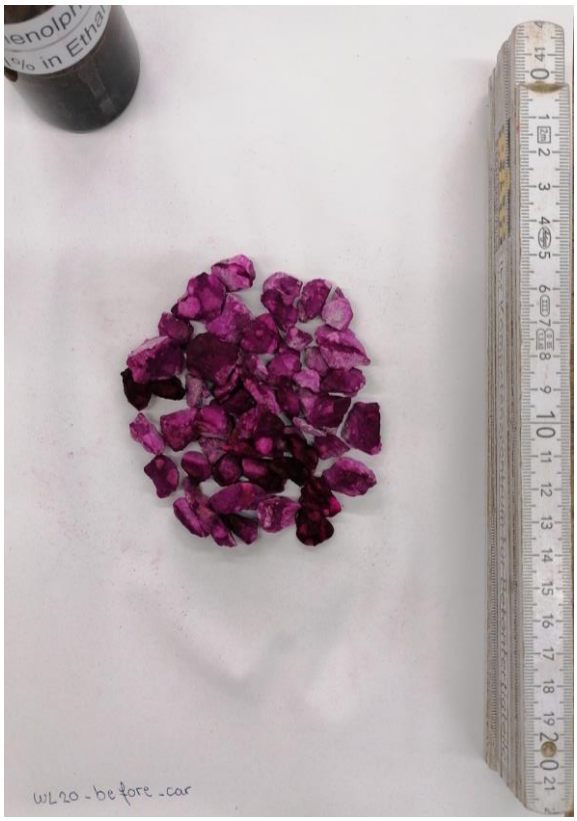

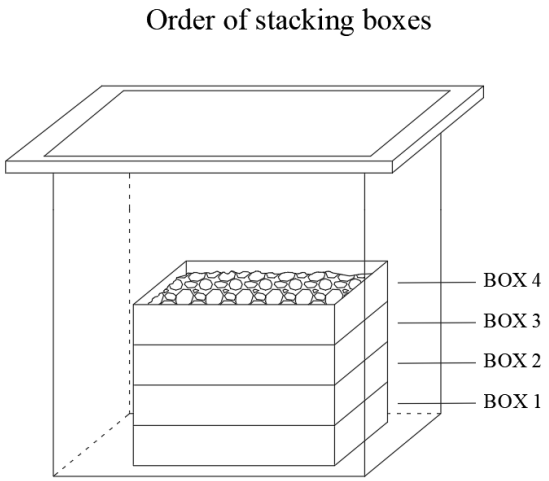

Fig. 19. Phenolphthalein test results before CO_2 curing for experiment WL20.

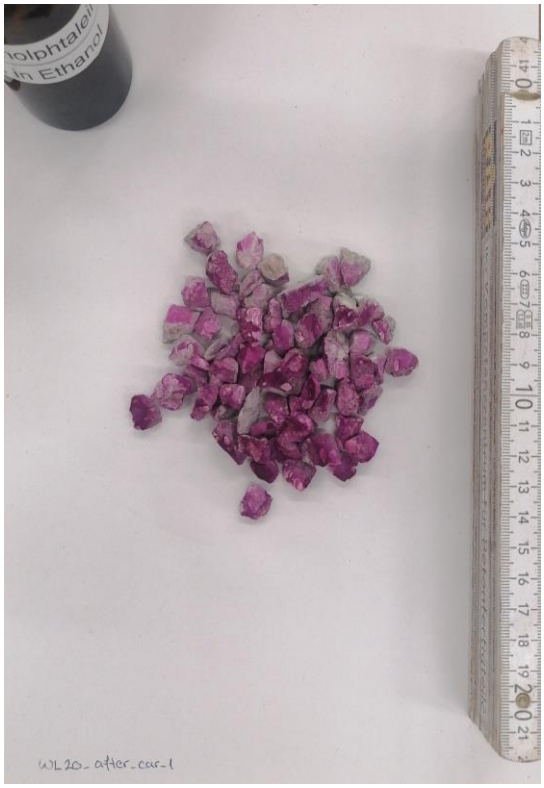

Box 1

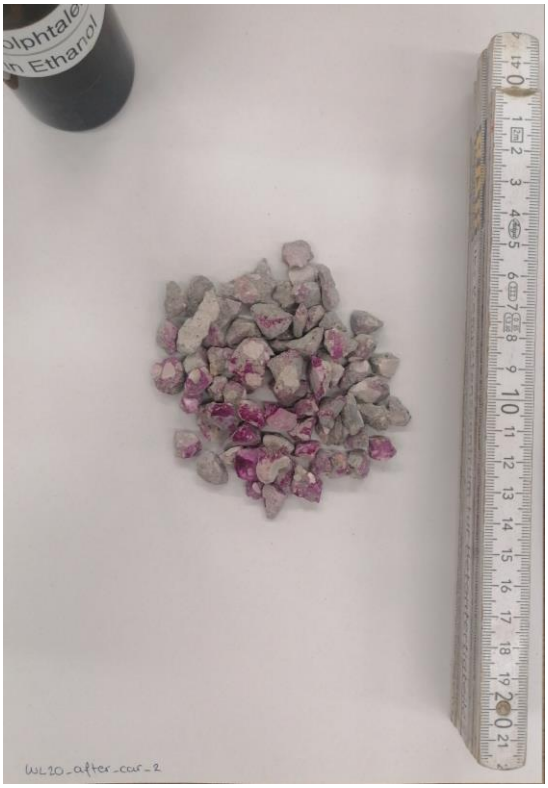

Box 2

Box 3

Box 4

Fig. 20. Phenolphthalein test results for each box of experiment WL20 after CO_2 curing.

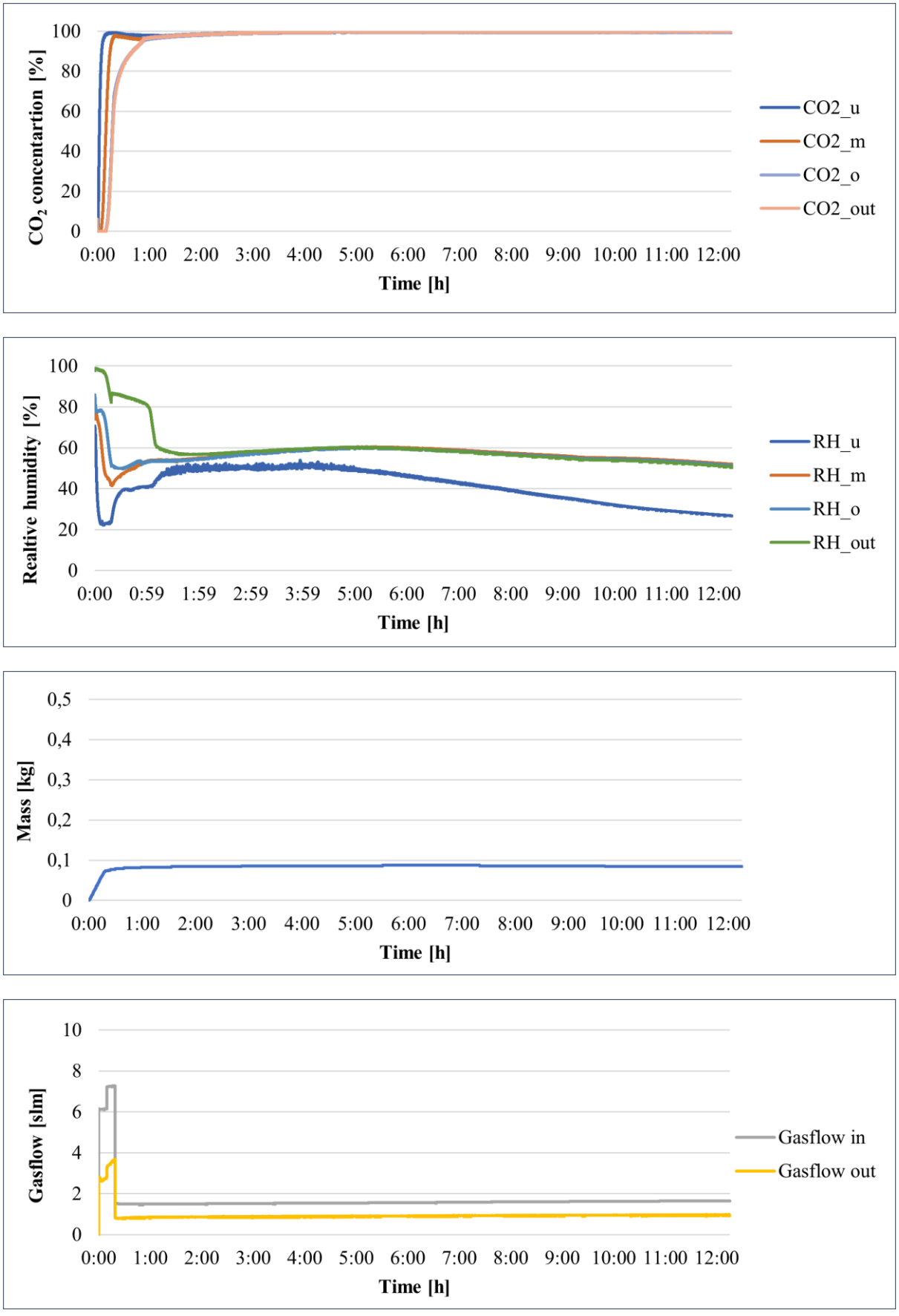

Fig. 21. The resulting diagrams for experiment WL20.

Appendix 4.8

Code: **WL21** Fraction: **1-2 mm** Duration: **8h**

Table 11. Properties of the examined RCA before and after CO_2 curing for experiment WL21.

		$m_{ø}$ = 12007,35 g m_1 = 12134,35 g	Δm = 127,00 g
MC_{before} = 4,52 % MC_{after} = 4,84 %	→ →	m_{w_0} = 542,73 g m_{w_1} = 587,30 g	Δm_w = -44,57 g
			Δm_{bal} = 198,00 g Δm_{gas} = 69,00 g
$\Delta M_{car.\ 1}$ = 84,43 g		$\Delta M_{car.\ 2}$ = 82,43 g	CO_2 uptake = **0,69 %**

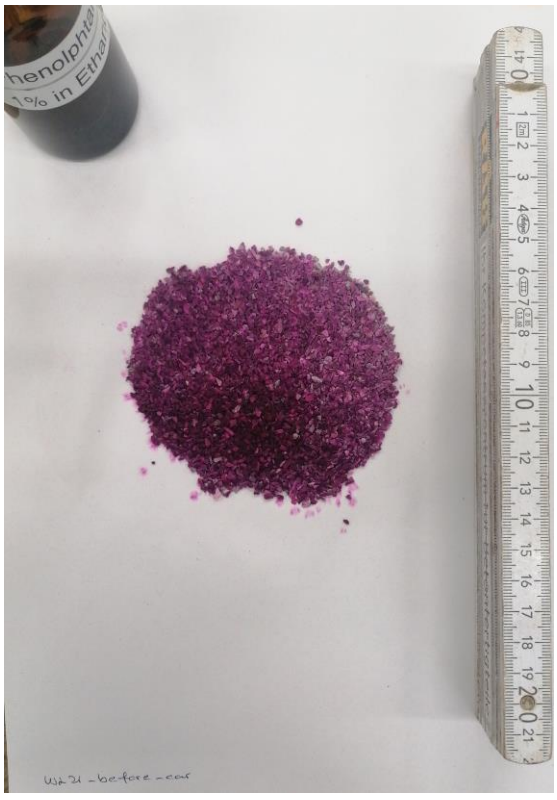

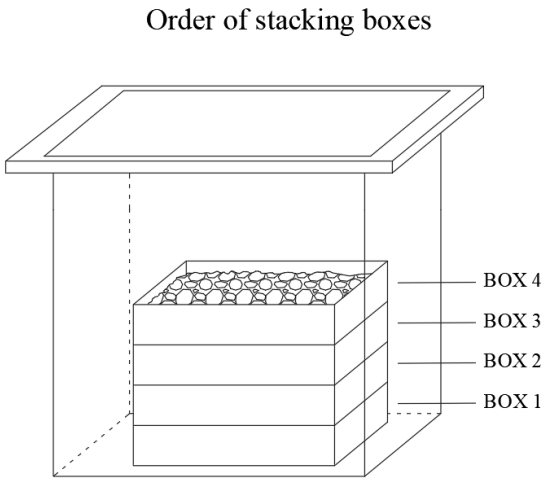

Fig. 22. Phenolphthalein test results before CO_2 curing for experiment WL21.

Box 1

Box 2

Box 3

Box 4

Fig. 23. Phenolphthalein test results for each box of experiment WL21 after CO_2 curing.

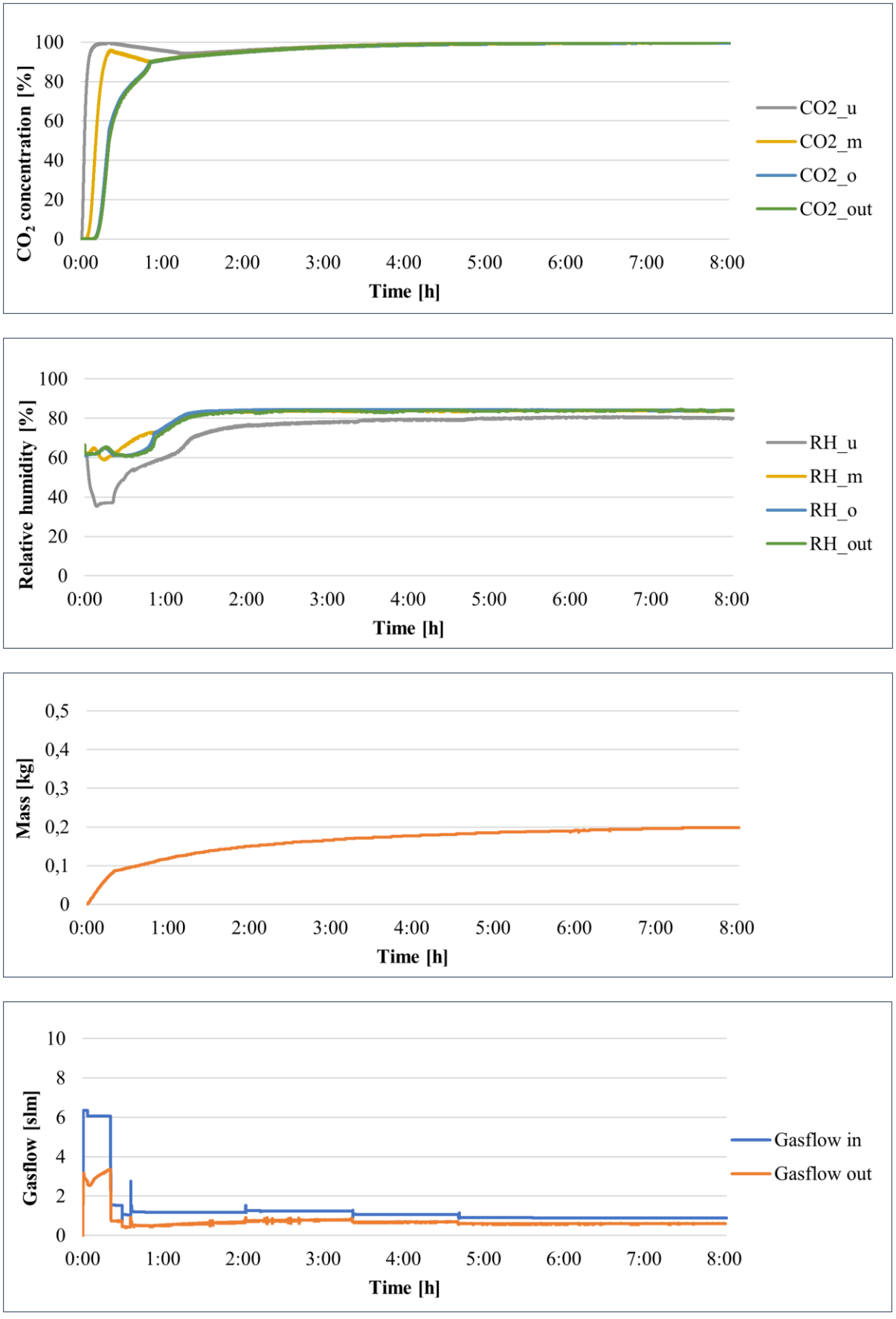

Fig. 24. The resulting diagrams for experiment WL21.

Appendix 4.9

Code: **WL22** Fraction: **0-0,25 mm** Duration: **4h 30min**

Table 12. Properties of the examined RCA before and after CO_2 curing for experiment WL22.

		$m_{ø}$ = 12005,30 g m_1 = 12349,70 g	Δm = 344,00 g
MC_{before} = 6,74 %	→	m_{w_0} = 809,16 g	Δm_w = -96,07 g
MC_{after} = 7,33 %	→	m_{w_1} = 905,23 g	
			Δm_{bal} = 436,00 g Δm_{gas} = 69,00 g
$\Delta M_{car.\ 1}$ = 270,92 g		$\Delta M_{car.\ 2}$ = 248,32 g	CO_2 uptake = **2,07 %**

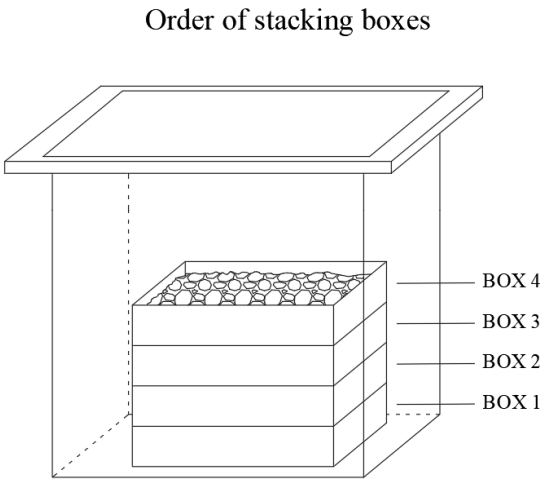

Fig. 25. Phenolphthalein test results before CO_2 curing for experiment WL22.

Box 1

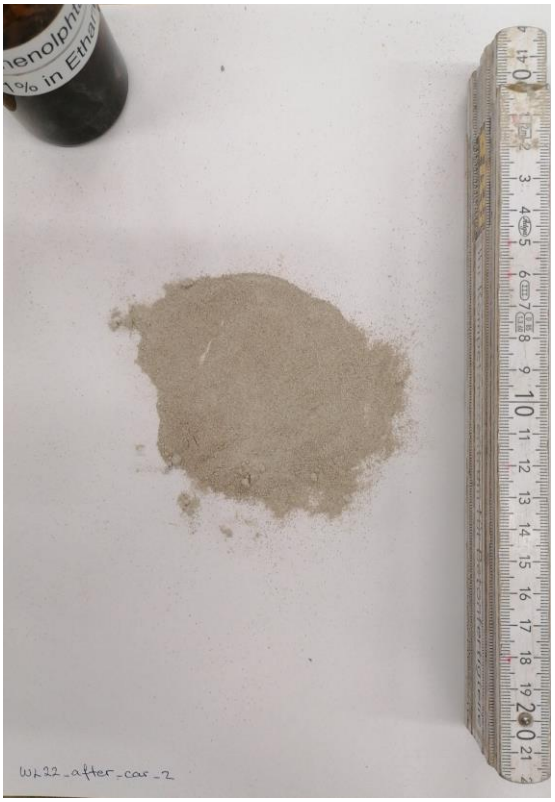

Box 2

Box 3

Box 4

Fig. 26. Phenolphthalein test results for each box of experiment WL22 after CO_2 curing.

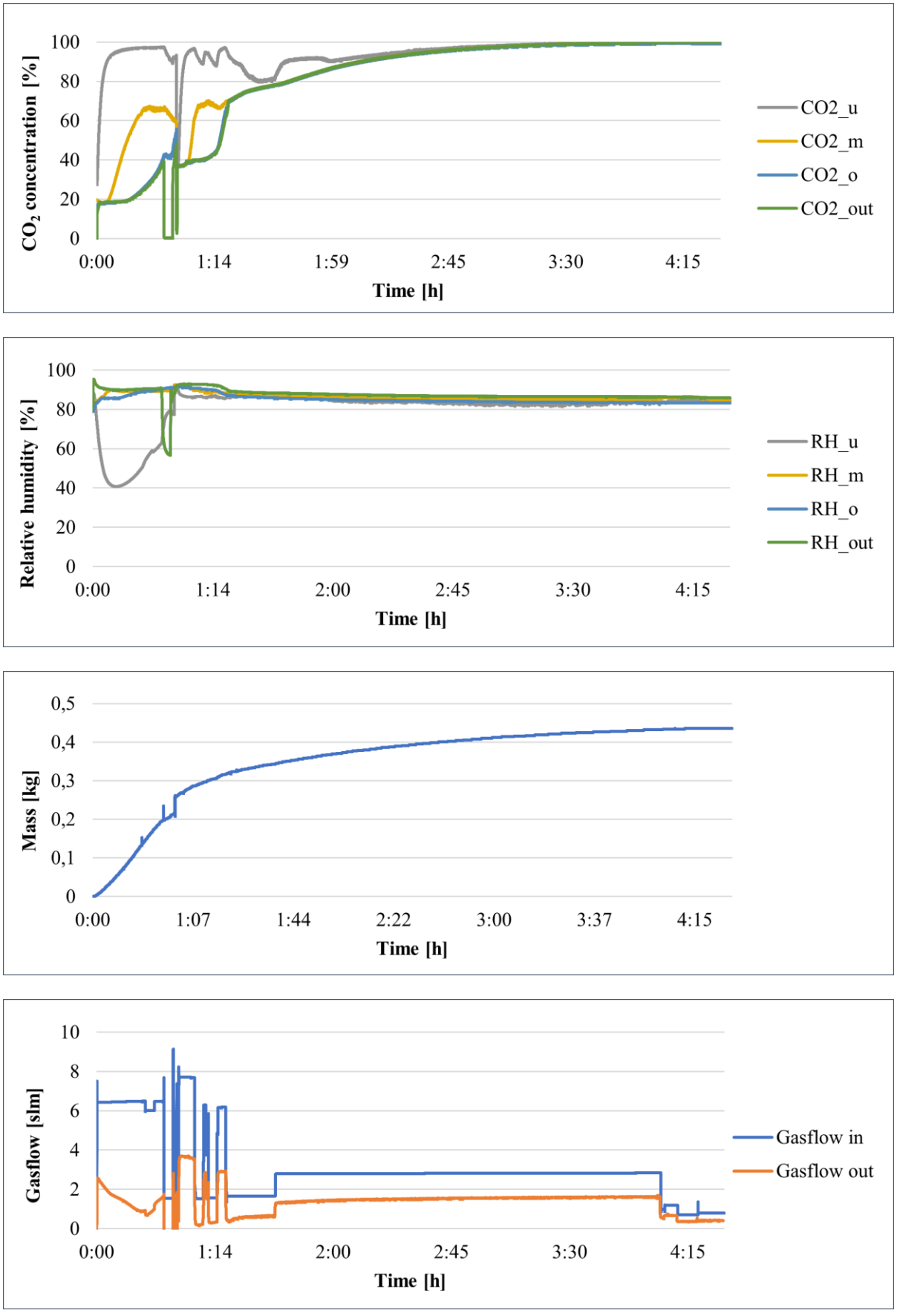

Fig. 27. The resulting diagrams for experiment WL22.

Appendix 4.10

Name: **WL23** Fraction: **0,25-0,5 mm** Duration: **4h**

Table 13. Properties of the examined RCA before and after CO_2 curing for experiment WL23.

		$m_{ø}$ = 11995,95 g m_1 = 12171,45 g	Δm = 175,50 g
MC $_{before}$ = 5,75 % MC $_{after}$ = 5,91 %	→ →	m_{w_0} = 689,77 g m_{w_1} = 719,33 g	Δm_w = -29,57 g
			Δm_{bal} = 275,00 g Δm_{gas} = 69,00 g
$\Delta M_{car.\ 1}$ = 176,43 g		$\Delta M_{car.\ 2}$ = 145,93 g	CO_2 uptake = **1,22 %**

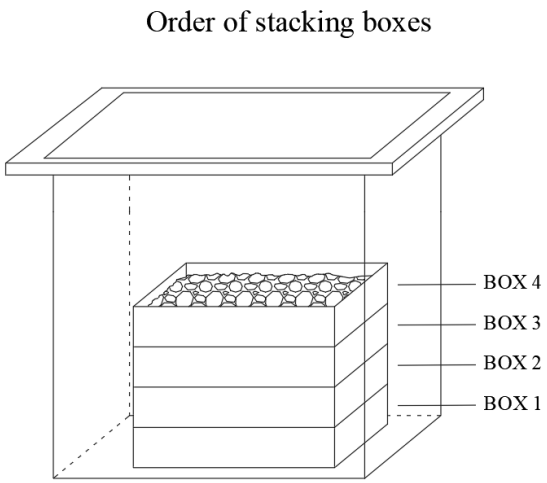

Fig. 28. Phenolphthalein test results before CO_2 curing for experiment WL23.

Box 1

Box 2

Box 3

Box 4

Fig. 29. Phenolphthalein test results for each box of experiment WL23 after CO_2 curing.

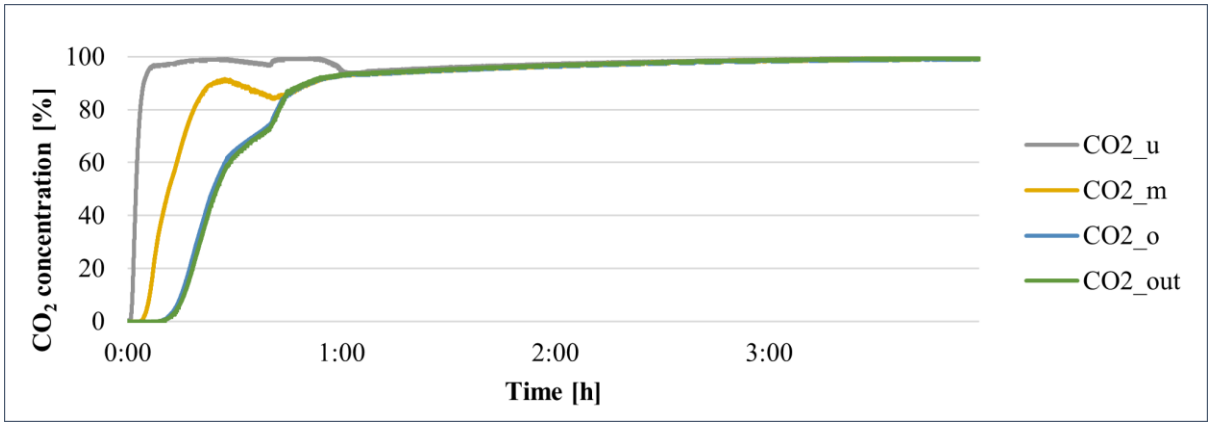

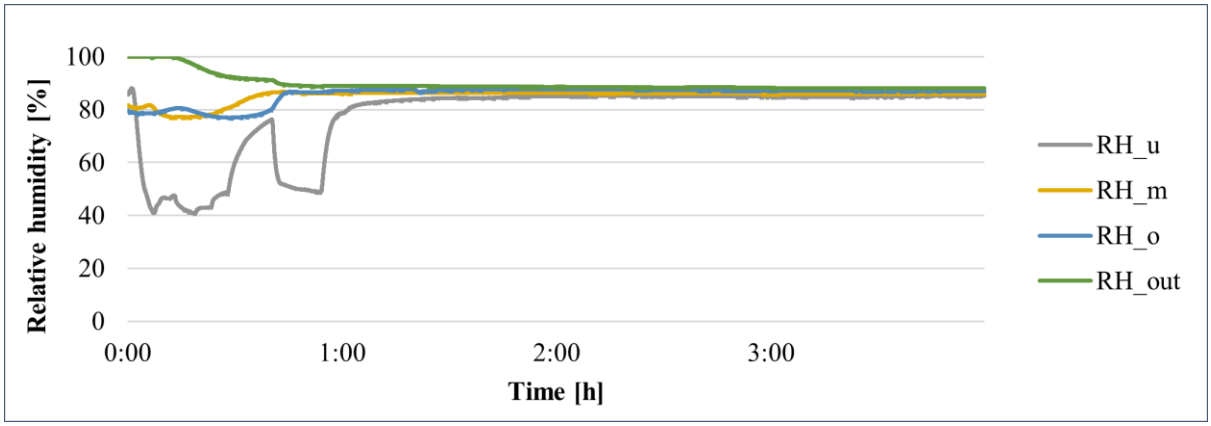

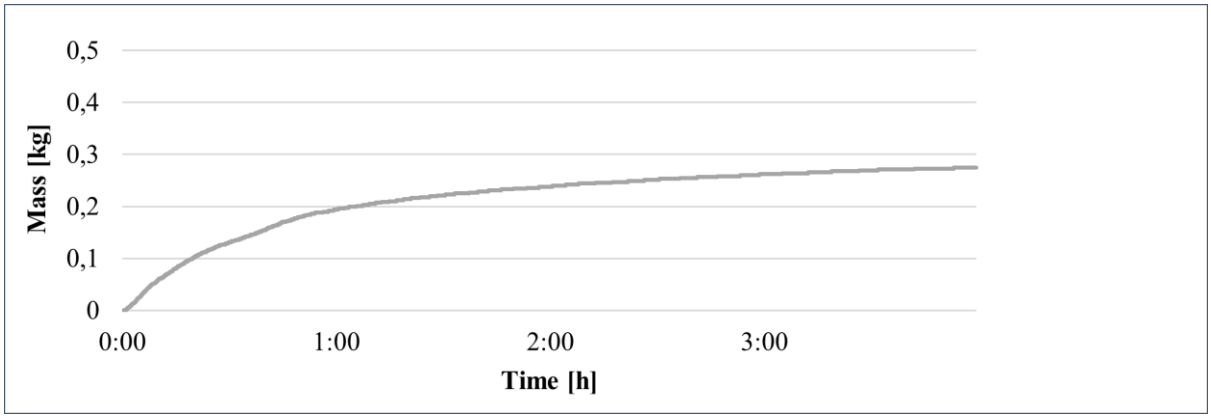

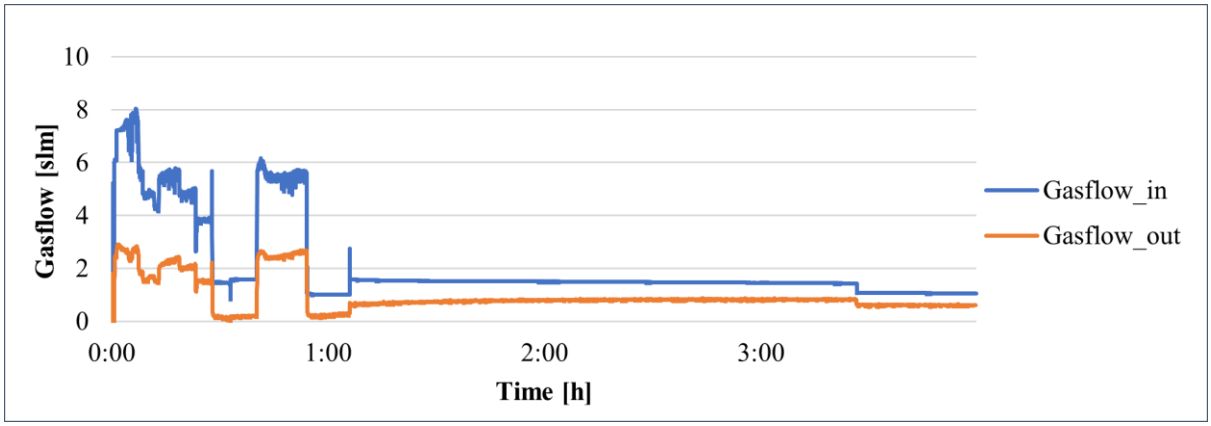

Fig. 30. The resulting diagrams for experiment WL23.

Appendix 4.11

Code: **WL24** Fraction: **0,5-1 mm** Duration: **8h**

Table 14. Properties of the examined RCA before and after CO_2 curing for experiment WL24.

		$m_{ø}$ = 11989,56 g m_1 = 12120,45 g	Δm = 130,89 g
MC_{before} = 5,08 %	→	m_{w_0} = 609,07 g	Δm_w = -5,44 g
MC_{after} = 5,07 %	→	m_{w_1} = 614,51 g	
			Δm_{bal} = 220,00 g Δm_{gas} = 69,00 g
$\Delta M_{car.\ 1}$ = 145,56 g		$\Delta M_{car.\ 2}$ = 125,45 g	CO_2 uptake = **1,05 %**

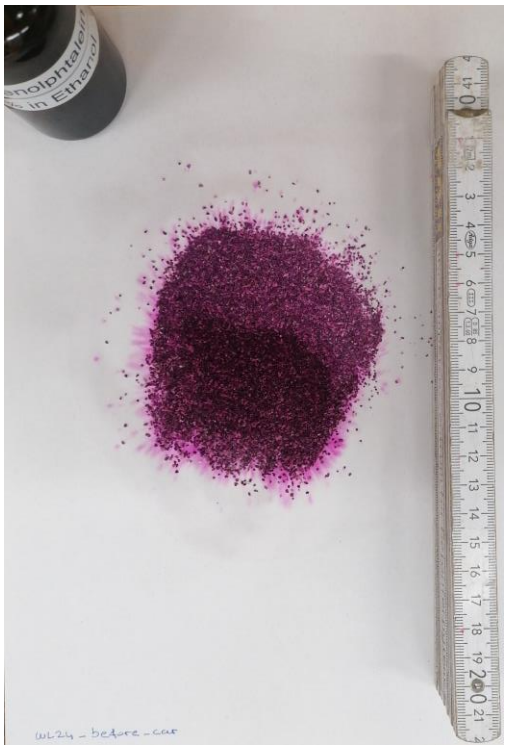

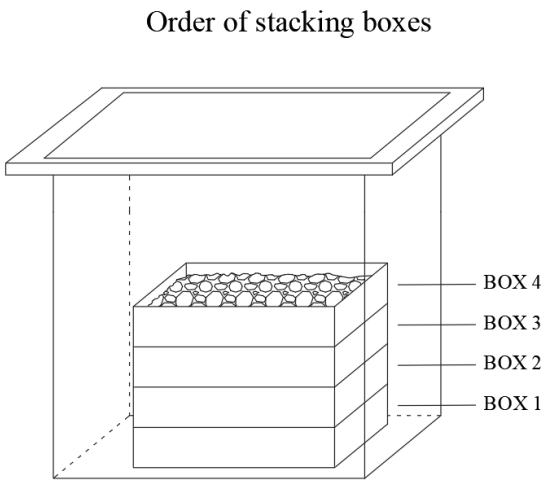

Fig. 31. Phenolphthalein test results before CO_2 curing for experiment WL24.

Box 1

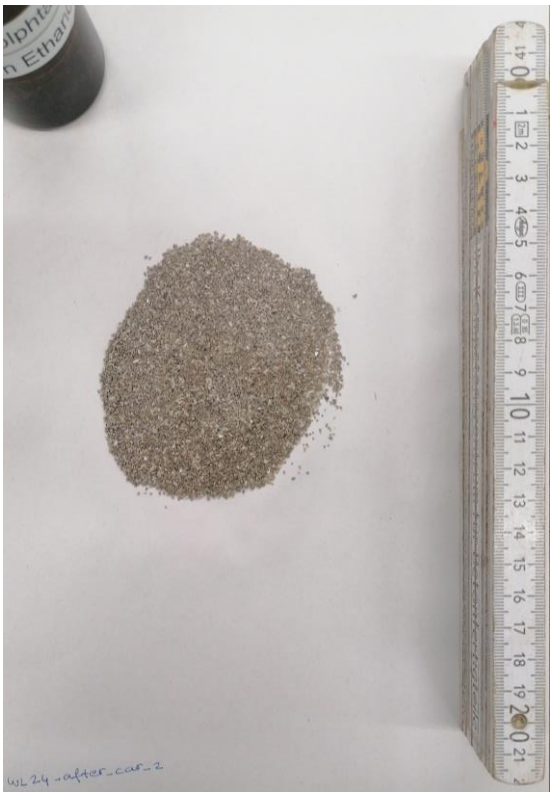

Box 2

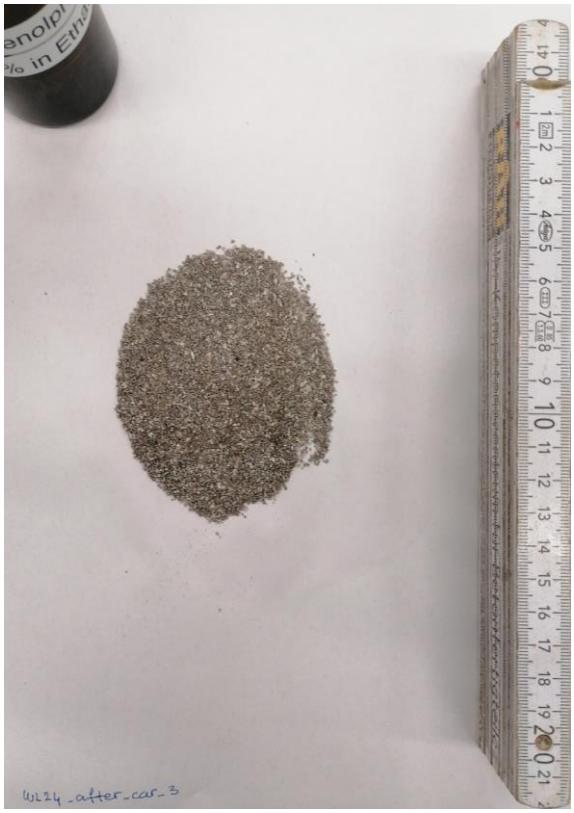

Box 3

Box 4

Fig. 32. Phenolphthalein test results for each box of experiment WL24 after CO_2 curing.

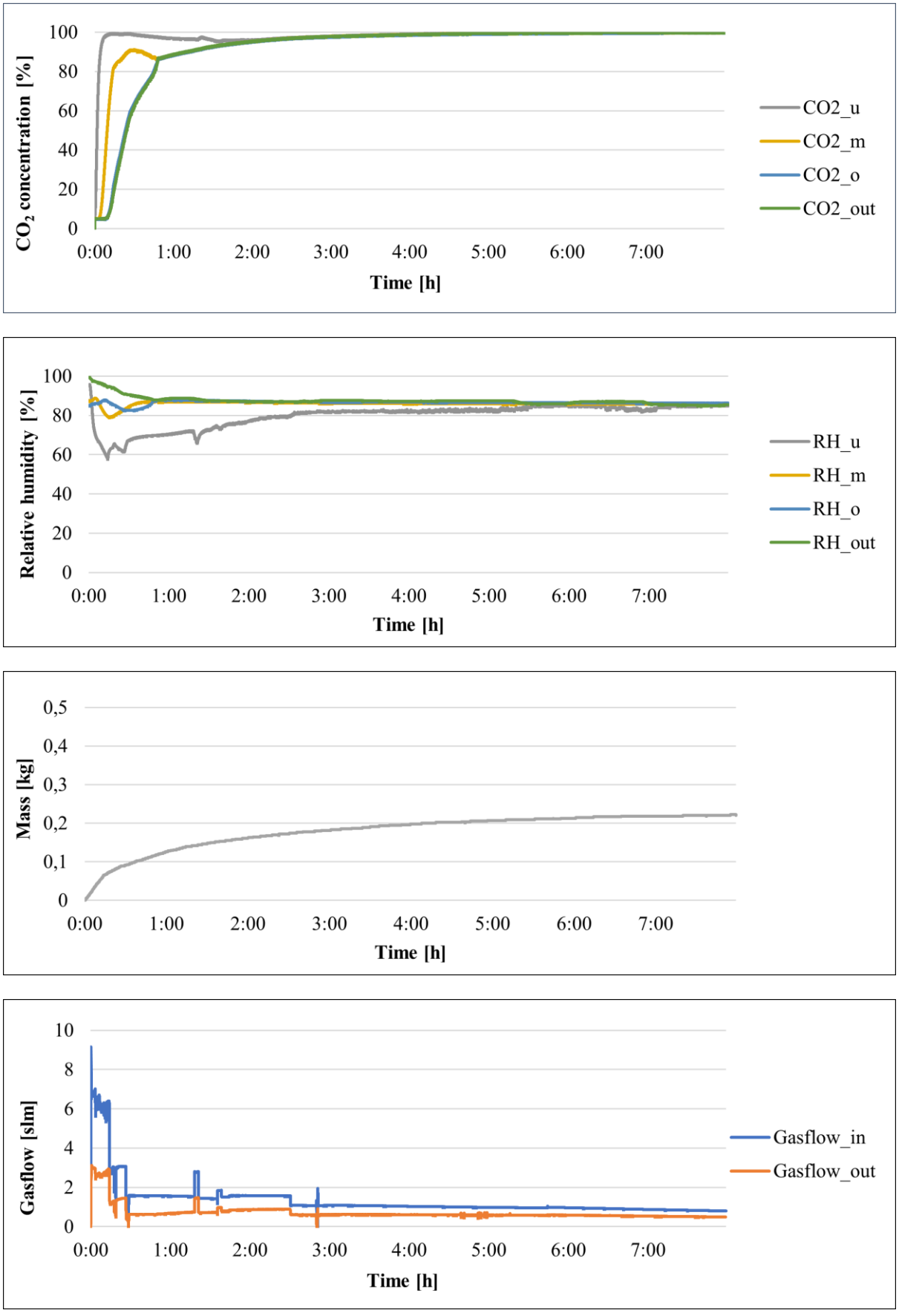

Fig. 33. The resulting diagrams for experiment WL24.

Appendix 4.12

Code: **WL25** Fraction: **0,25-0,5 mm** Duration: **4h**

Table 15. Properties of the examined RCA before and after CO_2 curing for experiment WL25.

		$m_{ø}$ = 10009,15 g m_1 = 10150,00 g	Δm = 140,85 g
MC $_{before}$ = 6,25 %	→	m_{w_0} = 625,57 g	Δm_w = 17,59 g
MC $_{after}$ = 5,99%	→	m_{w_1} = 607,99 g	
			Δm_{bal} = 229,00 g Δm_{gas} = 69,00 g
$\Delta M_{car.\ 1}$ = 177,59 g		$\Delta M_{car.\ 2}$ = 158,44 g	CO_2 uptake = **1,58 %**

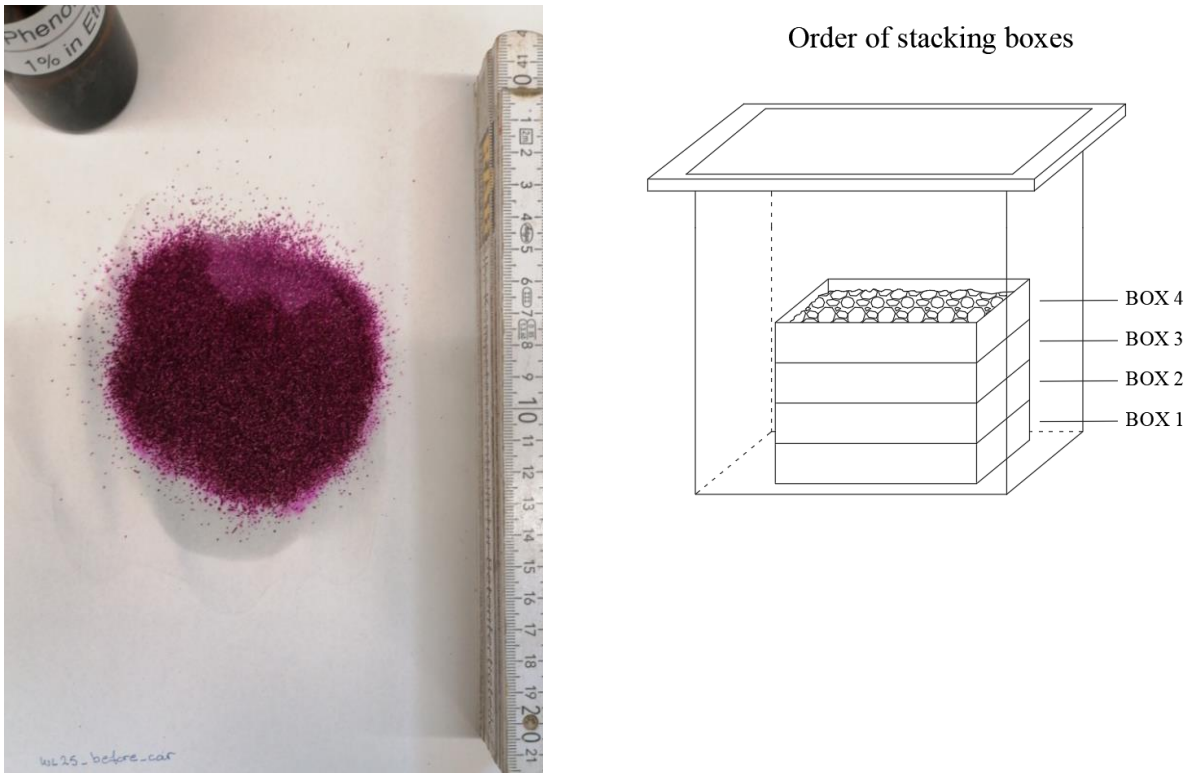

Fig. 34. Phenolphthalein test results before CO_2 curing for experiment WL25.

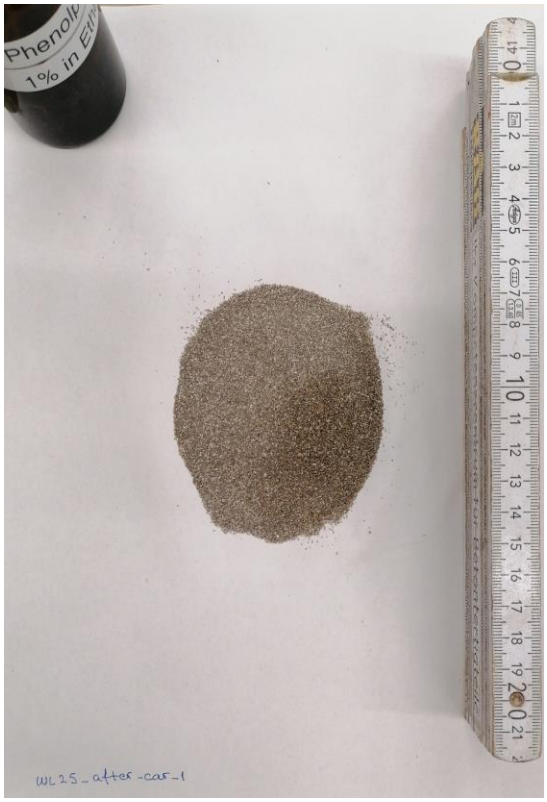

Box 1

Box 2

Box 3

Box 4

Fig. 35. Phenolphthalein test results for each box of experiment WL25 after CO_2 curing.

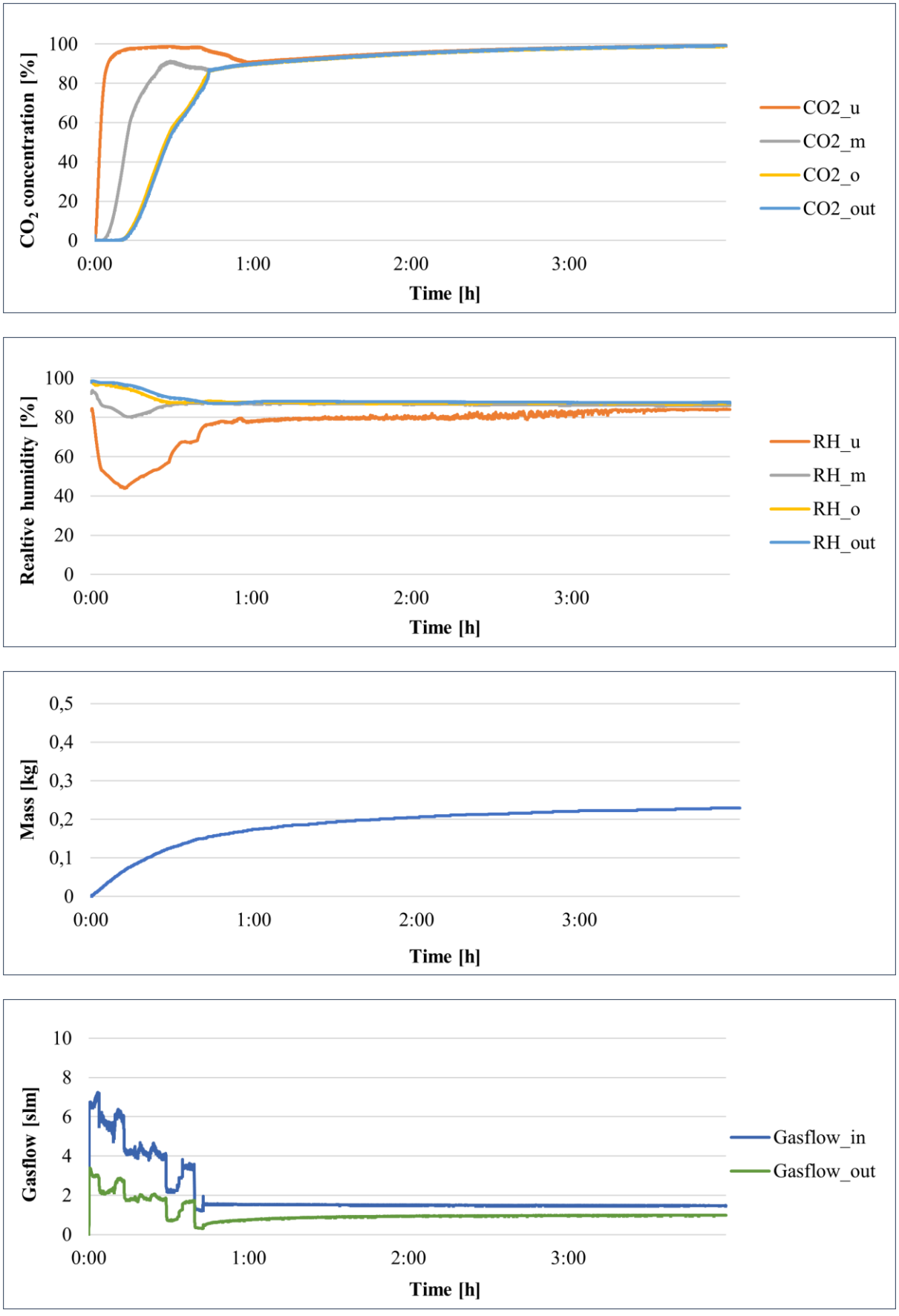

Fig. 36. The resulting diagrams for experiment WL25.

Appendix 4.13

Code: **WL26** Fraction: **8-16 mm** Duration: **12h**

Notes: In the box at the bottom of the chamber, complete carbonation did not occur. A significant drop in relative humidity was observed in the lower part of the chamber.

Table 16. Properties of the examined RCA before and after CO_2 curing for experiment WL26.

		$m_{ø}$ = 12050,40 g m_1 = 12075,75 g	Δm = 25,35 g
MC_{before} = 3,68 %	→	m_{w_0} = 443,33 g	Δm_w = -1,05 g
MC_{after} = 3,68 %	→	m_{w_1} = 607,99 g	
			Δm_{bal} = 80,00 g Δm_{gas} = 69,00 g
$\Delta M_{car.\ 1}$ = 9,95 g		$\Delta M_{car.\ 2}$ = 24,30 g	CO_2 uptake = **0,20 %**

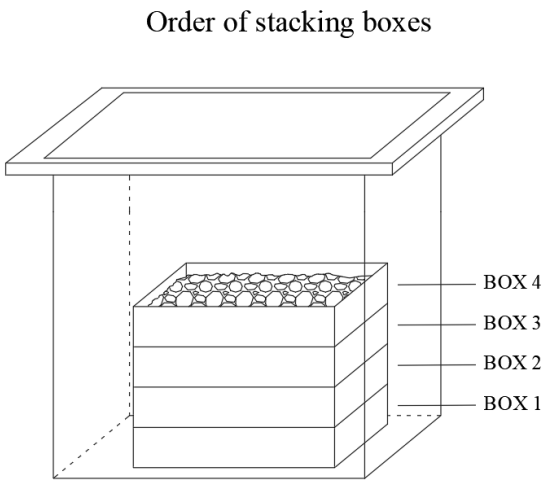

Fig. 37. Phenolphthalein test results before CO_2 curing for experiment WL26.

Box 1

Box 2

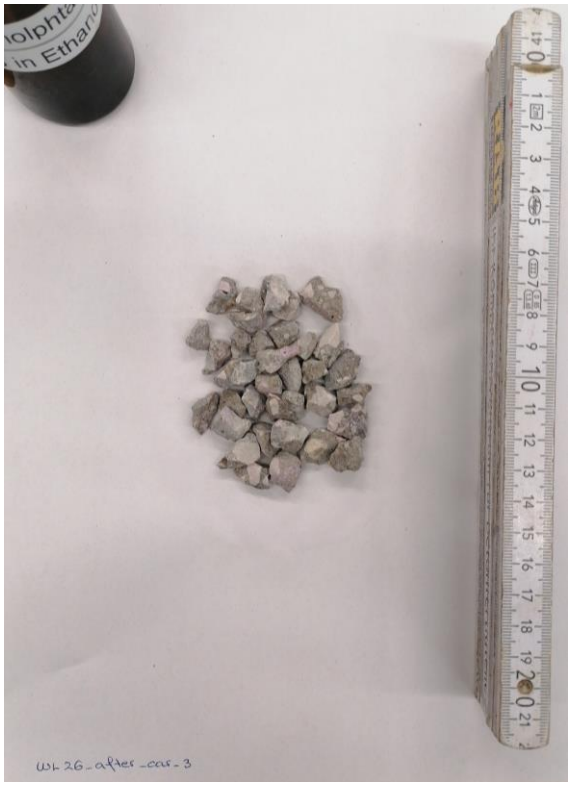

Box 3

Box 4

Fig. 38. Phenolphthalein test results for each box of experiment WL26 after CO_2 curing.

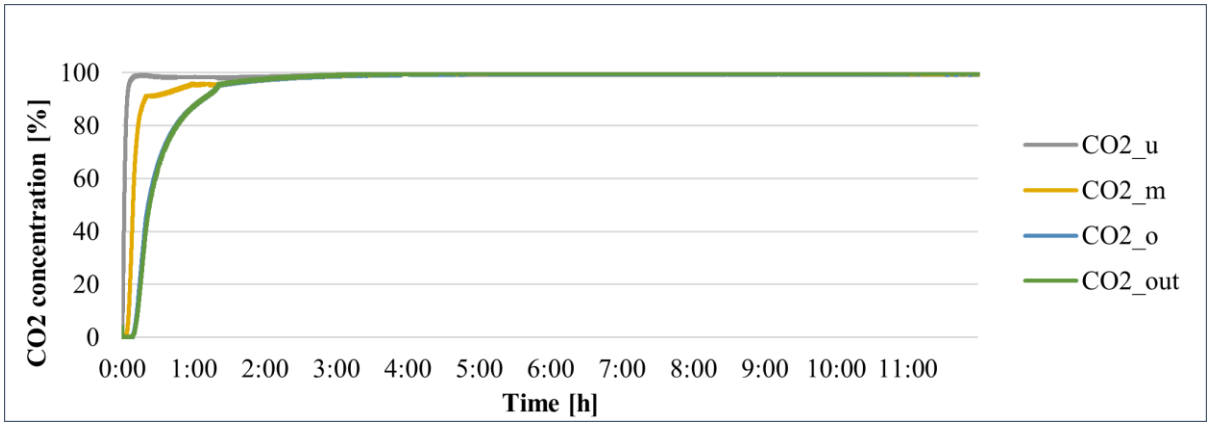

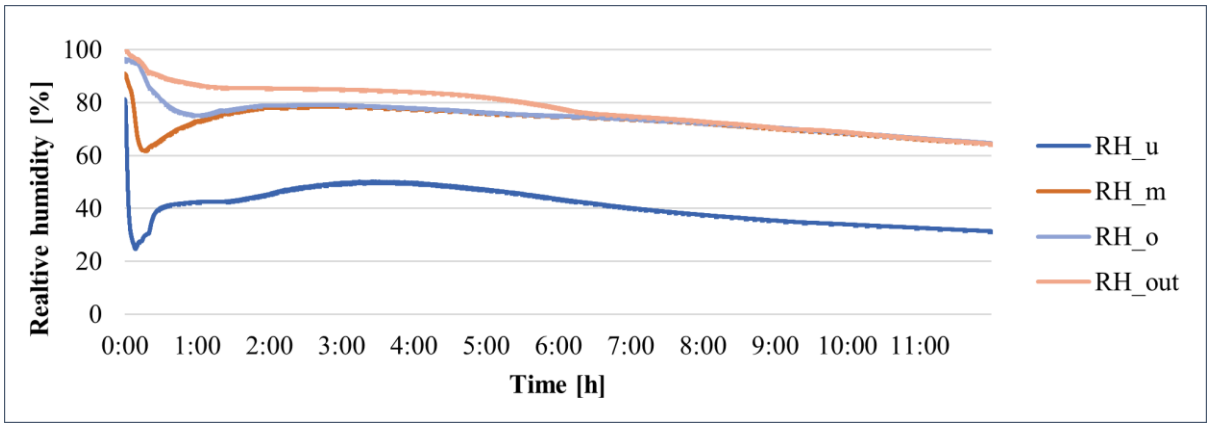

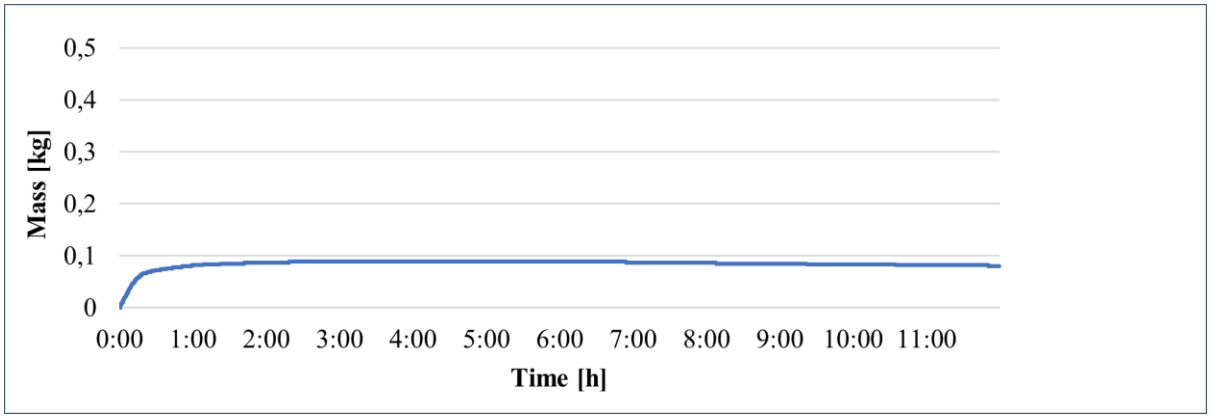

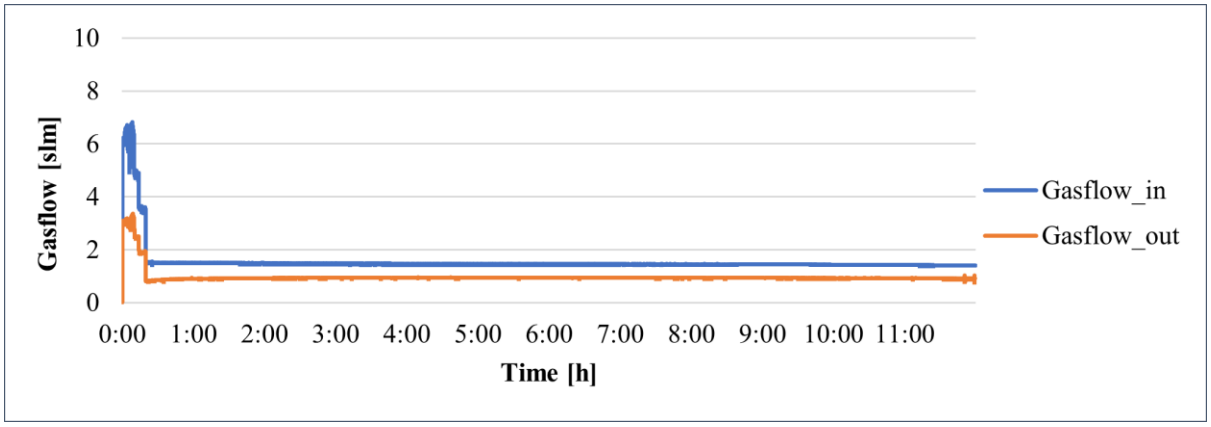

Fig. 39. The resulting diagrams for experiment WL26.

Appendix 4.14

Code: **WL27** Fraction: **0,5-1 mm** Duration: **8h**

Table 17. Properties of the examined RCA before and after CO_2 curing for experiment WL27.

		$m_{ø}$ = 12068,25 g m_1 = 12206,55 g	Δm = 138,30 g
MC_{before} = 5,25 %	→	m_{w_0} = 633,58 g	Δm_w = -37,78 g
MC_{after} = 5,50 %	→	m_{w_1} = 671,36 g	
			Δm_{bal} = 226,00 g Δm_{gas} = 69,00 g
$\Delta M_{car.\ 1}$ = 119,22 g		$\Delta M_{car.\ 2}$ = 100,52 g	CO_2 uptake = **0,83 %**

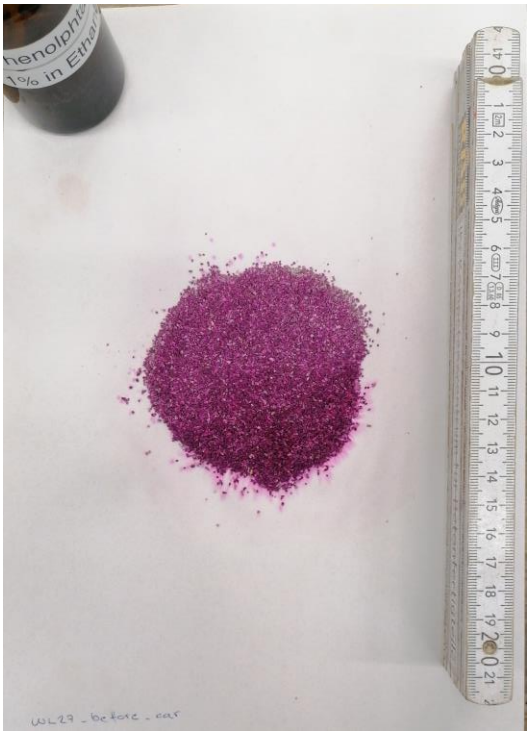

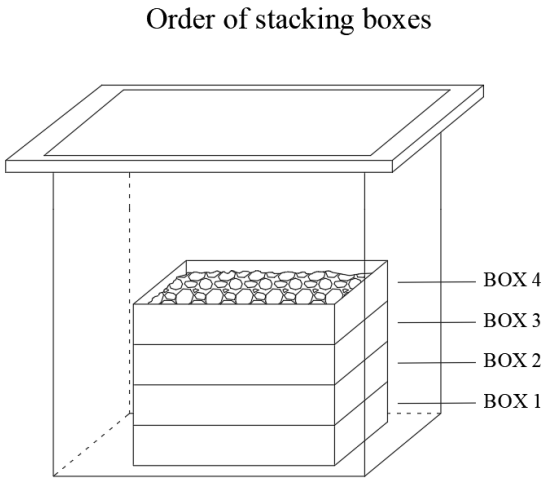

Fig. 40. Phenolphthalein test results before CO_2 curing for experiment WL27.

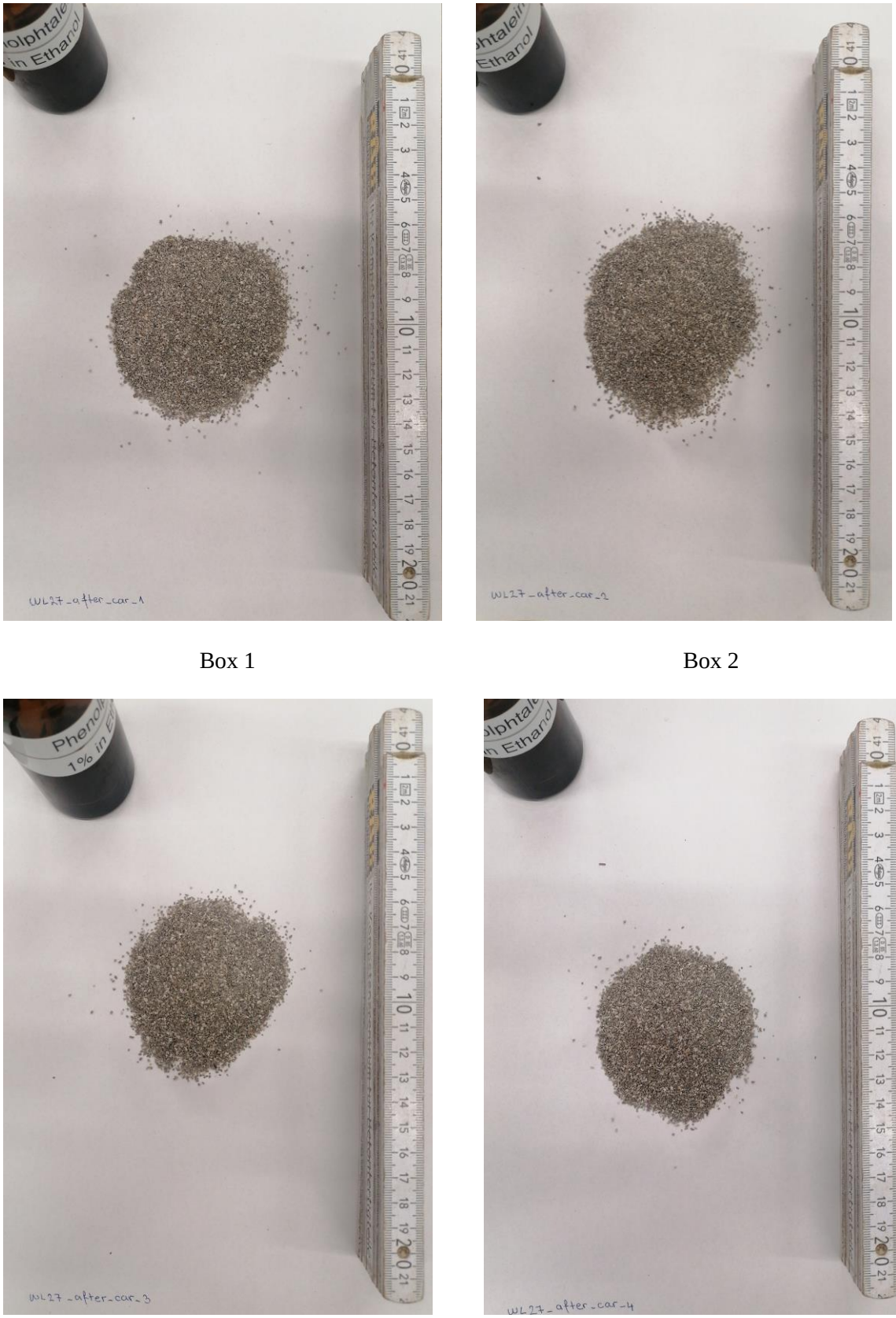

Box 1 Box 2

Box 3 Box 4

Fig. 41. Phenolphthalein test results for each box of experiment WL27 after CO_2 curing.

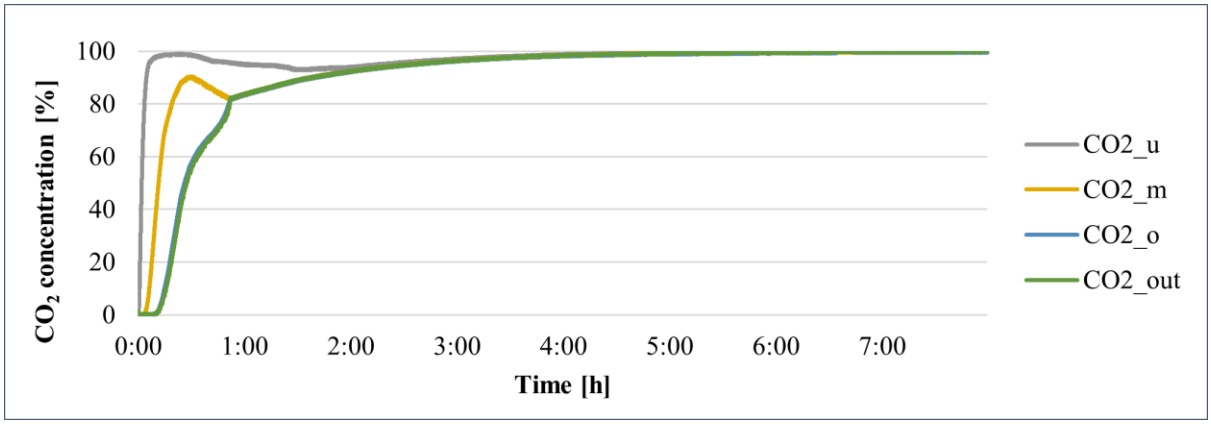

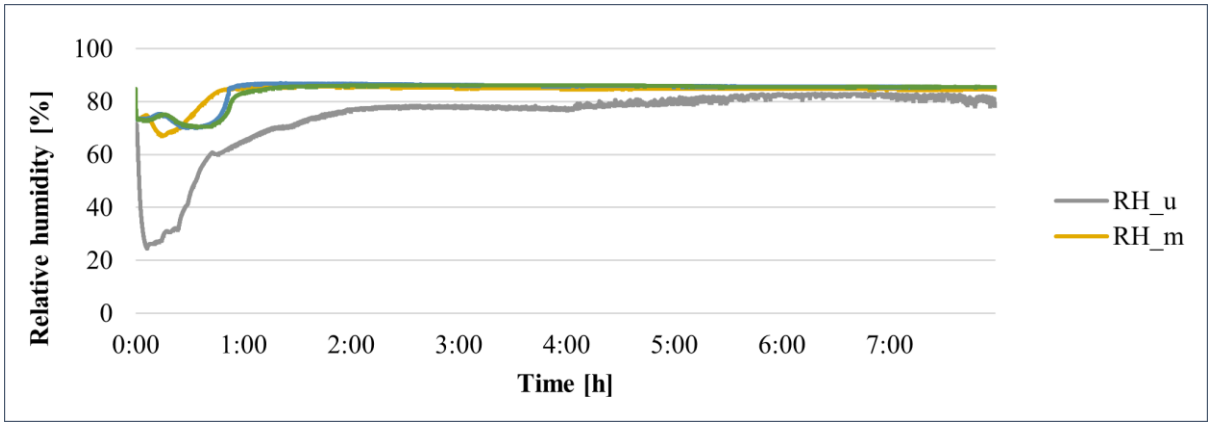

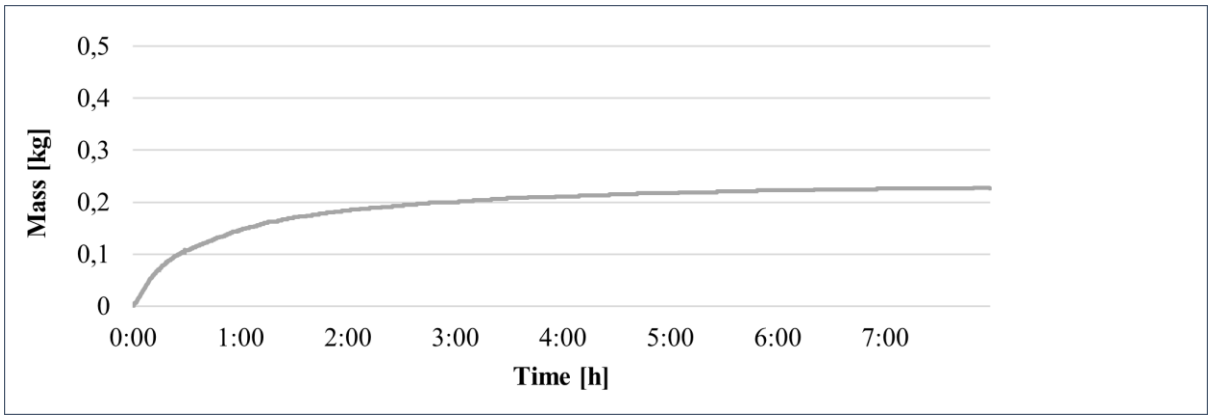

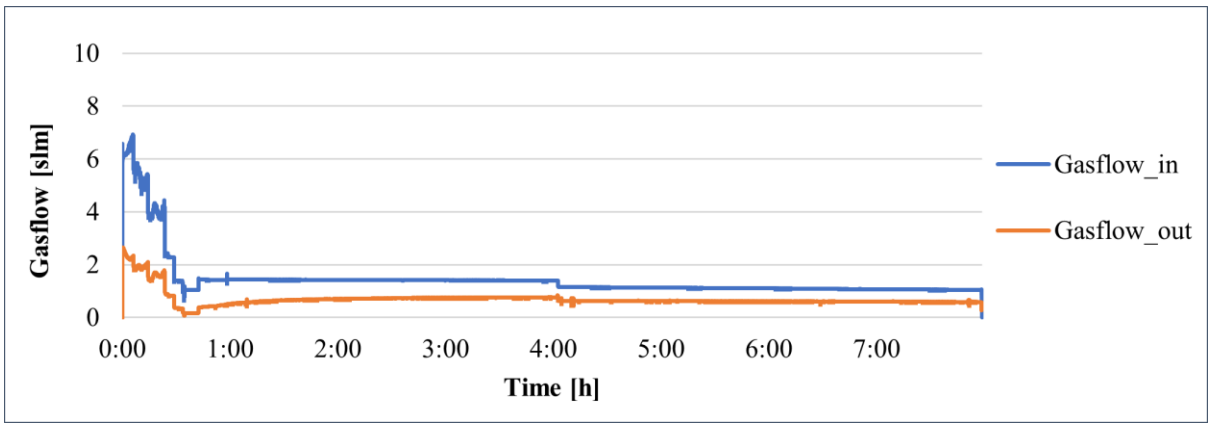

Fig. 42. The resulting diagrams for experiment WL27.